PNAS

www.pnas.org

Supplementary Information for:

Direct kinetic measurements and theoretical predictions of an isoprene-derived Criegee intermediate

Rebecca L. Caravan, Michael F. Vansco, Kendrew Au, M. Anwar H. Khan, Yu-Lin Li, Frank A. F. Winiberg, Kristen Zuraski, Yen-Hsiu Lin, Wen Chao, Nisalak Trongsiriwat, Patrick J. Walsh, David L. Osborn, Carl J. Percival, Jim Jr-Min Lin, Dudley E. Shallcross, Leonid Sheps, Stephen J. Klippenstein, Craig A. Taatjes & Marsha I. Lester.

Correspondence to: Marsha I. Lester
Email: milester@sas.upenn.edu

This PDF file includes:

1. Methods

1.1 Sandia transient absorption experiment. The UV-Vis spectra of methyl vinyl ketone oxide (MVK-oxide) and kinetics measurements with co-reactant SO_2 or formic acid were obtained using the Sandia broadband multi-pass transient absorption experiment as described previously (1, 2). Following the method of Barber *et al.* (3), MVK-oxide was produced by the 266 nm laser flash photolysis of 1,3-diiodobut-2-ene in the presence of excess O_2. The vapor of 1,3-diiodobut-2-ene was entrained into a He flow using a pressure- and temperature-controlled glass bubbler. Reactants (1,3-diiodobut-2-ene, O_2 and SO_2 or formic acid) and bath gases (He) were delivered via a set of calibrated mass flow controllers to the reactor (operated at 300 K and 10 Torr). Continuous broadband radiation was provided by a Xe arc lamp, leading to an effective path length in the range 30-40 m across the 300-450 nm spectral range. Time-resolved broadband spectra were obtained for each laser shot and were analyzed by a custom-built spectrometer. Experiments were performed under pseudo-first-order conditions such that $[O_2]$ >> [1,3-diiodobut-2-ene]. For bimolecular kinetics investigations, [co-reactant] >> [MVK-oxide]. Spectral analysis was performed by subtracting overlapping absorptions due to MVK and IO from the spectrum at long kinetic times, as discussed in the main text. Kinetic data were extracted by integrating over 330-367 nm to avoid perturbations from IO appearance at longer kinetic times. Analysis was conducted for wavelength ranges across the whole spectral range, and the resultant kinetics were consistent. The time traces were fitted with a single-exponential growth, single-exponential decay expression convolved with the instrument response function.
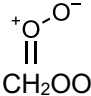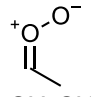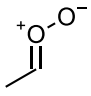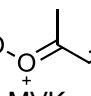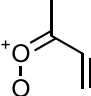
1.2 Sandia MPIMS. Complementary experiments to examine the kinetics of the iodoalkenyl + O_2 reaction and the products of *syn*-MVK-oxide + SO_2 and formic acid were performed using the Sandia Multiplexed Photoionization Mass Spectrometer (MPIMS) instrument (4). The MPIMS was interfaced with the tunable-VUV ionizing radiation of the Chemical Dynamics Beamline (9.0.2) of the Advanced Light Source (Lawrence Berkeley National Laboratory). 1,3-diiodobut-2-ene, O_2, He and SO_2 or formic acid were delivered to a halocarbon wax-coated quartz reactor (298 K, 10 Torr) as described above. MVK-oxide was produced using the method of Barber *et al.* (3), using a 248 nm excimer laser aligned along the length of the reactor. Reactants, intermediates and products were continuously sampled from a pinhole orifice in the reactor sidewall. The resultant molecular beam generated from expansion of the sampled gas into vacuum was intercepted orthogonally by the tunable-VUV radiation. The resultant ions were subsequently detected via orthogonal acceleration time-of-flight mass spectrometry. Experiments were performed at a photoionization energy of 8 eV in the absence of co-reactant, varying $[O_2]$ to establish the bimolecular rate coefficient for the iodoalkenyl radical + O_2 reaction (see section 3.1). The iodoalkenyl time profiles were fitted with a single exponential decay convolved with the instrument response function. Using the measured bimolecular rate coefficient for iodoalkyenyl + O_2, experimental conditions were designed such that pseudo-first-order conditions were maintained: $[O_2]$ >> [1,3-diiodobut-2-ene] and [SO_2 or formic acid] >> [MVK-oxide]. Investigations of SO_3 production from the reaction of MVK-oxide with SO_2 were performe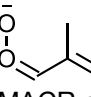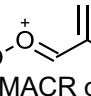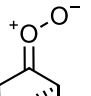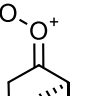d using a photoionization energy of 13 eV, above the ionizing threshold of 12.80 eV (5). High-resolution mass spectrometry was utilized to identify SO_3 via its exact mass. SO_3 time traces were fitted with a single-exponential growth single-exponential decay (to account for wall and diffusional loss) expression convolved with an instrument response function. Products of the MVK-oxide + formic acid reaction were investigated through experiments at a fixed ionization energy of 10.5 eV in addition to photoionization efficiency scans at ionization energies between 8.50 and 10.50 eV at 0.05 eV increments. High-resolution mass spectrometry was utilized to identify product formation at m/z 87 and 99.

1.3 IAMS transient absorption experiment. UV-Vis absorption spectra and kinetics were also recorded using the IAMS transient absorption experiment, detailed previously (6, 7). MVK-oxide was generated using the method of Barber *et al.* (3) via the 248 nm laser photolysis of 1,3-diiodobut-2-ene. The vapor pressure of 1,3-diiodobut-2-ene (heated to ~307 K) was entrained in O_2 or N_2, then mixed with O_2 prior to entering the photolysis reactor. A set of calibrated mass flow controllers were used to deliver N_2, O_2, 1,3-diiodobut-2-ene and SO_2 (or humidified N_2) to the reactor, which was held at 298 K. Pseudo-first-order conditions were maintained such that $[O_2]$ >> [1,3-diiodobut-2-ene], and for bimolecular investigations, $[SO_2]$ or [water] >> [MVK-oxide]. Prior to mixing, the concentrations of 1,3-diiodobut-2-ene and SO_2 were monitored in separate absorption cells by their UV absorption spectra. Absolute SO_2 concentrations were derived by comparing the integrated absorbance to the integrated cross section (8) within 200-250 nm. The concentration of SO_2 was also measured in the photolysis reactor using UV absorption for some

experiments to confirm the concentration calculation. The error from this calibration process is ~8%, including uncertainties in the spectrum measurement, pressure measurement, and uncertainty of the mass flow controllers. The error in [SO_2] from the reported absolute cross section is about 5–10% (8). Thus, the total error of [SO_2] is estimated to be 11–14%. [water] was derived in a similar manner with a humidity-temperature sensor. To prevent contamination of the reactor windows, slow flows of N_2 were used to purge the inner surfaces of the windows. To enhance the sensitivity of the absorption measurement, the probe light was focused and passed through the reactor 6 times using a spherical mirror and a SiO_2 prism resulting in an effective absorption length of ~ 426 cm. The spectra were acquired by using a grating spectrometer (Andor SR303i) and an electron-multiplying charge-coupled device (EMCCD, Andor Newton970, DU970N-UVB). The absorption change (after the photolysis pulse) at 340 or 375 nm (selected by a 10 nm bandpass filter) was monitored in real time by using a balanced photodiode detector and recorded by an oscilloscope.
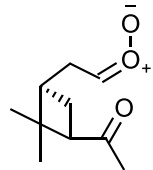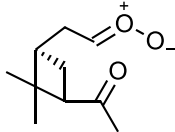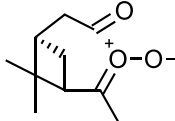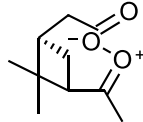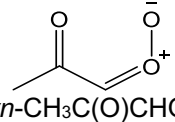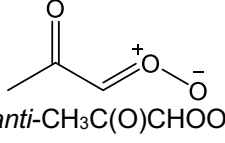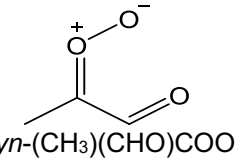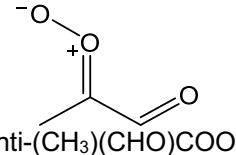
1.4 Global atmospheric modelling. Model simulations were conducted to quantify the impact of the MVK-oxide reactions with SO_2 and formic acid on the troposphere using the 3-dimensional global chemistry transport model, STOCHEM-CRI. STOCHEM is based upon a Lagrangian approach, with the chemical outputs being mapped onto a 5° latitude by 5° longitude Eulerian grid with 9 vertical layers. The Lagrangian approach has been used as it allows the advection of the 50,000 air parcels to be uncoupled from the chemical processes within these parcels. It is an 'offline' model with the radiation codes and transport driven by archived meteorological data, produced by the UKMO Unified Model (UM) at a grid resolution of 1.25° longitude, 0.8333° latitude, and 12 unevenly spaced (with respect to altitude) vertical levels with an upper boundary of 100 hPa (9). More details about the meteorological parameterizations in STOCHEM can be found in Collins *et al.* (10) and Derwent *et al.* (11). The chemical mechanism used in STOCHEM, is the common representative intermediates mechanism version 2 and reduction 5 (CRI v2-R5), referred to as 'STOCHEM-CRI' (12-15). The mechanism consists of 229 chemical species and 627 reactions. The emissions data employed in the STOCHEM model were adapted from the Precursor of Ozone and their Effects in the Troposphere (POET) inventory (http://accent.aero.jussieu.fr/database_table_inventories.php). The surface emissions from biomass burning, vegetation, oceanic and soil are distributed using monthly two-dimensional source maps at a resolution of 5° longitude $\times$ 5° latitude (16). The anthropogenic surface emissions have been distributed using the method developed by the International Institute for Applied Systems Analysis (IIASA) (17). The surface emissions of isoprene are emitted at a rate proportional to the cosine of the solar zenith angle during the day, with no emissions at night. More details about the emissions data of CO, NOx, SO_2, CH_4 and non-methane volatile organic compounds are given by Khan *et al.* (18).

The improved CRI v2-R5 mechanism of STOCHEM-CRI utilized in this study incorporates Criegee intermediates (CIs) formed from the ozonolysis reactions of six alkenes: ethene, propene, *trans*-but-2-ene, isoprene, α-pinene and β-pinene. Individual CIs are accounted for with their explicit formation and loss processes in the model. The chemical loss processes of unimolecular decomposition and/or reaction with water monomer and water dimer strongly dominate, which result in very short atmospheric lifetimes of CIs. The detailed information about the formation and loss processes of CIs used in the model can be found in McGillen *et al.* (19) and Chhantyal-Pun *et al.* (20). The loss of MVK-oxide by unimolecular decay, reactions with water monomer and dimer, and with SO_2 have been updated from the study McGillen *et al.* (19) and Chhantyal-Pun *et al.* (20) with the rate coefficients detailed in Table S1. Reactions of other functionalized CIs with SO_2 and formic acid have also been included. The reaction products from CH_2OO + water dimer have been updated, following recent experimental characterization by Sheps *et al.* (21) that revealed little formic acid production from this reaction. As a result of this, global modelled formic acid concentrations are reduced by 3% compared with previous model evaluations. Following the inclusion of the CI field, each air parcel contains 248 species that compete in 786 chemical reactions and utilize a time-step of 5 minutes.

Table S1. Reactions of Criegee intermediates and associated rate coefficients accounted for in the atmospheric model utilized in this work. The rate coefficients in bold font are those updated from previous work (19, 20).

Criegee intermediate	Rate coefficients[a]	References
CH₂OO	$k_{(H2O)2}$: 3.92 × 10⁻¹⁶ exp(2930/T)	Smith *et al.* (22)
syn-CH₃CHOO	k_{uni}: 2.76 × 10⁻⁷³T²⁷·⁸⁸ exp(3978/T) **k_{SO2}: 2.4 × 10⁻¹¹** **k_{HCOOH}: 2.5 × 10⁻¹⁰**	Fang *et al.* (23) **Taatjes *et al.* (24)** **Welz *et al.* (25)**
anti-CH₃CHOO	k_{H2O}: 1.3 × 10⁻¹⁴ cm³ s⁻¹ $k_{(H2O)2}$: 5.23 × 10⁻²⁰ exp(6124/T) **k_{SO2} 6.7 × 10⁻¹¹** **k_{HCOOH} 5.0 × 10⁻¹⁰**	Lin *et al*. (26) Lin *et al*. (26) **Taatjes *et al.* (24)** **Welz *et al.* (25)**
syn-MVK oxide	k_{uni}[b]: 2.46 × 10⁻⁷⁶ T²⁹·⁰⁹ exp(3545/T) **k_{H2O}: 3.4 × 10⁻¹⁹** **$k_{(H2O)2}$: 9.2 × 10⁻¹⁶** **k_{SO2}: 3.9 × 10⁻¹¹ cm³ s⁻¹** **k_{HCOOH}: 3.0 × 10⁻¹⁰ cm³ s⁻¹**	Barber *et al.* (3) **Anglada and Solé** (27) **Anglada and Solé** (27) **This study** **This study**
anti-MVK oxide	k_{uni}: 1.94 × 10¹² exp(-6150/T)	Barber *et al.* (3)
syn-MACR oxide	k_{uni}: 1.59 × 10¹¹ T⁰·⁴⁴exp(-6102/T)	Vereecken *et al.* (28)
anti-MACR oxide	k_{H2O}: 2.13 × 10⁻¹⁹ T¹·⁷⁴ exp(-929/T) $k_{(H2O)2}$: 2.24 × 10⁻¹⁹ T¹·⁷³ exp(1313/T) k_{uni}: 5.93 × 10⁸ T¹·⁴⁶ exp(-7832/T)	Vereecken *et al.* (28) Vereecken *et al.* (28) Vereecken *et al.* (28)
syn-nopinone oxide	k_{uni}: 1.9 × 10⁹ T¹·³³ exp(-8425/T) k_{H2O}: 8.46 × 10⁻²³ T²·⁶⁴ exp(121/T)	Vereecken *et al.* (28) Vereecken *et al.* (28)
anti-nopinone oxide	k_{uni}: 2.76× 10⁻⁷³T²⁷·⁸⁸ exp(3978/T)	Same k_{uni} as used for *syn*-CH₃CHOO

[a]The units of the unimolecular and bimolecular rate coefficient are s⁻¹ and cm³ s⁻¹, respectively.
[b]Note that OH produced from the unimolecular decomposition of stabilized *syn*-MVK-oxide is omitted from the model. This is a relatively minor source of OH and is anticipated to have minimal perturbation on the reactions assessed herein.

Criegee intermediate	Rate coefficients[a]	References
syn-pinonaldehyde oxide	k_{uni}: $2.76 \times 10^{-73} T^{27.88}$ exp(3978/T)	Same k_{uni} as used for *syn*-CH_3CHOO
anti-pinonaldehyde oxide	k_{H2O}: 1.3×10^{-14} cm^3 s^{-1} $k_{(H2O)2}$: 5.23×10^{-20} exp(6124/T) **k_{SO2}: 6.7×10^{-11}** **k_{HCOOH}: 5.0×10^{-10}**	Same k_{H2O}, $k_{(H2O)2}$ **k_{SO2} and k_{HCOOH}** as used for *anti*-CH_3CHOO
anti-isopinonaldehyde oxide	k_{uni}: $2.76 \times 10^{-73} T^{27.88}$ exp(3978/T)	Same k_{uni} as used for syn-CH_3CHOO
syn-isopinonaldehdye oxide	k_{uni}: $6.95 \times 10^{-66} T^{25.7}$ exp(2391/T)	Vereecken *et al.* (28)
syn-$CH_3C(O)CHOO$	k_{H2O}: $2.18 \times 10^{-19} T^{1.43}$ exp(1268/T) $k_{(H2O)2}$: $2.26 \times 10^{-19} T^{1.43}$ exp(3279/T) **k_{SO2}: 2.4×10^{-11}** **k_{HCOOH}: 2.5×10^{-10}**	Vereecken *et al.* (28) Vereecken *et al.* (28) **Same k_{SO2} and k_{HCOOH} as used for *syn*-CH_3CHOO**
anti-$CH_3C(O)CHOO$	k_{H2O}: 1.3×10^{-14} cm^3 s^{-1} $k_{(H2O)2}$: 5.23×10^{-20} exp(6124/T) **k_{SO2}: 6.7×10^{-11}** **k_{HCOOH}: 5.0×10^{-10}**	Same k_{H2O}, $k_{(H2O)2}$, **k_{SO2} and k_{HCOOH}** as used for *anti*-CH_3CHOO
syn-$(CH_3)(CHO)COO$	k_{uni}: $2.76 \times 10^{10} T^{0.78}$ exp(-5162/T) k_{H2O}: $7.81 \times 10^{-20} T^{1.68}$ exp(757/T) $k_{(H2O)2}$: $8.07 \times 10^{-20} T^{1.67}$ exp(2828/T)	Vereecken *et al.* (28) Vereecken *et al.* (28) Vereecken *et al.* (28)
anti-$(CH_3)(CHO)COO$	k_{uni}: $2.76 \times 10^{-73} T^{27.88}$ exp(3978/T)	Same k_{uni} as used for *syn*-CH_3CHOO

[a]The units of the unimolecular and bimolecular rate coefficient are s^{-1} and cm^3 s^{-1}, respectively.
[b]Note that OH produced from the unimolecular decomposition of stabilized *syn*-MVK-oxide is omitted from the model. This is a relatively minor source of OH and is anticipated to have minimal perturbation on the reactions assessed herein.

1.5 Computational kinetics and mechanistic investigations. Coupled cluster calculations were performed using MOLPRO (29), with the CCSDT(Q) calculations employing Kállay's MRCC supplement (30). Density functional theory calculations were performed using G09 (31). The master equation calculations were undertaken with the MESS code (32, 33), and the variable reaction coordinate transition state theory (TST) calculations were performed with VaReCoF (34).

2. Computational MVK-oxide isomerization kinetics

As discussed in the main text, there are four low lying conformers of MVK-oxide. A proper analysis of the experimental observations requires some understanding of the timescales for isomerization between these conformers. A high-level *ab initio* kinetics analysis for the unimolecular dissociation rates of *syn*- and *anti*-MVK-oxide was reported by Barber *et al.* (3). This previous analysis is readily adapted to predict the rates of isomerization between the four conformers under temperature and pressure conditions of relevance to Earth's atmosphere.

The focus of Barber *et al.* (3) involved dissociation of MVK-oxide at specific excitation energies (ca. 6000 cm^{-1}) obtained through direct IR-excitation. At these energies, isomerizations between the *cis* and *trans* forms of *syn*-MVK-oxide (and similarly *cis*- and *trans-anti*-MVK-oxide) are rapid relative to the dissociation timescale. Thus, the two *cis* and *trans* conformers were treated as merged species for both the *syn* and *anti* forms. For the present analysis, we instead treat all four conformers as distinct species within the master equation and directly explore both the *cis-trans* and *syn-anti* isomerizations.

This analysis indicates that: (i) all four conformers are kinetically stable (i.e., their isomerization rate coefficients are smaller than the collisional relaxation rates), (ii) the *cis-trans* isomerization rates are fast on the timescale of the present experiments, and (iii) the *syn-anti* isomerization rates are slow on the timescale of experiment. The first finding indicates that, at least in principle, one can properly derive bimolecular rate coefficients separately for each of the individual conformers. However, the second finding indicates that the experimental observations cannot resolve the *cis* and *trans* conformers as separate species and so the observed reactive decays will instead correspond to the Boltzmann weighted average of the rate coefficients for the *cis* and *trans* pair of species. Meanwhile, the third finding indicates that the *syn*- and *anti*-conformers should exhibit distinct decays.

The underlying energies for this master equation analysis of the isomerization are as reported by Barber *et al.* (3). They were largely obtained from CCSD(T)-F12b/CBS(cc-pVTZ-F12,cc-pVQZ-F12)//B2PLYPD3/cc-pVTZ evaluations coupled with CCSDT(Q)/cc-pVDZ corrections for higher order excitations, CCSD(T)/CBS(cc-pcVTZ,cc-pcVQZ) core-valence corrections, and B2PLYP-D3/cc-pVTZ anharmonicity corrections. For the two *syn*- to *anti*- torsional saddle points, the barrier heights were instead based on CASPT2 analyses due to the presence of significant multireference effects arising from the breaking of the O=O double bond in the zwitterionic resonant form of MVK-oxide. To facilitate interpretation of the present isomerization kinetics analysis, these conformer energies and isomerization barriers are reported again in Table S2.

In the present master equation analysis, the CH_3 groups were again treated as 1-dimensional hindered rotors with the torsional potentials as described by Barber *et al.* (3). For the C_2H_3 rotors, with our current codes, there is some difficulty in assigning the state density from the quantized hindered rotor states for the overall torsional motion to specific conformational states. Here we considered two simple approximations and found that the predicted rates agreed to within ~10%. In particular, the simplest approximation involved the treatment of these modes as harmonic oscillators. An alternative treatment replaced the full torsional potential with a symmetrized potential that roughly corresponds to restricting the range of torsional space for that rotor to +/- 90 degrees from the given conformer. The isomerization rates predicted with the harmonic separation approximation are reported in Table S3. The *syn-anti* and *anti-syn* rates are too small to be kinetically relevant (10^{-3} s^{-1} or less) and so are not reported here. For comparison purposes, the corresponding conformer-specific unimolecular dissociation rate coefficients are also reported therein. The bath gas for these calculations was presumed to be N_2, although minimal bath gas dependence is anticipated. The conformer-specific partition functions and Boltzmann thermal probabilities reported in Table S4 allow for the conversion of these conformer-specific isomerization and dissociation rate coefficients to more averaged quantities such as the *syn*- and *anti*- rate coefficients.

In summary, *syn-anti* isomerization of MVK-oxide will be negligibly slow due to the high barriers (Table S2) associated with rotation about C=O bond, and thus *syn*- and *anti*-conformers of MVK-oxide can be treated as distinct species. By contrast, the theoretical analysis demonstrates the rapid rate for *cis-trans* isomerization (ca. 10^7 s^{-1}, Table S3) for both *syn*- and *anti*-conformers of MVK-oxide due to the much lower barriers (Table S2) associated with rotation about the C-C single bond. The corresponding timescale for *cis-trans* isomerization is sub-microsecond, which is significantly faster than the experimental timescale of milliseconds. As a result, the *cis* and *trans* forms will rapidly interconvert with population of the lower energy *trans* form strongly favored over the higher energy *cis* form under thermal conditions.

Table S2. Stationary point energies (kcal mol^{-1}) for MVK-oxide isomerization.

Species	CCSD(T)-F12b				T(Q) Corr.	T(Q) Corr.	Core Val.	E0	Anh.	Total[a]
	DZ-F12	TZ-F12	QZ-F12	CBS	DZ	6-31G*	CBS TZ-QZ	B2 TZ	B2 TZ	
syn-trans	0.0	0	0	0	0	0	0	0	0	0
syn-cis	1.93	1.94	1.94	1.94	0.01	0.04	0.05	-0.19	0.00	1.76
anti-trans	2.70	2.72	2.74	2.75	-0.07	-0.03	0.01	-0.10	-0.03	2.57
anti-cis	2.84	2.79	2.79	2.78	0.20	0.21	0.01	0.03	-0.01	3.05
syn-cis to *syn-trans*	8.09	8.17	8.17	8.17	0.45	0.41	0.01	-0.63	-0.03	7.97
anti-cis to *anti-trans*	11.46	11.56	11.56	11.56	0.41	0.37	0.01	-0.71	-0.03	11.25
syn-trans to *anti-trans*[a]	-	-	-	-	-	-	-	-	-	30.93[a]
syn-cis to *anti-cis*[a]	-	-	-	-	-	-	-	-	-	30.63[a]

[a]The total energies for the *syn-anti* zero-point corrected barriers are derived from CASPT2(4e,4o)/cc-pVTZ calculations of the singlet-triplet splitting at the saddle point coupled with CCSD(T)-F12 based evaluations of the triplet energy as described in detail by Barber *et al.* (3). Also, as reported by Barber *et al.* (3) the total energy includes a minor (≤ 0.01 kcal mol^{-1}) contribution from relativistic effects.

Table S3. Predicted MVK-oxide *cis-trans* isomerization rate coefficients (s^{-1}) and conformer-specific dissociation rate coefficients (s^{-1}) for a range of temperatures and pressures.

T/K	P/atm.	*syn-trans syn-cis*	*syn-cis syn-trans*	*anti-trans anti-cis*	*anti-cis anti-trans*	*syn-trans*	*syn-cis*	*anti-*	*anti-*
225	0.01	4.1e3	1.3e5	1.9e3	5.1e3	-	-	2.1	3.7
250		1.6e4	3.4e5	9.0e3	2.2e4	1.6	8.6	28	45
275		4.6e4	6.8e5	3.0e4	6.5e4	6.3	31	230	330
298		1.0e5	1.1e6	7.0e4	1.4e5	22	110	1.1e3	1.5e3
350		3.7e5	2.6e6	2.8e5	5.1e5	240	1.9e3	1.4e4	1.8e4
400		-	-	6.7e5	1.2e6	4.0e3	-	7.7e5	9.8e4
225	0.1	2.1e4	6.6e5	7.1e3	1.9e4	-	-	2.6	4.7
250		9.0e4	1.9e6	3.8e4	9.1e4	1.7	6.4	39	63
275		2.8e5	4.1e6	1.4e5	3.1e5	6.5	29	350	520
298		6.4e5	7.3e6	3.6e5	7.4e5	23	110	1.8e3	2.6e3
350		2.6e6	1.8e7	1.7e6	3.1e6	320	1.9e3	3.2e4	4.2e4
400		-	-	4.5e6	7.7e6	5.6e3	-	2.2e5	2.8e5
225	1	6.5e4	2.1e6	1.6e4	4.1e4	-	-	2.4	6.0
250		3.2e5	6.7e6	9.7e4	2.3e5	1.6	7.3	38	78
275		1.1e6	1.7e7	4.1e5	9.0e5	6.5	29	360	650
298[a]		2.9e6	3.3e7	1.2e6	2.5e6	24	102	2.1e3	3.3e3
350		1.3e7	9.6e7	7.0e6	1.3e7	390	1.6e3	4.3e4	6.0e4
400		3.8e7	1.9e8	2.2e7	3.8e7	3.3e3	2.1e4	3.6e5	4.7e5

[a]At 298 K and 1 atm, the average decay rate for the *syn*-conformers is 33 s^{-1} based on a Boltzmann average [$Q_1 k_1 + Q_2 k_2/(Q_1+Q_2)$, where Q_i is the partition function for conformer i (*cis* or *trans*), c.f. Table S4. Similarly, the Boltzmann averaged decay rate for *anti*-conformers is 2140 s^{-1}.

Table S4. MVK-oxide partition functions and thermal probabilities.[a]

T/K	Partition Functions (cm^3)[b]				P_{trans}		P_{syn}[e]
	syn-trans	*syn-cis*	*anti-trans*	*anti-cis*	*syn*[b]	*anti*[d]	
225	2.5e32	4.1e32	3.8e32	4.2e32	0.969	0.725	0.994
250	4.8e32	7.9e32	7.3e32	8.1e32	0.954	0.705	0.988
275	8.9e32	1.5e33	1.4e33	1.5e33	0.937	0.687	0.981
298	1.5e33	2.6e33	2.5e33	2.6e33	0.919	0.674	0.973
350	5.1e33	9.0e33	8.2e33	8.7e33	0.877	0.651	0.949
400	1.5e34	2.8e34	2.5e34	2.6e34	0.835	0.635	0.922

[a]Note that the thermal probabilities reported here (P_{trans}, P_{syn}, etc.) are for an equilibrium distribution of MVK-oxide conformers and do not reflect the nascent or time-dependent populations from the experiments.
[b]Partition functions defined relative to their conformer-specific ground state energy.
[c]Thermal probability of the *trans* conformer within *trans-* and *cis-syn*-MVK-oxide.
[d]Thermal probability of the *trans* conformer within *trans-* and *cis-anti*-MVK-oxide.
[e]Thermal probability of the *syn-* conformer of MVK-oxide.

3. MVK-oxide kinetics and reaction mechanisms
3.1 MVK-oxide formation and unimolecular decay.
Iodoalkenyl + O₂ kinetics for MVK-oxide formation. To establish the rate of formation of MVK-oxide from the iodoalkenyl ($\cdot C_4H_6I$) + O_2 reaction, the rate coefficient for the reaction was measured by direct monitoring of the iodoalkenyl radical at m/z 181 using MPIMS at a photoionization energy of 8 eV. This energy was chosen such that it was below the threshold for dissociative ionization of the photolytic precursor ($C_4H_6I_2$) appearing at the mass of the iodoalkenyl radical. A bimolecular rate coefficient of $(1.70 \pm 0.07) \times 10^{-13}$ cm^3 s^{-1} for the reaction of C_4H_6I + O_2 is established (Figure S1) – around an order of magnitude slower than for the equivalent CH_2OO formation reaction (CH_2I + O_2) (35). This is rationalized by the resonance stabilization of the iodoalkenyl radical in the present case – comparisons can be drawn with R + O_2 reactions, where the rate coefficients are typically an order of magnitude slower for resonance stabilized R, due to the loss of resonance stabilization on addition of O_2.
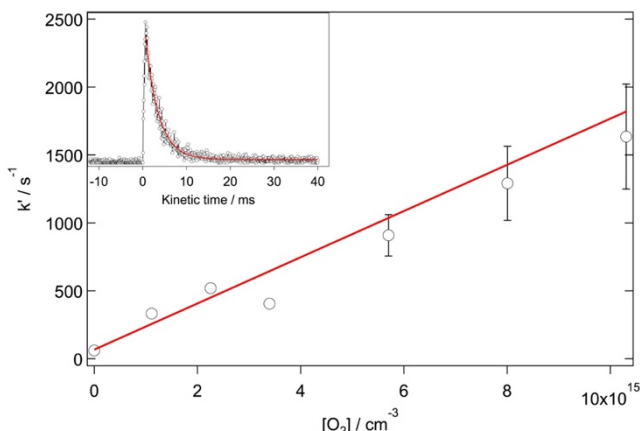
Fig. S1. First order rate coefficient for the loss of the iodoalkenyl radical as a function of [O_2], recorded at a photoionization energy of 8 eV using the Sandia MPIMS experiment. An example kinetic trace of the iodoalkenyl radical is inset. Kinetic traces are fitted with a single exponential decay expression convolved with the instrument response function. The bimolecular rate coefficient is obtained from a linear fit to k' vs. [O_2], weighted to the 95% confidence limit error bars (note that the error bars for the first four points are smaller than the symbols). From this a bimolecular rate coefficient of $(1.70 \pm 0.07) \times 10^{-13}$ cm^3 s^{-1} is obtained.
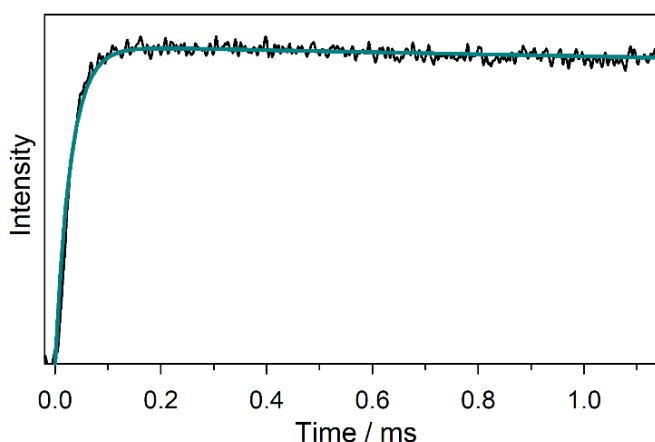
Fig. S2. Enlarged inset from Figure 1 (lower panel) from the main text. Kinetic time trace for MVK-oxide from the Sandia experiment (black) integrated between 330-367 nm compared with the simulated thermal unimolecular decay for *syn*-conformers to 2-hydroperoxyl-buta-1,3-diene (cyan) with $k(T) = 33$ s^{-1} (T = 298 K). Thermal rates are computed using *ab initio* master equation modeling in the high-pressure limit (3). The simulations include an experimental rise time for MVK-oxide appearance of 30 μs from the reaction of the iodoalkenyl radical + O_2.

3.2 MVK-oxide + SO₂.

Further experimental evidence for SO₃ formation. Using the bimolecular rate coefficient measured via the Sandia transient absorption experiment, and assuming a first order loss rate of 300 s^{-1} (based on the transient absorption measured first order loss, and consistent with previous smaller CI first order losses in the MPIMS experiments), the signal appearing at the exact mass of SO₃ (m/z = 79.96) at 13 eV can be evaluated versus the fraction of MVK-oxide undergoing reaction with SO₂. A linear increase in the amplitude of the signal at m/z 79.96 is observed with increasing fraction of MVK-oxide undergoing reaction with SO₂ (Figure S3). This, together with the exact mass determination (Figure S3, inset) and the bimolecular rate coefficient for formation (main text, Figure 3) provides further experimental evidence that SO₃ is a direct product of the MVK-oxide + SO₂ reaction.
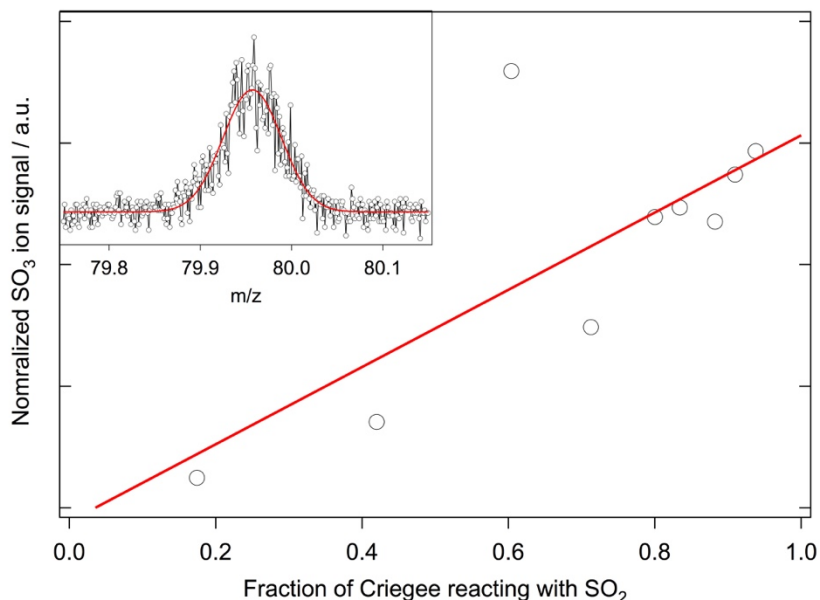
Fig. S3. Linear relationship of SO₃ amplitude, (summed over the kinetic time of 0-60 ms), and the estimated fraction of MVK-oxide reacting with SO₂. SO₃ data were obtained via MPIMS at a photoionization energy of 13 eV, using the absorption experiment bimolecular rate coefficient of 3.9×10^{-11} cm³ s^{-1} and assuming a first-order loss of 300 s^{-1}, consistent with the Sandia broadband multi-pass transient absorption experiment data and previous MPIMS experiments of Criegee intermediate chemistry. A Gaussian fit to m/z 80 to determine the exact mass is shown in the inset. The Gaussian fit retrieved a mass value of (79.957 ± 0.007) amu consistent with the exact m/z of SO₃ (79.95683 amu).

Ab initio calculations, computational kinetics and mechanistic investigations. For the reaction of MVK-oxide with SO₂, *ab initio* kinetics calculations were performed in order to gain a better understanding of the expected temperature- and pressure-dependencies of both the rate coefficient and product branching. The experimental observation that the rate coefficient is independent of pressure suggests that the rate is governed by the capture rate for the formation of the initial complex. However, there may still be strong temperature- and pressure-dependencies to the branching between stabilization of this complex and formation of bimolecular products (primarily SO₃ + methyl vinyl ketone (MVK)). This branching has significant ramifications for the net SO₃ formation rate.

To our best knowledge, there are no prior theoretical studies of the reaction of SO₂ with MVK-oxide. However, there is considerable prior work on the reaction of SO₂ with CH₂OO (36-40) and many of the conclusions from those studies are relevant to the reaction with MVK-oxide. These prior studies examined a great variety of possible pathways, with the quantitative analysis of the kinetics complicated by the present of both diradical and concerted pathways. Unfortunately, quantitative predictions for such diradical channels generally require multi-reference electronic structure treatments. A similar competition between diradical and concerted pathways arises in the ozonolysis of Criegee intermediates, as discussed for example in the recent analysis of the dynamics of Criegee intermediate stabilization for the ozonolysis of ethylene by Pfeifle *et al.* (41).

A particularly detailed exploration of the kinetics was provided in the recent study of Kuwata *et al.* (40). For simplicity, in this first analysis, we restrict our attention to the analogue of the dominant pathway from their study. In particular, we consider the addition to form both *endo* and *exo* van der Waals complexes (MVKO…SO$_2$) (3a/3b in the notation of Kuwata *et al.*), the conversion of these complexes to secondary ozonides (SOZ) (via TS-4a/TS-4b to 5a/5b), the interconversion of *endo/exo* forms (via TS-6), but with the loss of symmetry now yielding different secondary ozonides (SOZ'), and then dissociation of SOZ' to SO$_3$ + MVK (via TS7a/TS7b). (Again, MVK-oxide is often denoted in shorthand as MVKO.)

The energetics along these pathways were calculated for both *syn-trans-* and *syn-cis-*MVK-oxide at the CCSD(T)/CBS//B2PLYP-D3/cc-pVTZ level. The CBS extrapolation is based on calculations with Dunning's tight d supplemented correlated consistent basis sets [cc-pV(n+d)Z] (42). A correction for higher order electronic excitation was estimated from CCSDT(Q)/6-31G* calculations for related aspects of the CH$_2$OO + SO$_2$ system. In particular, we estimate higher level corrections of 0.41, 0.80, 1.49, -0.72, and 1.23 kcal mol^{-1} for the van der Waals minima, the transition state from the van der Waals minima to the SOZ, the SOZ, the transition state from the SOZ to SO$_3$ + MVK, and the products SO$_3$ + MVK, respectively. The calculated stationary point energies are reported in Table S5 and a schematic illustration of the reaction pathways is provided in Figure S4.
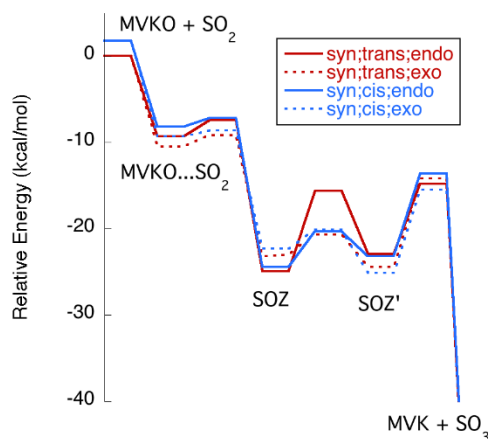
Fig. S4. Schematic plot of the expected lowest energy path for the reaction of MVK-oxide (denoted MVKO here) with SO$_2$ (cf., Table S5). Note that the *exo/endo* labeling is based on the structures of the first two complexes. The conversion to the SOZ' actually reverses this labeling, which is not accounted for in this plot. In particular, for SOZ and SOZ' the *endo* forms are lower in energy.

Species	B2PLYP-D3[b]	CCSD(T)[c]				E$_0$[d]	Total[e]	Total[f]	T1[g]
	TZ	DZ	TZ	QZ	CBS	B2/TZ		+Corr.	
syn-trans + SO$_2$	0.0	0.0	0.0	0.0	0.0	0.0	0.0	0.0	0.035
									0.022
trans; endo[h]									
MVKO;st…SO$_2$	-12.4	-9.4	-9.8	-10.6	-11.1	1.4	-9.7	-9.3	0.027
MVKO;st …SO$_2$ = SOZ	-11.1	-7.4	-8.4	-9.3	-10.0	1.8	-8.2	-7.4	0.024
SOZ	-26.1	-25.8	-28.9	-29.1	-29.2	2.9	-26.4	-24.9	0.017
SOZ=SOZ'	-16.5	-14.7	-18.5	-19.0	-19.4	2.4	-17.0	-15.6	0.017
SOZ'	-24.6	-24.6	-27.0	-27.1	-27.2	2.8	-24.4	-22.9	0.018
SOZ' = MVK + SO$_3$	-12.8	-11.0	-14.3	-15.0	-15.4	1.3	-14.1	-14.8	0.026
MVK + SO$_3$	-64.3	-64.2	-70.3	-71.3	-72.0	1.1	-70.8	-69.6	0.014
									0.019
trans; exo[h]									
MVKO;st …SO$_2$	-14.1	-11.1	-11.4	-12.0	-12.4	1.6	-10.9	-10.5	0.027
MVKO;st …SO$_2$ = SOZ	-13.1	-9.9	-10.7	-11.4	-11.9	1.9	-10.0	-9.2	0.024
SOZ	-24.9	-24.7	-27.3	-27.5	-27.6	2.8	-24.7	-23.2	0.017
SOZ=SOZ'	-21.9	-21.6	-24.6	-24.7	-24.8	2.6	-22.2	-20.7	0.017
SOZ'	-25.6	-25.6	-28.4	-28.6	-28.7	2.8	-25.9	-24.4	0.017
SOZ' = MVKO + SO$_3$	-12.2	-10.7	-13.8	-14.5	-14.9	1.4	-13.5	-14.2	0.026
MVKO + SO$_3$	-64.3	-64.2	-70.3	-71.3	-72.0	1.1	-70.8	-69.6	0.014
syn-cis + SO$_2$	2.3	1.3	1.8	2.0	2.02	-0.2	1.8	-	0.037
cis; endo[h]									
MVKO;sc …SO$_2$	-11.5	-8.8	-8.9	-9.5	-10.0	1.4	-8.6	-8.2	0.028
MVKO;sc …SO$_2$ = SOZ	-10.9	-8.0	-8.4	-9.1	-9.6	1.6	-8.0	-7.2	0.024
SOZ	-25.6	-25.7	-28.5	-28.6	-28.6	2.7	-25.9	-24.4	0.017
SOZ=SOZ'	-21.4	-20.9	-24.1	-24.2	-24.2	2.5	-21.8	-20.3	0.017
SOZ'	-24.7	-24.4	-27.0	-27.3	-27.4	2.6	-24.7	-23.2	0.017
SOZ' = MVKO + SO$_3$	-11.4	-10.0	-13.1	-13.7	-14.2	1.3	-12.9	-13.6	0.026
MVKO + SO$_3$	-64.0	-64.5	-70.0	-70.8	-71.4	1.0	-70.4	-69.2	0.014
cis; exo[h]									
MVKO;sc …SO$_2$	-12.6	-10.0	-10.1	-10.7	-11.2	1.4	-9.7	-9.3	0.028
MVKO;sc …SO$_2$ = SOZ	-12.2	-9.3	-9.9	-10.6	-11.1	1.7	-9.4	-8.6	0.025
SOZ	-23.9	-24.0	-26.4	-26.5	-26.5	2.7	-23.8	-22.3	0.017
SOZ=SOZ'	-21.3	-21.2	-24.1	-24.1	-24.2	2.5	-21.6	-20.1	0.017
SOZ'	-26.2	-26.1	-29.0	-29.2	-29.3	2.7	-26.6	-25.1	0.017
SOZ' = MVKO + SO$_3$	-13.6	-12.3	-15.2	-15.8	-16.2	1.4	-14.8	-15.5	0.026
MVKO + SO$_3$	-64.0	-64.5	-70.0	-70.8	-71.4	1.0	-70.4	-69.2	0.014

syn,trans = syn,cis; endo[h]									
MVKO…SO₂	-5.6	-3.9	-3.6	-4.4	-4.9	1.0	-3.8	-3.4	0.024
MVKO…SO₂; geom. B	-4.5	-2.6	-2.7	-3.4	-3.9	0.7	-3.2	-2.8	0.024
SOZ	-23.6	-23.4	-26.5	-26.7	-26.8	2.5	-24.3	-22.8	0.017
SOZ; geom. B	-23.9	-23.8	-26.7	-27.0	-27.1	2.5	-24.6	-23.1	0.017
syn,trans = syn,cis; exo[h]									
MVKO…SO₂	-7.4	-5.8	-5.6	-6.3	-6.7	1.1	-5.6	-5.2	0.024
SOZ	-23.1	-23.0	-25.5	-25.7	-25.8	2.6	-23.2	-21.7	0.018
SOZ; geom. B	-23.2	-23.2	-25.7	-25.8	-25.9	2.6	-23.3	-21.9	0.017

[a]All energies are relative to *syn-trans*-MVK-oxide (denoted MVKO) + SO₂. [b]B2PLYP-D3/cc-pVTZ electronic energies. [c]CCSD(T) electronic energies for the cc-pVDZ, cc-pVTZ, cc-pVQZ and an estimate of the CBS limit. [d]B2PLYP-D3/cc-pVTZ vibrational zero-point energy. [e]The total energy taken as the sum of the CCSD(T)/CBS//B2PLYP-D3/cc-pVTZ energy and the B2PLYP-D3/cc-pVTZ zero-point energy. [f]The total energy corrected by estimated T(Q) corrections obtained from CCSDT(Q)/6-31G* calculations for related geometries in the CH₂OO + SO₂ system. [g]The T1 diagnostic.[h]The pathways are labeled as *exo/endo* according to the initial van der Waals complex (MVKO…SO₂) and SOZ. The transition from SOZ to SOZ' converts between the *endo* and *exo* forms.
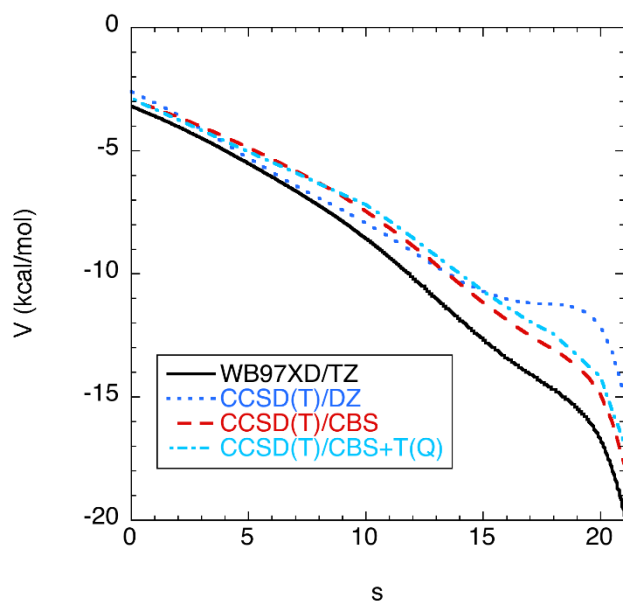
Figure S5. Plot of the minimum energy path (MEP) potential for the addition of SO₂ to *syn-trans*-MVK-oxide evaluated at various levels, all along the ωB97XD/cc-pVTZ minimum energy potential (MEP).

For the SO₂ + CH₂OO system, there has been some debate as to whether or not there is a saddle point for the formation of the long-range van der Waals complex. We examined this question herein via calculations along the minimum energy path determined at the ωB97XD/cc-pVTZ level. Interestingly, calculations at the CCSD(T)/CBS//ωB97XD/cc-pVTZ level show no saddle point, even with the inclusion of a CCSDT(Q)/6-31G* correction. This finding strongly suggests that there is no saddle point for this reaction.

Notably, the resonance stabilization in MVK-oxide changes the picture for reaction with SO₂ (Figure S5). In particular, we now find a saddle point with an imaginary frequency in the 100-200 cm⁻¹ range for each of the ωB97XD/6-31+G*, ωB97XD/cc-pVTZ, and B2PLYP-D3/cc-pVTZ methods for both *syn-trans* and *syn-cis* isomers and for *endo* and *exo* pathways (Table S5). The resonance stabilization also decreases

the depth of the SOZ and SOZ' wells relative to reactants from ~35 kcal mol^{-1} for CH_2OO to ~24 kcal mol^{-1} for MVK-oxide.

We used direct sampling *ab initio* variable reaction coordinate transition state theory (VRC-TST) to explore the rate coefficient for forming the van der Waals complex. For this VRC-TST analysis, we considered four separate electronic structure methods (MP2/cc-pVDZ, MP2/cc-pVTZ, ωB97XD/6-31+G*, and ωB97XD/cc-pVTZ) finding only modest variation (~20% near room temperature) in the predicted long-range capture rate coefficient, as illustrated in Figure S6. The reaction coordinate was presumed to be defined by the separation between the two centers-of-mass of the two fragments and the separation was constrained to 4.2 Å and larger. A dynamical correction factor of 0.85, based on reference comparisons of trajectories and TST (43) is included.
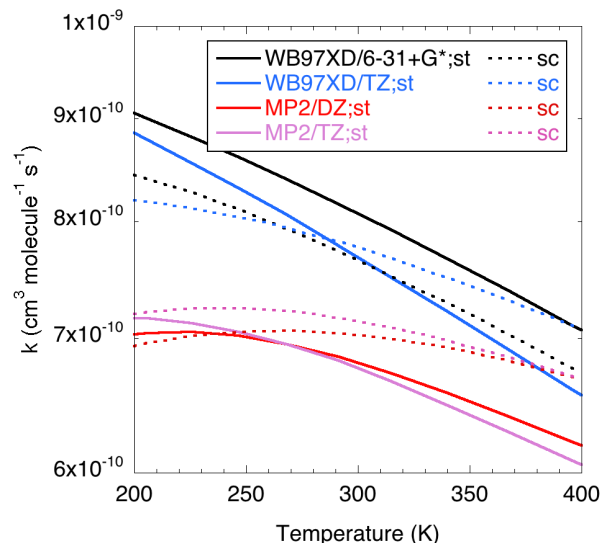
Fig. S6. Plot of the VRC-TST predicted rate coefficient for the high-pressure addition of SO_2 to *syn-trans* (st) and *syn-cis* (sc) MVK-oxide evaluated with four different *ab initio* methods.

The pressure-dependence of branching between stabilization and SO_3 + MVK formation was explored though an *ab initio* transition state theory-based master equation (AITSTME) model for the overall kinetic process. This master equation model employs standard exponential down energy transfer probabilities, with a temperature-dependent expression for the average downwards energy transferred given by $<\Delta E_{down}> = 400 \ (T/298)^{0.85}$ cm^{-1} and a Lennard-Jones collision rate appropriate for collision with N_2. As part of this analysis we presume rapid equilibration of the *endo* and *exo* forms of both the MVKO;st …SO_2 and MVKO;sc …SO_2 van der Waals complexes. The entrance channel flux is obtained from the MP2/cc-pVTZ VRC-TST calculations, while the flux for the other channels are obtained from the T(Q) corrected CCSD(T)/CBS//B2PLYP-D3/cc-pVTZ analysis employing rigid-rotor harmonic oscillator (RRHO) treatments for all but the CH_3 rotors, which are treated as one-dimensional hindered rotors.

The AITSTME predictions for the SO_2 + MVK-oxide rate coefficients are illustrated in Figures S7 (a) and (b) for the *syn,trans*- and *syn,cis*- forms of MVK-oxide, respectively. As noted in the main text, the total rate coefficient is predicted to be effectively pressure-independent, with no back reaction from the SOZ to the reactants. However, there is predicted to be a fairly strong temperature-dependence due to the effect of the TS connecting the van der Waals complexes and the SOZ. The total rate coefficients for the *syn,trans*- and *syn,cis*- forms are well reproduced by the expressions $2.3 \times 10^9 \ T^{-7.28} \exp(-1031/T)$ and $2.5 \times 10^{10} \ T^{-7.50} \exp(-1202/T)$ cm^3 s^{-1} for temperatures ranging from 200 to 400 K. At 300 K the *syn,trans*- and *syn,cis*- rates coefficients are predicted to be 6.5×10^{-11} and 1.2×10^{-10} cm^3 s^{-1}, respectively.

The total rate coefficient predicted for the *syn,trans* isomer is a factor of 1.7 larger than the value observed experimentally for the thermal average (3.9×10^{-11} cm^3 s^{-1}). This modest overprediction may indicate either the need for a variational treatment of the TS from the van der Waals complex to SOZ, or shortcomings in the electronic energies of that saddle point. The former may be quite significant because the submerged nature of the saddle point implies that the variational deviation from the saddle point can

be quite significant even at low temperature. Furthermore, this TS effectively corresponds to that for an addition process, which commonly have significant variational effects. Meanwhile, a simple increase by 0.5 kcal mol^{-1} for each of the saddle point energies (roughly the expected uncertainty) for the TSs connecting the van der Waals complexes to the SOZ reduces the predicted *syn,trans* rate coefficient to 4.6 × 10^{-11} cm^3 s^{-1} at room temperature and 1 atm. Further explorations of the reason for this modest overprediction are left for future work.

The decreased stability reduces the possibility for stabilization of the SOZ prior to decomposition to SO$_3$, whilst the additional vibrational degrees of freedom increases it. Nevertheless, for pressures below 1 atm the branching to stabilized SOZ is predicted to be negligible, while by 10 atm the stabilization amounts to ~50% of the overall reaction. Ambiguity in the energy transfer parameters suggests that even at 1 atm there may be some stabilization of the SOZ.

(a)   **(b)**
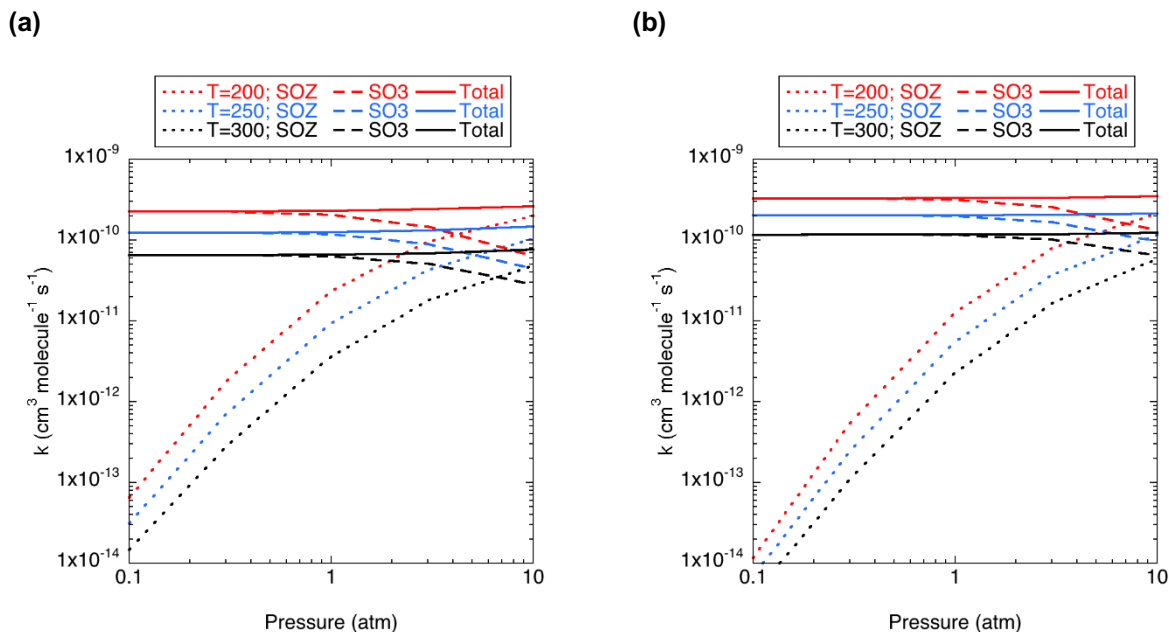
Fig. S7. The predicted temperature- and pressure-dependencies of the total rate coefficient, the rate coefficient to form any of the SOZ, and the rate coefficient to form SO$_3$ + MVK for the reaction of (a) *syn-trans*-MVK-oxide with SO$_2$ and (b) *syn-cis*-MVK-oxide with SO$_2$.

3.3 MVK-oxide + formic acid.

Ionization energy calculations of the reaction product. A variety of theoretical calculations were performed to complement the experimental observations of the ionization of the MVK-oxide + formic acid reaction product. These analyses included density functional theory (DFT) based conformational analyses of $C_5H_8O_4$, CCSD(T) based calculations of the vertical ionization energies for the different conformers, DFT evaluations of the relaxation energies for the vertically excited ions (and thus adiabatic ionization energies), a DFT mapping of an ion dissociation path, and a CCSD(T) based calculation of the daughter appearance energy for the ground conformer.

In analogy with calculations for the CH_2OO + formic acid reaction, the reaction product was presumed to be 2-hydroperoxybut-3-en-2-yl formate ($CH_2CHC(CH_3)OCHO$, HPBF), as shown in Scheme 5 of the main text (44). The low energy conformers of this species were determined through random sampling of 200 sets of the 6 torsional angles followed by ωB97XD/6-31+G* (45) geometry optimizations for each starting geometry. This optimization was performed in two steps, with first just the torsional angles optimized, and then the full set of internal coordinates optimized. The resulting set of 9 conformers that had energies within 3.5 kcal mol^{-1} of the ground state conformer were then reoptimized at the B2PLYP-D3/cc-pVTZ level (46). The vertical ionization energies for the set of 9 conformers with energies within 3 kcal mol^{-1} of the ground state were evaluated as the sum: CCSD(T)-F12b/cc-pVDZ-F12 + MP2-F12/cc-pVTZ-F12 – MP2-F12/cc-pVDZ-F12, which is meant to approximate the CCSD(T)-F12b/cc-pVTZ-F12//B2PLYP-D3/cc-pVTZ level (47). These values are reported in Table S6. For the ground conformer, the appearance energy for the daughter ion (obtained by simply pulling off the HO_2 and then allowing the $C_5H_7O_2^+$ structure to relax) is predicted to be 9.82 eV using the methodology above to approximate the CCSD(T)-F12b/cc-pVTZ-F12//B2PLYP-D3/cc-pVTZ level of theory.

Table S6. Energies of relevance to the ionization of HPBF.

HPBF conformer	Conformer energy (kcal mol^{-1})[a]	Vertical excitation (eV)[b]	Relaxation energy (kcal mol^{-1})
1	0.0	10.41 (10.70)	33.1
2	0.6	10.37 (10.80)	31.5
3	1.0	10.31 (10.47)	29.6
4	1.7	10.48 (10.71)	36.1
5	2.2	10.13 (10.39)	54.5
6	3.	10.10	35.9
7	3.1	10.52	42.6
8	3.1	10.76	48.4
9	3.2	10.14	36.8

[a]B2PLYP-D3/cc-pVTZ calculated zero-point corrected energy of the given conformer relative to the ground conformer.
[b]B2PLYP-D3/cc-pVTZ and approximate CCSD(T)-F12b/cc-pVTZ-F12 vertical electronic excitation energies for the given conformer. The latter energies are given in parentheses, and were obtained from the sum: CCSD(T)-F12b/cc-pVDZ-F12 + MP2-F12/cc-pVTZ-F12 – MP2-F12/cc-pVDZ-F12, all evaluated at the B2PLYP-D3/cc-pVTZ geometries.
[c]B2PLYP-D3/cc-pVTZ calculated relaxation energies for the parent cation (from the vertically excited geometry to the optimized geometry).

The relaxation of the HPBF$^+$ ions was explored for each of the 9 lowest neutral conformers through B2PLYP-D3/cc-pVTZ optimizations of the ion initiated at the neutral geometry. In each case the calculated relaxation energy exceeds 29 kcal mol^{-1} and the relaxation involves substantial geometrical transformations. For the ground state, the relaxation energy is 33 kcal mol^{-1}. For such large relaxations, adiabatic ionization will have very poor Franck-Condon overlaps resulting in low experimental signals at the adiabatic threshold. Instead, the ionization process is likely to be dominated by nearly vertical transitions.

Notably, the vertical ionization states have energies that substantially exceed the threshold for C-O fission to produce HO_2 + $CH_2CHC(CH_3)OCHO^+$. A schematic plot of the minimum energy path for dissociation of one conformer of the HPBF$^+$ ions is provided in Figure S8. This minimum energy path was mapped through constrained optimizations (with the CO distance fixed) at the ωB97XD/6-31+G* level. For this conformer, the daughter ion is 16 kcal mol^{-1} below the vertical excitation energy. Furthermore, CO fission

from the adiabatic minimum requires only 13 kcal mol^{-1}, suggesting that the dissociation of that parent ion should be rapid. At the B2PLYP-D3/cc-pVTZ level the HPBF$^+$ vertical excitation states for the 9 lowest conformers range from 17 to 33 kcal mol^{-1} higher than the ground state of HO$_2$ + CH$_2$CHC(CH$_3$)OCHO$^+$. Thus, it is expected that the ionization process will directly produce CH$_2$CHC(CH$_3$)OCHO$^+$ (HO$_2$-loss) daughter ions, as is observed experimentally (Figure 5, main text). The correlation between the energy of the observed rise in the daughter ion signal and the calculated vertical ionization energies further suggests that the ionization process primarily involves nearly vertical transitions.
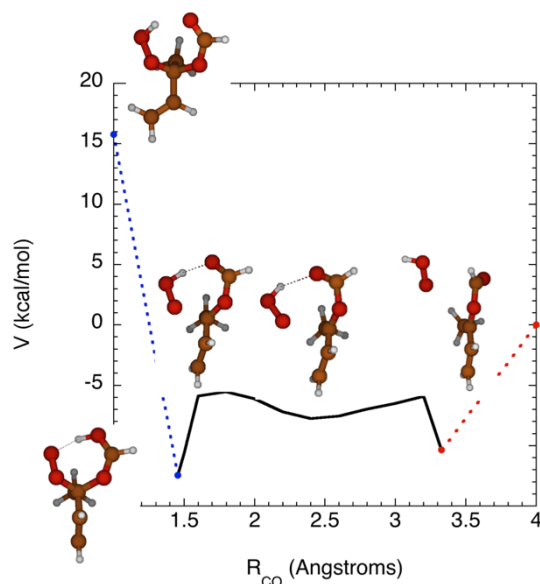
Fig. S8. Schematic plot of the process from vertical excitation of HPBF$^+$ through to CO fission to product HO$_2$ + CH$_2$CHC(CH$_3$)OCHO$^+$.

Kinetics calculations of MVK-oxide + formic acid. For the reaction of MVK-oxide with formic acid, it is interesting to ponder why the experimentally observed rate coefficient is so large and yet not quite as large as what one would predict on the basis of long-range capture theory. Understanding this behavior has important ramifications for the expected temperature- and pressure-dependencies of the rate coefficient. One possibility is that this reduction from the long-range capture rate is indicative of the effect of entropic loss in the transition state for formation of the initial chemically bound complex. In this case, one would expect the rate coefficient to be nearly independent of temperature and pressure. Alternatively, the reduction may arise from redissociation of the initial formed complex back to reactants. This would culminate in significant temperature- and pressure-dependencies. To interrogate these possibilities, we must examine in detail both the overall reaction pathway as well as the minimum energy path potential for the initial formation of the complex.

There are a variety of possible reaction channels for the reaction of formic acid with CIs, as discussed, for example, in a recent study by Vereecken (44), where the reaction of CH$_2$OO with formic acid was considered in detail. Vereecken found that the primary reaction pathway involves H-transfer from the acid to the CI in concert with CO bond formation, followed by stabilization of the resulting functionalized hydroperoxide, hydroperoxymethyl formate (HPMF). Notably, even though there are exothermic exit channels arising from OO bond fission of the complex, stabilization was predicted to dominate over bimolecular product formation. Addition over the C=O bond to form a cyclic ozonide was found to have a submerged barrier, however, the TS for this pathway was very tight, and the corresponding addition rate was predicted to be quite small (~ 10^{-13} cm^3 s^{-1}). By contrast, *ab initio* variational TST calculations predicted the pathway to form the functionalized hydroperoxide has a rate coefficient of 1.0 × 10^{-10} cm^3 s^{-1} - in excellent accord with the experimentally observed value of 1.1 × 10^{-10} cm^3 s^{-1} (25).

For the reaction of MVK-oxide with formic acid we restricted our attention to the analogue of Vereecken's predicted primary reaction pathway for CH$_2$OO based on the previous work described above. We find that, notably, the resonance stabilization in MVK-oxide leads to a significant destabilization of the

functionalized hydroperoxide pathway relative to reactants. A schematic illustration of the CCSD(T)-F12/cc-pVTZ-F12//B2PLYPD3/cc-pVTZ predicted reaction path energies is shown in the main text (Figure 6) and the corresponding energies are provided in Table S7.

The initial approach along the reaction co-ordinate leads to a planar van der Waals complex, which is a minimum at some levels of theory and a saddle point at others (see Table S7). Proceeding on from there leads to a clear long-range minimum followed by a well-defined (imaginary frequency of 598 cm^{-1}), but strongly submerged, saddle point that separates the global long-range minimum from the functionalized hydroperoxide product, HPBF. As discussed in the main text, HPBF is much more weakly bound than in its CH_2OO analogue (30 vs. 44 kcal mol^{-1} (44)), due to the additional resonance stabilization present in MVK-oxide. Correspondingly, the OO fission pathway of HPBF to produce OH + an alkoxy radical is now significantly endothermic relative to initial reactants. Nevertheless, as discussed below, the overall kinetics is predicted to be quite similar, with the reaction dominated by direct addition to form the functionalized hydroperoxide species.

Table S7. Reaction path energies for the reaction of *syn-trans*-MVK-oxide with formic acid.[a]

Species	R_{CO} (Å)	B2PLYP-D3[b] TZ	E0[c] B2/TZ	CCSD(T)-F12[d] cc-pVTZ-F12	Total[e]	T1[f]
syn-trans + OCHOH	-	0.0	0.0	0.0	0.0	-
syn-trans…OCHOH (long-range C$_s$)	5.68	-11.7	0.9	-10.8	-9.9	0.027
syn-trans…OCHOH (short-range C$_1$)	2.89	-17.0	1.1	-15.8	-14.7	0.024
syn-trans…OCHOH= vinyl hydroperoxideHPBF	2.26	-14.5	-0.9	-12.6	-13.5	0.020
HPBF	1.48	-30.8	2.8	-33.0	-30.3	0.015
alkoxy + OH	-	17.7	-2.7	16.6	13.4	0.019

[a] All energies are in kcal mol^{-1} relative to *syn-trans*-MVK-oxide + formic acid.
[b] Stationary point electronic energy from B2PLYP-D3//cc-pVTZ calculations.
[c] Zero-point energy (ZPE) from B2PLYP-D3//cc-pVTZ calculations.
[d] CCSD(T)-F12b/cc-pVTZ-F12 B2PLYP-D3/cc-pVTZ electronic energies.
[e] Sum of CCSD(T)-F12b/cc-pVTZ-F12// B2PLYP-D3/cc-pVTZ energies and B2PLYP-D3/cc-pVTZ ZPEs.
[f] T1 diagnostic for the CCSD(T)-F12b/cc-pVTZ-F12// B2PLYP-D3/cc-pVTZ calculations.

There are now three distinct regions of the potential energy surface that may provide the kinetic bottleneck for the addition process, as illustrated in Figure S9. The longer-range portion of the MEP (labelled A in Figure S9) was derived from the minimum center-of-mass constrained sampling of random orientations of the two reactants. The two shorter ranged portions (B and C in Figure S9) of the MEPs were derived from reaction path following initiated at the larger of the separations on that portion of the curve. At low temperatures, the longest ranged portion (A in Figure S9) of the curve provides the greatest bottleneck, while at higher temperatures the saddle point region (C in Figure S9), which occurs at a CO separation of 2.27 Å, should provide the dominant bottleneck due to its lower entropy. However, the deeply submerged nature of this saddle point (i.e., with a ZPE corrected energy of -13.5 kcal mol^{-1}) suggests that this bottleneck may only become important at quite high temperature. The intermediate regime (B in Figure S9) may also provide an important bottleneck at intermediate temperatures.
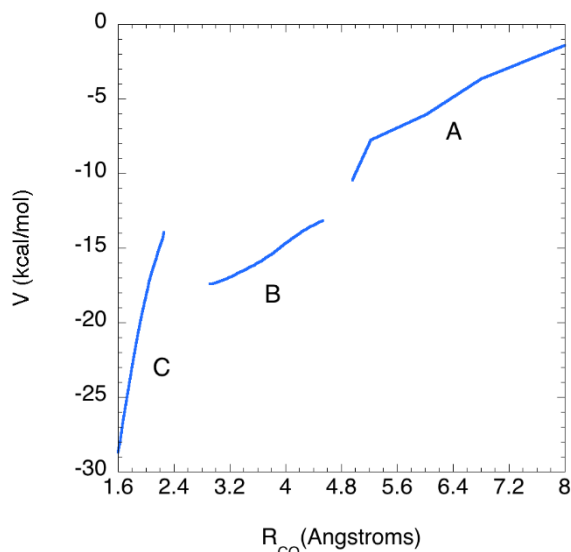
Fig. S9. The ωB97XD/6-31+G* calculated minimum energy path (MEP) for the addition of formic acid to the syn-trans form of MVK-oxide. The three disjoint curves correspond to physically distinct aspects of the addition process.

We have used direct sampling *ab initio* variable reaction coordinate transition state theory to explore the effect of the long-range bottleneck on the addition kinetics. For this VRC-TST analysis, we considered four separate electronic structure methods (MP2/cc-pVDZ, MP2/cc-pVTZ, ωB97XD/6-31+G*, and ωB97XD/cc-pVTZ) finding only modest variation (~10% near room temperature) in the predicted long-range capture rate coefficient, as illustrated in Figure S10. For these calculations, the reaction coordinate was presumed to be defined by the separation between the two centers-of-mass of the two fragments and the separation was constrained to 4.2 Å and larger. A dynamical correction factor of 0.85, based on reference comparisons of trajectories and TST (43), is also included.
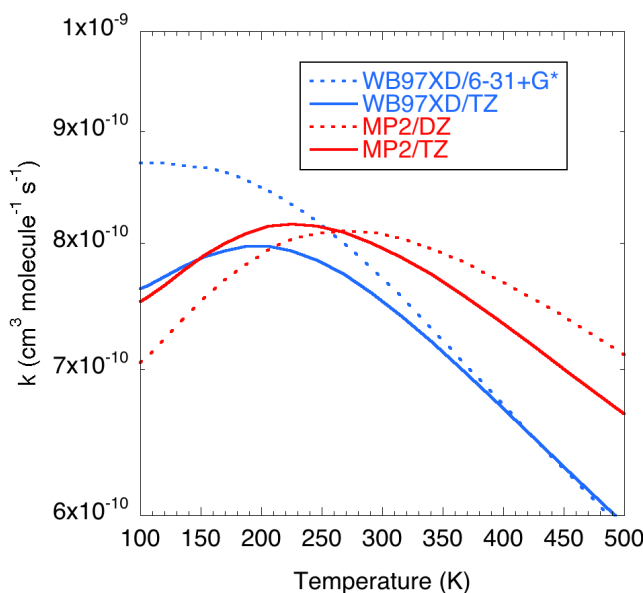
Fig. S10. Temperature-dependence of the predicted VRC-TST rate coefficients for capture to form the van der Waals complex, calculated using four different levels of theory.

Notably, the predicted room-temperature long-range capture rate coefficient of ~8 × 10^{-10} cm^3 s^{-1} is considerably greater than what might be expected on the basis of dipole-dipole capture theory. This is likely due to additional contributions from dispersion interactions. Furthermore, this value is about 3 times larger than that observed experimentally ((3.0 ± 0.1) × 10^{-10} cm^3 s^{-1}). Related calculations for addition to *syn-cis*-MVK-oxide yield essentially identical predictions for the capture rate (i.e., differing by 10% or less).

From our experience, we would expect uncertainties in the VRC-TST predictions to be on the order of 10-20%. Thus, the apparent overprediction of the rate coefficient suggests that some other bottleneck is operative. The effect of the two inner transition state regions (B and C in Figure S9) were included here through microcanonical (E-resolved) variational TST implementing ωB97XD/6-31+G* based evaluations of the minimum energy path properties coupled with CCSD(T)-F12/cc-pVTZ-F12 evaluation of the energy for the starting point on the path. For simplicity, the vibrational modes were all treated as harmonic oscillators, aside from the CH_3 rotor, which was treated as a 1-dimensional hindered rotor in both the reactants and the transition. The inclusion of such variational TST treatments for the two separate inner bottlenecks leads to only a modest reduction in the predicted formation rate coefficient for HPBF. For example, at 300 K the predicted recombination rate coefficient at 10 bar is now 5.0 × 10^{-10} cm^3 s^{-1}. Although, there is considerably greater uncertainty in our estimate of the effect of these inner transition state regions, it still appears that there must be another bottleneck to HPBF formation. One possibility is that there is substantial back dissociation of the initially formed HPBF. To explore this issue, we have implemented an *ab initio* transition state theory-based master equation model for the overall kinetic process. This master equation model employs standard exponential down energy transfer probabilities with a temperature dependent expression for the average downwards energy transferred given by < ΔE_{down}> = 300 $(T/298)^{0.85}$ cm^{-1}, and Lennard-Jones collision rate appropriate for N_2. For HPBF, we have optimized 100 randomly sampled sets of torsional angles to estimate the lowest torsional conformer, and then performed one-dimensional mappings of the 6 hindered rotor modes. The resultant master equation-based predictions for the temperature- and pressure-dependencies of the recombination rate coefficient are shown in Figure 7 of the main text and the results discussed therein.

3.4 MVK-oxide + water monomer.

Ab initio calculations, computational kinetics and mechanistic investigations. For the reaction of MVK-oxide with water, the present experimental analysis is only able to obtain an upper bound to the rate coefficient. Thus, it is interesting to consider what theory predicts for the actual rate coefficient for this reaction. This reaction has been the subject of previous theoretical studies by Anglada and coworkers (27, 48, 49), Kuwata *et al.* (50) and Vereecken *et al.* (28) (based on the results of Anglada and Solé (27)) . The recent study of Anglada and Solé (27) was based on CCSD(T)/aug-cc-pVTZ//B3LYP/6-311++G(2df,2p) energetic analyses, while that of Kuwata *et al.* employed MCG3///QCISD/6-31G* energies. A recent survey by Vereecken *et al.* (28) suggested that the rates predicted by Anglada and Solé should be reduced by a factor of 7.1 on the basis of comparisons of related calculations for $CH_3CHOO + H_2O$. This rate reduction was correlated with an increase in the barrier height by 1.16 kcal mol^{-1}, which apparently was needed due to the lack of post-CCSD(T) calculations.

Here, we proceed beyond these earlier works with higher level calculations of the energies. We also explore the role of one additional form of H_2O-catalysis, where the water molecule is simply a spectator molecule that lowers the isomerization barriers relative to isolated MVK-oxide + H_2O. For example, this spectator catalysis can enhance the rate of the internal H-transfer from MVK-oxide to form a vinyl hydroperoxide-type species. It also catalyzes the transformation from the *cis* to *trans* forms of MVK-oxide. The present *ab initio* evaluations begin with a B2PLYP-D3/cc-pVTZ density functional-based analysis of the rovibrational properties of the stationary points. Our prior kinetic analyses of CI isomerization reactions have indicated good performance for this double-hybrid functional. At these geometries, we determine CCSD(T)/CBS limit energies from CCSD(T)-F12 calculations for the cc-pVTZ-F12 and cc-pVQZ-F12 basis sets. We also evaluate CCSDT(Q)/6-31G* corrections for high order excitations, core-valence corrections from the CBS limit of CCSD(T) for the cc-pcVTZ and cc-pcVQZ bases, and anharmonicity corrections evaluated with B2PLYP-D3/cc-pVTZ based vibrational perturbation theory. For validation purposes, we also perform a closely related analysis for the reaction of CH_2OO with H_2O.

An initial study of $CH_2OO + H_2O$ provides some validation for the present approach for MVK-oxide + H_2O. Various components of the stationary point energies for $CH_2OO + H_2O$ are provided in Table S8. The 0.1 kcal mol^{-1} difference in the T(Q) correction for the 6-31G* and cc-pVDZ bases provides some indication of the basis set dependence of this correction. For the MVK-oxide + H_2O reaction our computational resources constrain us to the 6-31G* basis set. Notably, the differences between the deviations in the B2PLYP-D3 and CCSD(T) calculated ZPEs decrease quite substantially with increasing basis set. Nevertheless, at the complete basis set (CBS) limit the two values likely still differ by about 0.2 kcal mol^{-1} for the TS. This difference may simply be a result of the significant multireference effects in CH_2OO, which can yield different errors in the B2PLYP-D3 and CCSD(T) estimates. It is not clear *a priori* which is correct. Overall, it seems reasonable to expect high accuracy for the present scheme, with overall uncertainties of ~ 0.3 kcal mol^{-1} (51).

Table S8. Stationary Point Energies (kcal mol^{-1}) for $CH_2OO + H_2O$.[a]

Species	CCSD(T)-F12b			T(Q) Corr.	Core Val.		ZPE Harm.		ZPE Anh.	Total[b]
	DZ-F12	TZ-F12	QZ-F12	6-31G*	DZ	CBS	B2TZ	CCSD(T)DZ,TZ	B2TZ	
$CH_2OO + H_2O$	0.0	0.0	0.0	0.0	0.00	0.0	0.0	0.0	0.0	0.0
$CH_2OO…H_2O$	-8.34	-8.41	-8.40	0.26	0.14	0.00	2.28	2.61,2.39	-0.14	-6.11 (-6.27)
TS; tau a	-0.03	-0.18	-0.22	0.81	0.72	0.25	2.78	3.35,3.14	-0.39	3.12 (3.48)
TS; tau b	0.92	0.76	0.73	0.82	0.73	0.25	2.70	3.23,3.06	-0.43	3.97 (4.35)
$OHCH_2OOH$	-47.62	-47.65	-47.73	1.47	1.43	0.11	5.27	5.73,5.60	-0.13	-41.09 (-40.93)

[a] All energies are relative to $CH_2OO + H_2O$. Aside from the CCSD(T) ZPE calculations all energies were evaluated at the B2PLYPD3/cc-pVTZ geometries.
[b] The total zero-point corrected energy from CCSD(T)-F12b/CBS + T(Q)/DZ correction + Core Valence correction + anharmonic ZPE(B2PLYPD3/cc-pVTZ). The numbers in parentheses are the W3X-L//QCISD/TZ calculations from Long *et al.* (52).

Long *et al.* (52) also examined the $CH_2OO + H_2O$ reaction in detail, finding similar results to the present work, but with 0.4 kcal mol^{-1} higher saddle point energies. The higher barriers predicted by Long *et al.* appear to arise primarily from their use of a scaling-based relation to treat the anharmonic ZPE, in contrast with the explicit spectroscopic perturbation theory evaluations performed herein. The method used by Long *et al.* limits the ZPE change from reactants to TS to fairly small numbers due to the cancellation in TS and reactant effects. Additionally, the present analysis also employs a somewhat more direct treatment of the higher order excitations and improved treatment of other aspects such as the geometries and frequencies.

Ab initio transition state theory calculations utilizing these energies combined with an Eckart tunneling model and rigid rotor harmonic oscillator state counts (employing the anharmonic fundamental frequencies) yield a predicted room temperature rate coefficient of 4.4×10^{-16} cm^3 s^{-1} for the $CH_2OO + H_2O$ reaction. For comparison, the most recent experimental measurement of $(3.2 \pm 1.2) \times 10^{-16}$ cm^3 s^{-1} (53) falls more or less midway between the present prediction and that of Long *et al.* $(2.4 \times 10^{-16}$ cm^3 $s^{-1})$, with the experimental error bars encompassing both theoretical predictions. Notably, the primary cause for the variation in the theoretical results appears to be the difference in the predicted barrier heights, with a 0.4 kcal mol^{-1} room temperature Boltzmann factor essentially identical to the ratio of the two predictions. It is perhaps worth noting that, due to the relatively low tunneling frequency ($\sim$ 500 cm^{-1}), tunneling has only a modest effect on the rate predictions; simply removing tunneling lowers our rate prediction by only 20%, while reducing the tunneling frequency by 20% only lowers the rate coefficient by 8%. Thus, the physically more meaningful small curvature tunneling treatment of Long *et al.* is unlikely to have much bearing on the discrepancy in the rate predictions.

Prior work has examined four separate types of TSs for the reaction of MVK-oxide + H_2O (27, 48-50). The primary transition state involves OH-insertion across COO. Here, this insertion was studied for both *exo* and *endo* orientations and for all 4 conformers of MVK-oxide. Another key transition state involves direct catalysis of the H-transfer from the CH_3 group to the terminal O via a bridging H_2O. Although the barriers for this pathway are considerably larger, the imaginary frequency is also much larger, which dramatically increases the tunneling rate (54). In the end, the rates for the two pathways are fairly comparable. A pathway involving OH-insertion across the CH_2CHCOO group has barriers that are of similar magnitude to those for the H_2O-catalyzed H-transfer from CH_3 to O. Finally, the barriers for an H_2O-catalyzed H transfer from the CH group to the terminal O were found to be too high for this pathway to be relevant. The present calculations of these stationary point energies for the reaction of all four isomers of MVK-oxide with H_2O are reported in Table S9. Then, in Table S10 we report the stationary point energies for a few of the spectator H_2O processes, again for all four isomers. For simplicity, the latter calculations focus on spectator catalysis related to the *trans* to *cis* isomerization process and the CI to vinyl hydroperoxide isomerization in the *syn* conformers. These processes are chosen due to their direct relevance to the present discussion, although others, such as a catalysis of the decomposition of the anti-forms may also be occurring.

A schematic plot of the key reaction pathways for the *syn-trans* conformer is provided in Figure S11. Notably, although the pathway for formation of the $C_2H_3C(OH)(CH_3)OOH$ species has the lowest barriers, the imaginary frequencies for the direct and spectator-catalyzed pathways to the $C_2H_3C(CH_2)OOH + H_2O$ products are about twice as large. Thus, it is not clear which pathway will contribute most to the kinetics.

Table S9. Stationary point energies (kcal mol^{-1}) for MVK-oxide + H_2O. All energies are relative to the *syn-trans* conformer of MVK-oxide + H_2O.

Species	Label	CCSD(T)-F12b			T(Q) Corr.	Core Val.	E0	Anh.	Total
		DZ-F12	TZ-F12	CBS	6-31G*	CBS	B2/TZ	B2/TZ	
syn-trans	1a	0.0	0.0	0.0	0.0	0.0	0.0	0.0	0.0
syn-trans…H_2O	2a	-8.82	-8.89	-8.92	0.39	-0.01	2.09	-0.07	-6.52
2a = 3a		7.22	7.16	7.12	0.93	0.23	1.10	-0.42	8.97
VHPOH;*trans*	3a	-32.55	-32.44	-32.38	1.60	0.13	3.99	-0.10	-26.76
2a = 3a'		8.76	8.70	8.67	0.96	0.23	1.11	-0.43	10.53
VHPOH;*trans'*	3a'	-32.36	-32.23	-32.17	1.60	0.13	3.88	-0.09	-26.64
2a = 4a		13.08	12.86	12.75	0.82	-0.01	-1.64	0.24	12.16
VHP;*trans*…H_2O	4a	-20.76	-20.61	-20.54	1.31	-0.09	2.26	-0.09	-17.21
2a = 4a'		12.85	12.63	12.51	0.83	-0.01	-1.60	0.21	11.94
VHP;*trans*…H_2O	4a'	-21.18	-21.03	-20.95	1.31	-0.09	2.30	-0.22	-17.66
syn-cis	1b	1.93	1.94	1.94	0.04	0.0	-0.19	0.00	1.79
syn-cis…H_2O	2b	-6.96	-7.02	-7.05	0.48	-0.01	1.88	-0.09	-4.79
2b = 3b		7.44	7.39	7.37	1.00	0.23	1.21	-0.64	9.17
VHPOH;*cis*	3b	-33.24	-33.15	-33.11	1.64	0.11	3.99	-0.10	-27.40
2b = 3a'		9.04	8.99	8.97	1.00	0.23	0.97	-0.45	10.72
VHPOH;*trans'*	3a'	-32.36	-32.23	-32.17	1.60	0.13	3.88	-0.09	-26.64
2b = 4b		13.36	13.14	13.03	0.87	-0.02	-1.61	0.05	12.32
VHP;*cis*…H_2O	4b	-22.66	-22.53	-22.47	1.32	-0.10	2.36	-0.18	-19.06
2b = 4b'		13.14	12.91	12.80	0.88	-0.02	-1.54	-0.04	12.07
VHP;*cis*…H_2O'	4b'	-23.30	-23.16	-23.09	1.32	-0.10	2.46	-0.27	-19.68
anti-trans	1c	2.70	2.72	2.74	-0.03	0.01	-0.10	-0.03	2.60
anti-trans…H_2O	2c	-6.26	-6.28	-6.29	0.47	0.02	2.00	-0.17	-3.96
2c = 3c		7.97	7.92	7.89	0.93	0.23	0.96	-0.51	9.50
VHPOH;*trans*	3c	-32.21	-32.10	-34.76	1.62	0.12	3.98	-0.07	-26.38
2c = 3c'		7.43	7.35	7.32	0.90	0.22	1.04	-0.66	8.81
VHPOH;*trans'*	3c'	-34.20	-34.11	-34.06	1.64	0.11	3.92	-0.15	-28.54
2c = 5c		24.19	24.02	23.94			-2.30	0.04	21.68
AHP…H_2O	5c								-6.91
2c = 5c'		23.82	23.65	23.57			-2.30	0.02	21.29
AHP;*tau'*…H_2O	5c'								-6.61
anti-cis	1d	2.84	2.79	2.78	0.21	0.05	0.03	-0.01	3.06
anti-cis…H_2O	2d	-5.06	-5.15	-5.19	0.56	0.05	2.00	-0.30	-2.88
2d = 3d		9.31	9.24	9.20	1.03	0.24	1.00	-0.61	10.86
VHPOH;*cis*	3d	-32.71	-32.61	-32.57	1.63	0.12	3.97	-0.14	-26.98
2d = 3d'		9.52	9.43	9.38	1.00	0.24	0.97	-0.60	11.00
VHPOH;*cis'*	3d'	-33.63	-33.53	-33.48	1.63	0.11	3.98	-0.07	-27.83
2d = 6d		9.53	9.32	9.22	0.71	0.21	2.17	-0.57	11.74
VHPOH'	6d	-27.34	-27.31	-27.30	1.48	0.04	5.27	-0.15	-20.65
2d = 6d'		9.90	9.70	9.59	0.74	0.21	1.84	-0.73	11.65
VHPOH';*tau'*	6d'	-25.97	-25.92	-25.90	1.49	0.04	5.16	-0.18	-19.39

Table S10. Stationary point energies (kcal mol⁻¹) describing effect of spectator H_2O on MVK-oxide transformations. All energies are relative to the *syn-trans* conformer of MVK-oxide + H_2O.

Species	Label	CCSD(T)-F12b			T(Q) Corr.	Core Val.	E0	Anh.	Total
		DZ-F12	TZ-F12	CBS	6-31G*	CBS	B2/TZ	B2/TZ	
syn-trans	1a	0.0	0.0	0.0	0.0	0.0	0.0	0.0	0.0
syn-trans…H_2O = *syn-cis*…H_2O	stcH$_2$O	-1.60	-1.58	-1.56	0.72	-0.00	1.47	-0.22	0.41
syn-trans…H_2O = *syn-cis*…H_2O	stcH$_2$O'	-2.07	-2.05	-2.04	0.73	0.00	1.55	-0.40	-0.17
syn-trans…H_2O = VHP…H_2O;a	stVHPH	13.78	13.73	13.70	0.79	0.02	-0.95	-0.23	13.33
syn-trans…H_2O = VHP…H_2O;a;gb	stVHPH'	12.89	12.79	12.74	0.80	0.02	-0.60	-0.11	12.86
VHP…H_2O;a	VHPHt	-16.95	-16.73	-16.62	1.30	-0.09	1.32	-0.14	-14.22
VHP…H_2O;a;gb	VHPHt'	-16.92	-16.74	-16.65	1.33	-0.08	1.50	-0.30	-14.19
syn-cis	1b	1.93	1.94	1.94	0.04	0.0	-0.19	0.0	1.79
syn-cis…H_2O = VHP…H_2O;b	scVHPH	14.69	14.62	14.58	0.85	0.03	-0.82	-0.09	14.55
syn-cis…H_2O = VHP…H_2O;b;gb	scVHPH'	14.10	13.99	13.93	0.83	0.01	-0.63	-0.24	13.89
VHP…H_2O;b	VHPHc	-18.99	-18.77	-18.67	1.33	-0.09	1.39	-0.10	-16.15
VHP…H_2O;b;gb	VHPHc'	-18.93	-18.78	-18.70	1.34	-0.09	1.63	-0.25	-16.07
anti-trans	1c	2.70	2.72	2.74	-0.03	0.01	-0.10	-0.03	2.60
anti-trans…H_2O = *anti-cis*…H_2O	atcH$_2$O	0.87	0.88	0.89	0.72	0.01	1.52	-0.18	2.97
anti-trans…H_2O = *anti-cis*…H_2O	atcH$_2$O'	1.25	1.29	1.30	0.72	0.01	1.34	-0.19	3.19

Predicted rate coefficients for the reaction of water with each of the conformer of MVK-oxide were obtained from AITSTME calculations implementing the energies in Table S9 and S10 together with an Eckart tunneling model, rigid rotor harmonic oscillator state counts employing the anharmonic fundamental frequencies, and one-dimensional torsional treatments for the methyl rotors. The predictions are not sensitive to the energy transfer parameters for the relevant region of temperature and pressure. They are also not sensitive to the rate for forming the van der Waals complexes. Thus, these parameters are not described here. Suffice it to say, that we use physically realistic values. The rate coefficients are obtained from two separate master equations: one treating the *syn-trans*- and *syn-cis*- conformers, and one treating the *anti-trans*- and *anti-cis*- conformers. For simplicity, we ignore the coupling of the *syn*- and *anti*- conformers, which we do not expect to be significant. The most significant shortcoming in this analysis is in the use of the Eckart model to predict the tunneling rates. This shortcoming may affect our predictions of which pathway is of greatest significance kinetically.
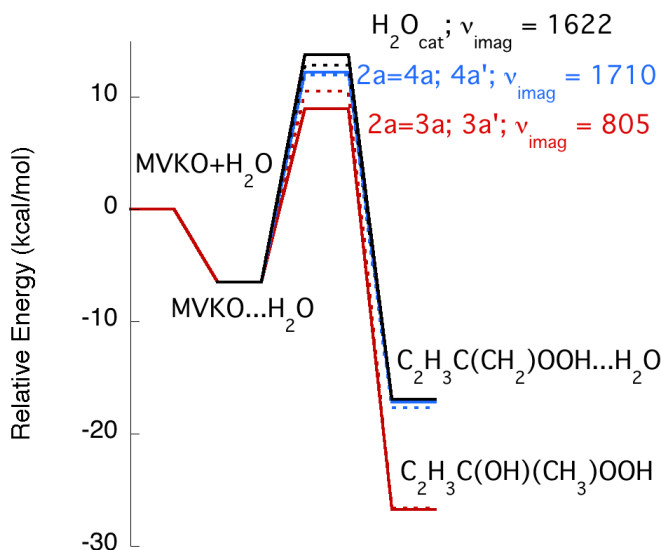
Fig. S11. Schematic plot of the reaction pathways for the reaction of H_2O with *syn-trans*-MVK-oxide (denoted MVKO here).

The AITSTME-predicted rate coefficients for the chemically significant reactions are summarized in Table S11. For simplicity, we do not report the rate coefficients for formation of the van der Waals wells, which are chemically irrelevant since the branching from those wells onto chemical products does not contribute significantly to the overall flux to chemical products. Similarly, we do not report the rate coefficients for isomerization between *cis* and *trans* conformers, since that process has already been calculated to happen rapidly enough to yield thermal distributions of the *cis* and *trans* conformers, as discussed in section 2 of the SI.

Table S11. Conformer-specific AITSTME predicted rate coefficients ($cm^3\ s^{-1}$) for the MVK-oxide + H_2O reaction.

Reactants\Products[a]	W2	P2	P3	W3	Total
Syn-trans	1.4×10^{-20}	9.3×10^{-21}	7.9×10^{-20}	-	1.0×10^{-19}
Syn-cis	1.2×10^{-19}	8.4×10^{-20}	4.2×10^{-20}	-	2.5×10^{-19}
Syn(thermal)	2.3×10^{-20}	1.5×10^{-20}	7.6×10^{-20}	-	1.1×10^{-19}
Anti-trans	1.1×10^{-18}	-	-	$<1 \times 10^{-23}$	1.1×10^{-18}
Anti-cis	2×10^{-19}	-	-	1.3×10^{-20}	2×10^{-19}
Anti(thermal)	8×10^{-19}	-	-	4.2×10^{-21}	8×10^{-19}

[a] W2 denotes $C_2H_3C(OH)(CH3)OOH$; P2 denotes $C_2H_3C(CH_2)OOH…H_2O$ via direct H_2O catalysis; P3 denotes $C_2H_3C(CH_2)OOH…H_2O$ via spectator H_2O catalysis; W3 denotes $C_2H_3C(OH)(CH3)OOH$ via the pathway leading to the 6d isomers in Table S10.

The total rate coefficient for the reaction of the thermal distribution of *syn-* conformers, *syn*(thermal), is predicted to be $1.1 \times 10^{-19}\ cm^3\ s^{-1}$, while that for the thermal distribution of *anti-* isomers, *anti*(thermal), is predicted to be $8 \times 10^{-19}\ cm^3\ s^{-1}$. Interestingly, for the *syn*(thermal) case, the spectator catalysis pathway has the largest contribution to the rate coefficient, but all pathways make a significant contribution. The rate coefficient determined in the present work is in accord with the previous work by Anglada and Solé ($3.4 \times 10^{-19}\ cm^3\ s^{-1}$) (27), and the adjusted value of Anglada and Solé by Vereecken *et al.* ($9.5 \times 10^{-20}\ cm^3\ s^{-1}$) (28), but the value obtained herein was achieved without empirical adjustment of the barrier height or other parameters.

4. Global chemical modelling evaluation of particulate formation from MVK-oxide + SO₂

The implications for the reaction of MVK-oxide with SO₂ on particle nucleation have been modelled with nucleation coefficients of 2 (55) and 1.5 (56) for H_2SO_4, and the results presented in Figures S12 and S13, respectively.
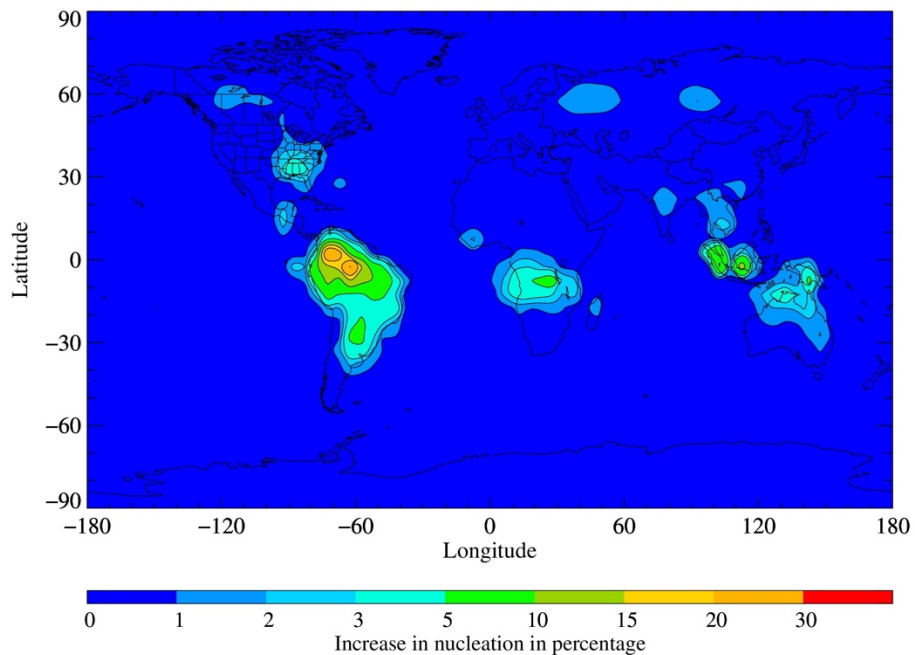
Fig. S12. The impact of the MVK-oxide reaction with SO₂ on particulate nucleation, using a nucleation coefficient for sulfuric acid of 2.
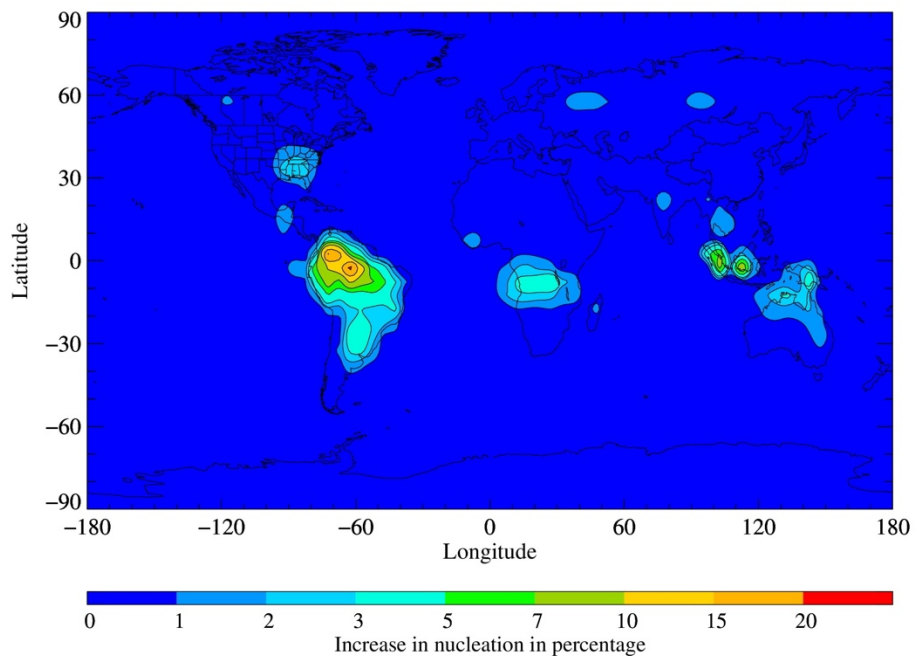
Fig. S13. The impact of the MVK-oxide reaction with SO₂ on particulate nucleation, using a nucleation coefficient for sulfuric acid of 1.5

27

5. *Ab initio* optimized geometries and frequencies
5.1 MVK-oxide.
Syn-trans

Relative energy = 0.0 kcal mol^{-1}
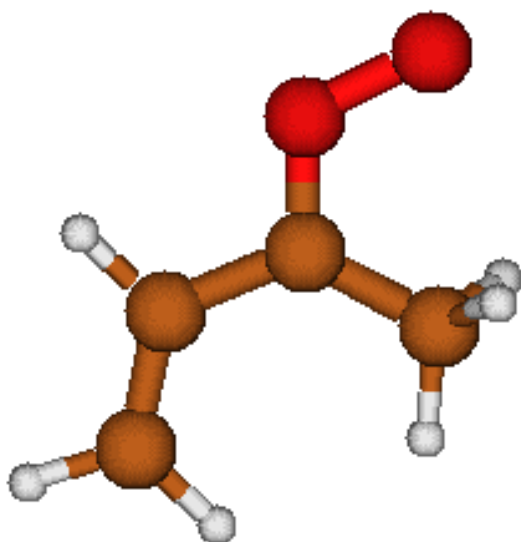
1	6	0	-0.281002	-2.428825	0.000000
2	6	0	0.489860	-1.332579	0.000000
3	6	0	0.000000	0.017627	0.000000
4	6	0	-1.397431	0.477385	0.000000
5	8	0	0.934365	0.910720	0.000000
6	8	0	0.561182	2.203583	0.000000
7	1	0	-1.359012	-2.376515	0.000000
8	1	0	0.163693	-3.411629	0.000000
9	1	0	1.567972	-1.424436	0.000000
10	1	0	-2.098829	-0.348501	0.000000
11	1	0	-1.553379	1.122502	0.866535
12	1	0	-1.553379	1.122502	-0.866535

Frequencies --	119.9147	198.1647	256.1167
Frequencies --	283.2193	331.6966	459.4209
Frequencies --	496.8539	609.8350	682.4911
Frequencies --	814.7146	950.8478	998.3597
Frequencies --	1026.7698	1041.7510	1047.8678
Frequencies --	1076.4570	1292.3767	1337.6406
Frequencies --	1400.1620	1449.9665	1453.0141
Frequencies --	1472.8403	1504.9644	1662.0030
Frequencies --	3052.6351	3097.5438	3178.5451
Frequencies --	3186.9118	3194.4379	3270.2727

Syn-cis
Relative energy = 3.05 kcal mol⁻¹
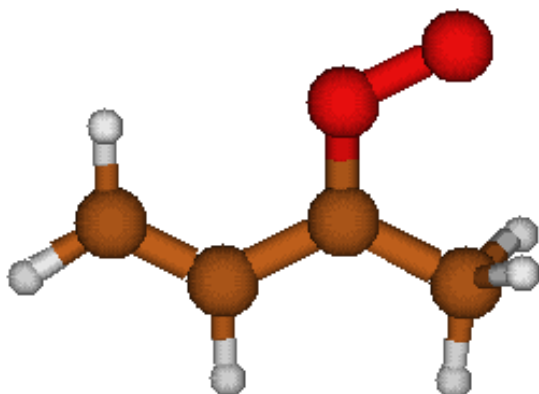
1	6	0	-2.181296	-0.839531	0.000000
2	6	0	-1.445765	0.279851	0.000000
3	6	0	0.000000	0.334288	0.000000
4	6	0	0.795556	1.572979	0.000000
5	8	0	0.625731	-0.789133	0.000000
6	8	0	1.976736	-0.749625	0.000000
7	1	0	-1.722960	-1.817168	0.000000
8	1	0	-3.258737	-0.787750	0.000000
9	1	0	-1.934488	1.244081	0.000000
10	1	0	0.161642	2.453346	0.000000
11	1	0	1.461921	1.566019	0.865256
12	1	0	1.461921	1.566019	-0.865256

Frequencies --	66.4658	206.2188	228.8220
Frequencies --	275.2111	327.6923	442.9534
Frequencies --	485.9721	623.2547	665.9256
Frequencies --	815.8805	971.1810	992.1262
Frequencies --	1024.2898	1041.0284	1044.4521
Frequencies --	1108.3087	1286.3487	1340.7090
Frequencies --	1397.3938	1418.9712	1451.4392
Frequencies --	1475.0005	1500.5024	1669.4449
Frequencies --	3044.5296	3088.3513	3171.9026
Frequencies --	3177.8055	3200.0465	3272.9201

Syn-trans=syn-cis
Relative energy = 7.97 kcal mol^{-1}
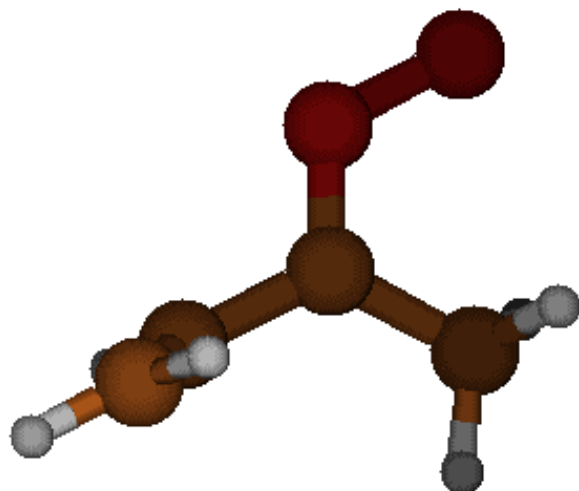
1	6	0	2.327858	-0.267919	0.425627
2	6	0	1.381300	-0.133215	-0.497496
3	6	0	-0.027092	0.153355	-0.167281
4	6	0	-0.602629	1.490867	0.045170
5	8	0	-0.796694	-0.864200	-0.093452
6	8	0	-2.103652	-0.635657	0.189406
7	1	0	2.105556	-0.189953	1.480296
8	1	0	3.351766	-0.466552	0.146356
9	1	0	1.626162	-0.217122	-1.550508
10	1	0	-1.070284	1.516480	1.033036
11	1	0	-1.432790	1.629417	-0.652467
12	1	0	0.145734	2.268058	-0.060451

Frequencies --	-155.8236	160.3454	206.9403
Frequencies --	272.9053	318.6863	393.4493
Frequencies --	519.1815	618.1650	677.8188
Frequencies --	801.6223	973.9469	989.5462
Frequencies --	996.7350	1008.2812	1048.2105
Frequencies --	1090.0645	1299.6607	1324.2466
Frequencies --	1397.9023	1440.7421	1448.6849
Frequencies --	1456.7181	1494.5998	1693.0250
Frequencies --	3035.8504	3076.2762	3155.4400
Frequencies --	3168.9422	3179.8447	3258.5054

Anti-trans
Relative energy = 2.57 kcal mol^{-1}
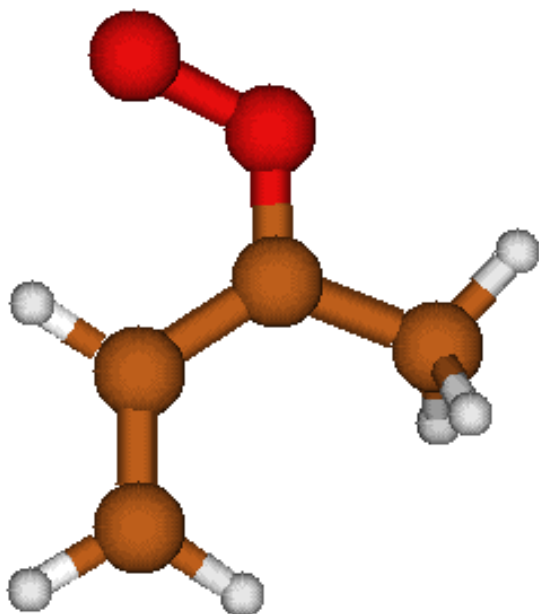
1	6	0	-1.894146	-1.185090	0.000000
2	6	0	-0.571837	-0.965527	0.000000
3	6	0	0.000000	0.349961	0.000000
4	6	0	-0.769734	1.622704	0.000000
5	8	0	1.282506	0.506388	0.000000
6	8	0	2.101575	-0.560185	0.000000
7	1	0	-2.612894	-0.378124	0.000000
8	1	0	-2.286939	-2.190359	0.000000
9	1	0	0.144815	-1.772424	0.000000
10	1	0	-0.083752	2.464487	0.000000
11	1	0	-1.409789	1.687253	0.880050
12	1	0	-1.409789	1.687253	-0.880050

Frequencies --	113.8309	150.9705	244.3138
Frequencies --	280.5671	326.0586	377.0466
Frequencies --	479.0748	640.2948	718.3130
Frequencies --	798.5875	977.2758	985.0386
Frequencies --	1021.2924	1049.6643	1057.6112
Frequencies --	1065.0237	1281.3674	1373.2418
Frequencies --	1391.3621	1436.2627	1469.0936
Frequencies --	1486.0836	1512.5356	1657.6094
Frequencies --	3054.8184	3111.1078	3162.1730
Frequencies --	3170.5660	3228.1091	3261.6980

Anti-cis
Relative energy = 3.05 kcal mol^{-1}
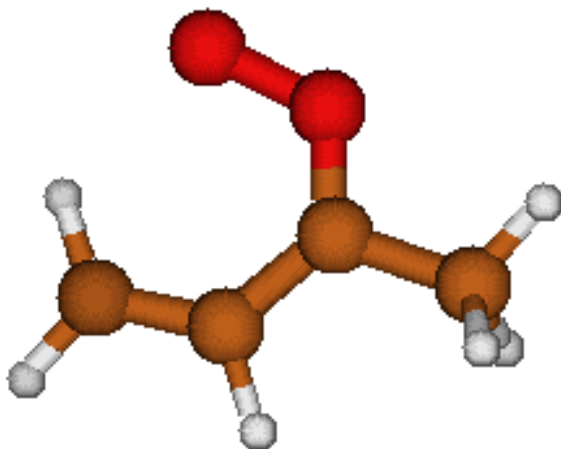
1	6	0	-1.352990	-1.521124	0.000000
2	6	0	-1.214381	-0.180848	0.000000
3	6	0	0.000000	0.576665	0.000000
4	6	0	-0.021963	2.069054	0.000000
5	8	0	1.191358	0.084982	0.000000
6	8	0	1.382201	-1.251687	0.000000
7	1	0	-0.494812	-2.166647	0.000000
8	1	0	-2.348757	-1.942692	0.000000
9	1	0	-2.104292	0.435798	0.000000
10	1	0	0.990778	2.459965	0.000000
11	1	0	-0.547687	2.442365	0.879064
12	1	0	-0.547687	2.442365	-0.879064

Frequencies --	116.7361	165.5085	285.0024
Frequencies --	305.2060	339.0183	368.0726
Frequencies --	411.2073	640.2272	717.5908
Frequencies --	823.6757	990.3387	1004.8285
Frequencies --	1029.1718	1053.3593	1054.9509
Frequencies --	1099.6379	1269.7395	1340.3444
Frequencies --	1418.9240	1438.3092	1463.9237
Frequencies --	1487.0283	1508.1717	1640.9833
Frequencies --	3054.6683	3110.9627	3165.1107
Frequencies --	3167.2660	3181.8932	3314.1293

Anti-trans=anti-cis
Relative energy = 11.25 kcal mol^{-1}
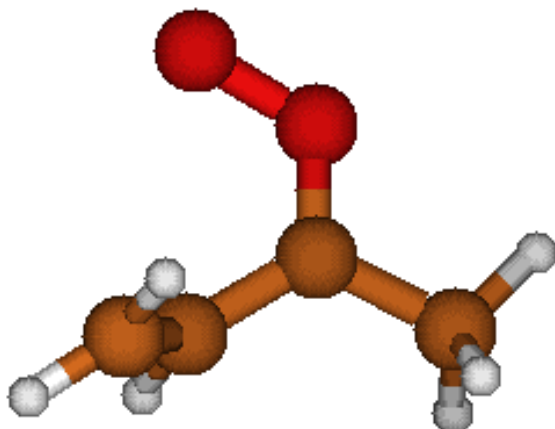
1	6	0	2.007829	-0.418699	-0.342971
2	6	0	0.984974	-0.461235	0.502459
3	6	0	-0.412755	-0.301218	0.080860
4	6	0	-1.331026	-1.454707	-0.099639
5	8	0	-0.925829	0.850993	-0.119854
6	8	0	-0.181649	1.963910	0.046691
7	1	0	1.863784	-0.218324	-1.394427
8	1	0	3.019565	-0.567451	0.002037
9	1	0	1.146198	-0.648731	1.558247
10	1	0	-2.328717	-1.110049	-0.356799
11	1	0	-1.377214	-2.045749	0.816530
12	1	0	-0.957925	-2.113760	-0.884538

Frequencies --	-172.4811	152.1270	208.0108
Frequencies --	231.6809	294.2586	330.2831
Frequencies --	521.8294	599.3025	696.2792
Frequencies --	802.6304	974.6524	982.0157
Frequencies --	993.4085	1013.3162	1031.6387
Frequencies --	1096.0715	1286.3799	1328.8923
Frequencies --	1414.9866	1434.1413	1473.1757
Frequencies --	1478.4513	1514.3980	1695.7927
Frequencies --	3046.9529	3100.6707	3156.9139
Frequencies --	3158.0516	3173.6061	3263.0241

5.2 MVK-oxide + H₂O.

All energies are relative to the *syn-trans* conformer of MVK-oxide + H_2O.

syn,trans…H₂O

Relative energy = -6.52 kcal mol^{-1}
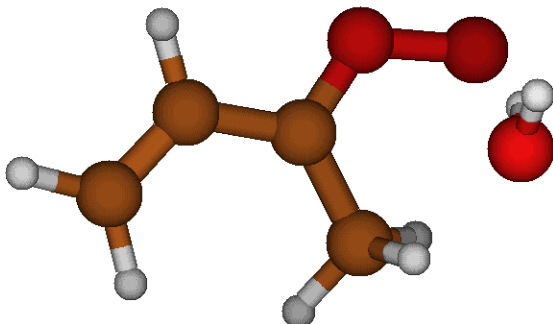
1	6	0	0.489007	0.264516	0.167706
2	8	0	-0.336591	1.153141	-0.251510
3	8	0	-1.577619	1.195747	0.327256
4	8	0	-2.306706	-1.265045	-0.649351
5	1	0	-2.721363	-1.216477	-1.512131
6	1	0	-2.264989	-0.342001	-0.331686
7	6	0	1.751470	0.296037	-0.529991
8	6	0	2.762595	-0.549002	-0.298507
9	1	0	1.836135	1.061648	-1.289087
10	1	0	2.703200	-1.329584	0.444164
11	1	0	3.678923	-0.475719	-0.863409
12	6	0	0.100681	-0.642904	1.258049
13	1	0	-0.415836	-0.058942	2.019359
14	1	0	0.957059	-1.164312	1.669279
15	1	0	-0.628323	-1.357237	0.868810

Frequencies --	44.9318	93.9248	113.8528
Frequencies --	148.0790	209.4653	225.2281
Frequencies --	259.7891	310.6386	351.0015
Frequencies --	410.5464	464.0009	493.3084
Frequencies --	601.9423	690.2681	758.4837
Frequencies --	815.3560	958.3834	978.0073
Frequencies --	1015.8055	1030.3811	1055.7593
Frequencies --	1072.2687	1304.8934	1342.0402
Frequencies --	1401.5251	1450.9373	1471.2367
Frequencies --	1490.9252	1510.5859	1665.5925
Frequencies --	1671.7086	3050.9581	3111.8539
Frequencies --	3179.8565	3186.4210	3200.7510
Frequencies --	3272.6727	3517.4754	3899.8520

syn,cis…H₂O
Relative energy = -4.79 kcal mol^{-1}
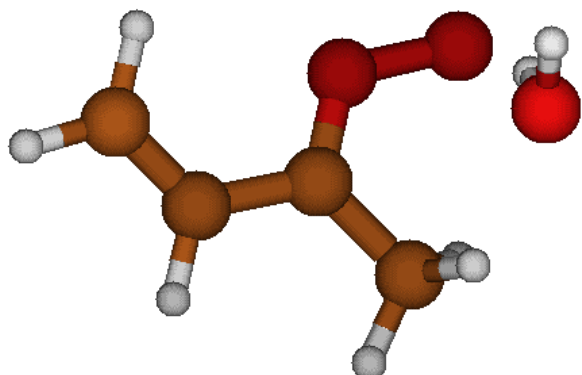
1	6	0	0.482794	0.413398	-0.218287
2	8	0	0.044784	-0.676190	-0.719244
3	8	0	-1.240344	-0.677599	-1.215796
4	8	0	-2.354573	-0.265627	1.250537
5	1	0	-2.586255	-1.076662	1.705565
6	1	0	-2.140465	-0.534429	0.334956
7	6	0	1.823278	0.368578	0.340056
8	6	0	2.541485	-0.747768	0.503219
9	1	0	2.223477	1.324114	0.646605
10	1	0	2.152041	-1.714733	0.221869
11	1	0	3.533280	-0.706893	0.925958
12	6	0	-0.352026	1.624801	-0.233754
13	1	0	-0.834194	1.706409	-1.207879
14	1	0	0.236074	2.504747	0.005606
15	1	0	-1.156078	1.498725	0.495949

Frequencies --	32.9371	76.5633	94.9279
Frequencies --	132.2298	197.4039	226.9238
Frequencies --	238.2559	309.3540	341.8078
Frequencies --	415.7916	448.5863	489.0176
Frequencies --	611.1751	670.6446	768.7060
Frequencies --	816.5299	943.1330	996.1371
Frequencies --	1023.4833	1034.5872	1052.8533
Frequencies --	1104.9161	1283.8398	1342.4179
Frequencies --	1401.5507	1444.1634	1454.9261
Frequencies --	1496.2033	1508.2471	1666.4515
Frequencies --	1677.4319	3043.2697	3104.8767
Frequencies --	3171.1756	3178.4725	3208.2614
Frequencies --	3274.0038	3499.0217	3900.5198

syn,trans…H₂O=syn,cis…H₂O
Geometry a
Relative energy = 0.41 kcal mol⁻¹
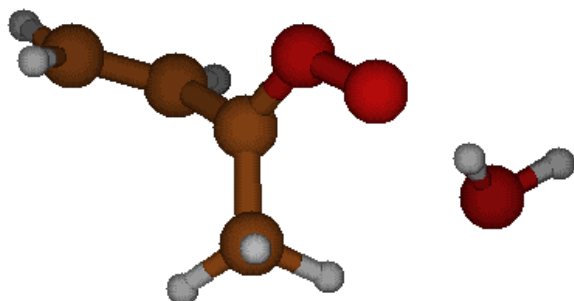
1	6	0	-2.880802	-0.049482	-0.250076
2	6	0	-1.657458	-0.463922	-0.559184
3	6	0	-0.447285	-0.007237	0.151529
4	6	0	0.079441	-0.630814	1.374894
5	8	0	0.149436	0.972956	-0.390681
6	8	0	1.333044	1.393574	0.189844
7	1	0	-3.054975	0.665315	0.541436
8	1	0	-3.741856	-0.413030	-0.790043
9	1	0	-1.491233	-1.180144	-1.355249
10	1	0	0.434330	0.156667	2.040266
11	1	0	0.961090	-1.219379	1.104128
12	1	0	-0.668603	-1.265176	1.837324
13	1	0	2.296332	-0.038523	-0.323660
14	8	0	2.473161	-0.973300	-0.554529
15	1	0	3.056417	-0.942845	-1.314258

Frequencies --	-144.9212	46.0741	103.9866
Frequencies --	128.5973	171.3865	211.5284
Frequencies --	253.0168	275.8132	337.9782
Frequencies --	387.2042	442.1334	525.8062
Frequencies --	620.9468	669.0667	774.3546
Frequencies --	803.3119	921.7968	988.7619
Frequencies --	995.4181	1009.7640	1040.3556
Frequencies --	1096.3749	1296.7309	1319.6798
Frequencies --	1392.2818	1447.3971	1467.5752
Frequencies --	1486.7451	1512.9638	1671.3128
Frequencies --	1696.1287	3037.5917	3100.0800
Frequencies --	3165.3029	3173.6130	3179.4224
Frequencies --	3260.9581	3483.9766	3901.7777
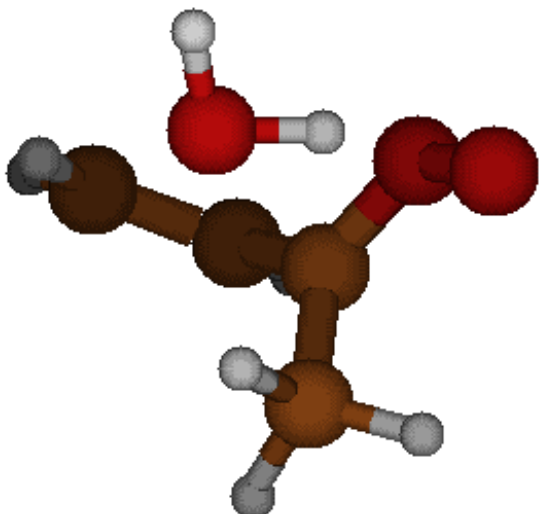
1	6	0	-2.279697	0.982306	-0.266373
2	6	0	-1.838890	-0.269776	-0.204644
3	6	0	-0.432410	-0.564433	0.130695
4	6	0	0.098045	-0.593244	1.502423
5	8	0	0.320806	-0.783591	-0.865900
6	8	0	1.669941	-0.963834	-0.607926
7	1	0	-1.614501	1.816222	-0.091944
8	1	0	-3.310818	1.197532	-0.502666
9	1	0	-2.493472	-1.113315	-0.386002
10	1	0	0.653299	0.334399	1.669393
11	1	0	0.823017	-1.403018	1.581226
12	1	0	-0.707523	-0.676043	2.224105
13	1	0	1.919619	0.786143	-0.201781
14	8	0	1.681904	1.677294	0.128239
15	1	0	2.066888	2.290007	-0.500239

Frequencies --	-146.2612	52.1943	112.8834
Frequencies --	142.5367	178.9859	209.4953
Frequencies --	248.4925	277.1258	337.6150
Frequencies --	391.8617	439.5577	542.9273
Frequencies --	606.7060	668.0224	782.7031
Frequencies --	806.2161	918.8306	987.8445
Frequencies --	1000.1376	1005.9314	1047.9252
Frequencies --	1101.3053	1293.0978	1325.9385
Frequencies --	1392.4906	1448.9594	1463.0891
Frequencies --	1487.0840	1515.9956	1675.3110
Frequencies --	1688.1794	3040.1213	3104.6560
Frequencies --	3165.0939	3176.6070	3176.9574
Frequencies --	3262.2919	3474.5887	3899.8450

syn-trans…H₂O = VHPOH
Geometry a
Relative energy = 8.97 kcal mol^{-1}
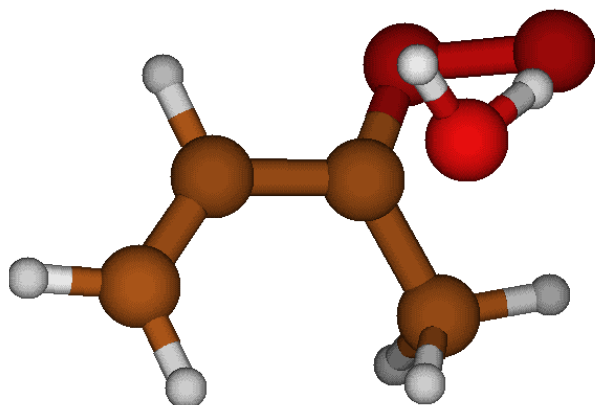
1	6	0	0.096795	0.004807	-0.275680
2	8	0	-0.842261	-0.766000	-0.754394
3	8	0	-2.127980	-0.227189	-0.370471
4	8	0	-0.725808	0.079180	1.554832
5	1	0	-0.583657	-0.790042	1.946386
6	1	0	-1.602700	-0.037664	0.859505
7	6	0	1.377145	-0.701605	-0.195220
8	6	0	2.536563	-0.108681	0.087187
9	1	0	1.319500	-1.768604	-0.361240
10	1	0	2.606455	0.952441	0.272096
11	1	0	3.449323	-0.681477	0.149333
12	6	0	0.037925	1.489363	-0.427360
13	1	0	-0.994569	1.812091	-0.442100
14	1	0	0.514369	1.740427	-1.376576
15	1	0	0.569104	1.981601	0.379287

Frequencies --	-806.5569	84.1812	184.9313
Frequencies --	211.2148	257.8291	313.1670
Frequencies --	342.9059	402.6911	471.3653
Frequencies --	498.2204	573.8569	601.3477
Frequencies --	680.0268	707.6429	788.8630
Frequencies --	898.6793	956.7308	987.6368
Frequencies --	1002.8543	1035.4158	1070.3564
Frequencies --	1106.5912	1305.3303	1336.5641
Frequencies --	1397.3269	1445.8988	1461.3039
Frequencies --	1505.8700	1509.4564	1601.4307
Frequencies --	1691.5810	1801.1955	3066.5856
Frequencies --	3161.1164	3178.8631	3200.7703
Frequencies --	3210.7818	3269.2248	3817.1273

Geometry b
Relative energy = 10.53 kcal mol^{-1}
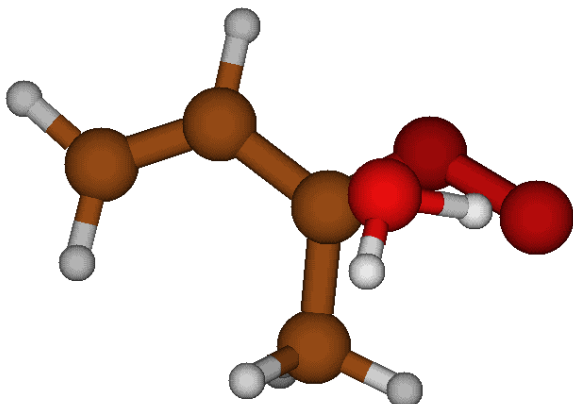
1	6	0	0.103536	-0.013306	-0.245140
2	8	0	-0.817370	-0.793650	-0.734748
3	8	0	-2.117430	-0.231700	-0.425306
4	8	0	-0.775030	-0.035873	1.550089
5	1	0	-1.637472	-0.081893	0.831802
6	1	0	-0.780862	0.844114	1.938907
7	6	0	1.375923	-0.717161	-0.072217
8	6	0	2.553002	-0.106230	0.052532
9	1	0	1.295142	-1.793937	-0.040268
10	1	0	2.648733	0.968963	0.031579
11	1	0	3.459806	-0.676776	0.183327
12	6	0	0.056207	1.465045	-0.471549
13	1	0	-0.974845	1.789186	-0.525408
14	1	0	0.544807	1.666803	-1.426620
15	1	0	0.591320	2.003239	0.304652

Frequencies --	-803.9253	89.1490	198.1131
Frequencies --	232.4033	249.7559	312.9024
Frequencies --	337.6056	411.8848	456.5700
Frequencies --	492.9717	565.7829	619.9861
Frequencies --	672.4764	715.7811	798.8568
Frequencies --	895.4729	949.0614	984.5613
Frequencies --	1000.1212	1035.2495	1066.5264
Frequencies --	1104.1322	1310.7011	1332.0434
Frequencies --	1394.1137	1437.9090	1464.7692
Frequencies --	1505.1144	1512.8790	1516.7876
Frequencies --	1693.5497	1878.6334	3062.7141
Frequencies --	3143.4079	3178.0814	3203.9525
Frequencies --	3213.6932	3266.9008	3841.4265

VHPOH
Geometry a
Relative energy = -26.76 kcal mol^{-1}
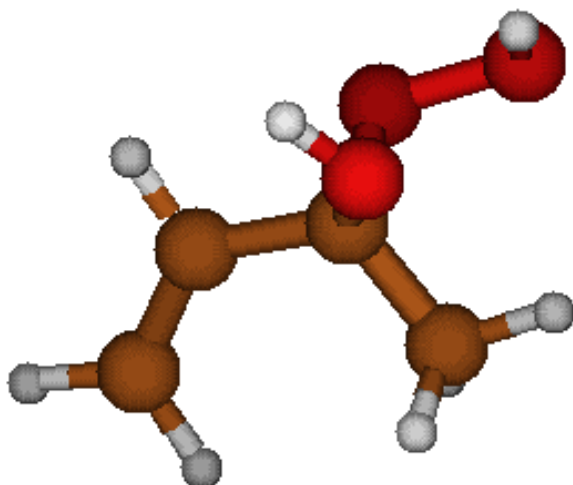
1	6	0	0.020989	0.026262	0.156928
2	8	0	-0.865799	-0.609365	-0.769894
3	8	0	-2.202317	-0.086467	-0.572193
4	8	0	-0.415309	-0.258740	1.479554
5	1	0	-0.188513	-1.173939	1.676847
6	1	0	-2.387080	-0.406142	0.323900
7	6	0	1.325600	-0.666074	-0.133761
8	6	0	2.488688	-0.069546	-0.361328
9	1	0	1.260053	-1.748513	-0.137088
10	1	0	2.589484	1.005022	-0.381339
11	1	0	3.382045	-0.650006	-0.536527
12	6	0	0.024121	1.530367	0.009457
13	1	0	-0.966596	1.912145	0.230255
14	1	0	0.288013	1.802094	-1.008646
15	1	0	0.733606	1.969865	0.705093

Frequencies --	69.7971	149.1262	229.3361
Frequencies --	236.1173	291.2859	315.2939
Frequencies --	351.1442	402.2086	425.4415
Frequencies --	443.5173	500.7283	623.4160
Frequencies --	689.5235	781.0899	894.8016
Frequencies --	937.1683	951.2917	980.5495
Frequencies --	1024.1114	1035.0427	1145.5435
Frequencies --	1169.0051	1196.1006	1331.0266
Frequencies --	1388.0185	1405.7064	1444.1300
Frequencies --	1463.5143	1506.7559	1507.7273
Frequencies --	1711.9751	3087.3529	3158.9796
Frequencies --	3165.8071	3177.3391	3180.8342
Frequencies --	3260.5345	3723.5227	3805.882

Geometry b
Relative energy = -26.64 kcal mol^{-1}
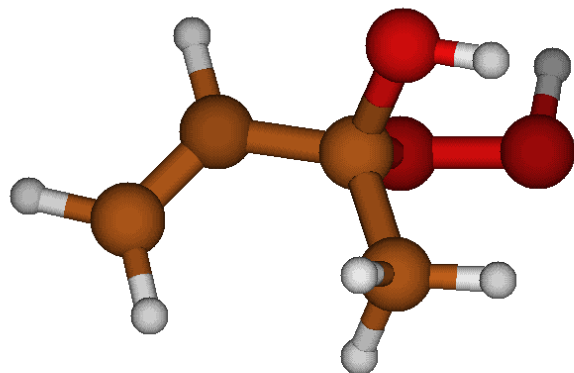
1	6	0	0.030843	0.089208	0.209106
2	8	0	-0.756425	-0.738745	-0.673282
3	8	0	-2.134789	-0.270440	-0.594456
4	8	0	-0.467702	0.018331	1.520913
5	1	0	-2.521566	-1.006508	-0.103769
6	1	0	-1.276349	0.540392	1.543603
7	6	0	1.352053	-0.627576	0.223052
8	6	0	2.451299	-0.233838	-0.406336
9	1	0	1.340614	-1.537943	0.806720
10	1	0	2.486929	0.670390	-0.995229
11	1	0	3.359558	-0.814596	-0.346054
12	6	0	0.054305	1.517581	-0.300845
13	1	0	-0.958279	1.915260	-0.303202
14	1	0	0.430458	1.555510	-1.319532
15	1	0	0.678967	2.132090	0.342213

Frequencies --	62.1506	143.7477	189.9464
Frequencies --	253.7147	259.8264	293.5761
Frequencies --	351.3994	397.9616	437.1932
Frequencies --	462.6130	501.3034	617.0535
Frequencies --	676.7290	780.9787	883.7850
Frequencies --	911.0227	966.8616	978.5326
Frequencies --	1034.2065	1041.8784	1129.4282
Frequencies --	1153.4620	1223.1173	1330.2207
Frequencies --	1355.9002	1403.4147	1425.9346
Frequencies --	1466.3463	1504.2881	1520.7190
Frequencies --	1714.6837	3074.3526	3150.2909
Frequencies --	3160.6100	3172.8632	3197.4643
Frequencies --	3258.7111	3781.4294	3815.6786

syn-trans…H₂O = VHP…H₂O
Geometry a
Relative energy = 12.16 kcal mol^{-1}
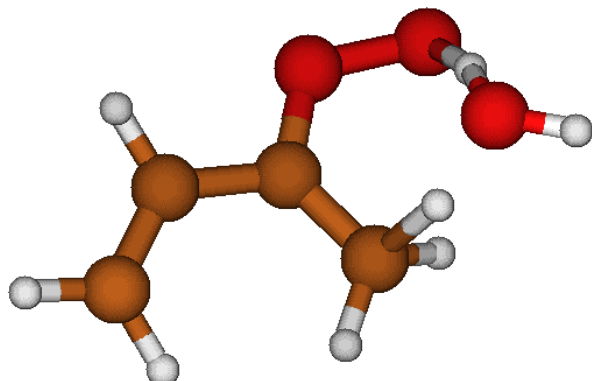
1	6	0	0.026254	0.979209	0.829133
2	6	0	-0.438225	-0.193280	0.208507
3	8	0	0.336152	-1.213066	-0.044070
4	8	0	1.697094	-1.068073	0.366731
5	6	0	-1.764129	-0.411668	-0.364713
6	6	0	-2.805521	0.398811	-0.174064
7	1	0	0.961596	1.294094	-0.049447
8	1	0	-0.721674	1.731460	1.029025
9	1	0	0.726908	0.788151	1.636374
10	1	0	2.016119	-0.046645	-0.270412
11	8	0	2.026235	1.020553	-0.786263
12	1	0	2.790270	1.513493	-0.470245
13	1	0	-1.861072	-1.305408	-0.965125
14	1	0	-3.760971	0.181580	-0.626388
15	1	0	-2.737305	1.289526	0.431854

Frequencies --	-1715.1668	73.6559	131.7662
Frequencies --	254.6795	264.3027	328.9123
Frequencies --	440.4471	475.9273	483.4808
Frequencies --	539.4930	576.1226	637.3117
Frequencies --	679.2480	713.9916	778.2489
Frequencies --	878.0055	922.1894	929.3425
Frequencies --	993.8413	1031.4964	1035.2753
Frequencies --	1067.0307	1094.4327	1313.0413
Frequencies --	1329.9010	1356.8597	1408.6694
Frequencies --	1451.5531	1475.2206	1567.4922
Frequencies --	1608.5694	1690.1443	1838.4171
Frequencies --	3124.7152	3178.8874	3204.4247
Frequencies --	3233.5887	3269.6241	3835.9575

Geometry b
Relative energy = 11.94 kcal mol^{-1}
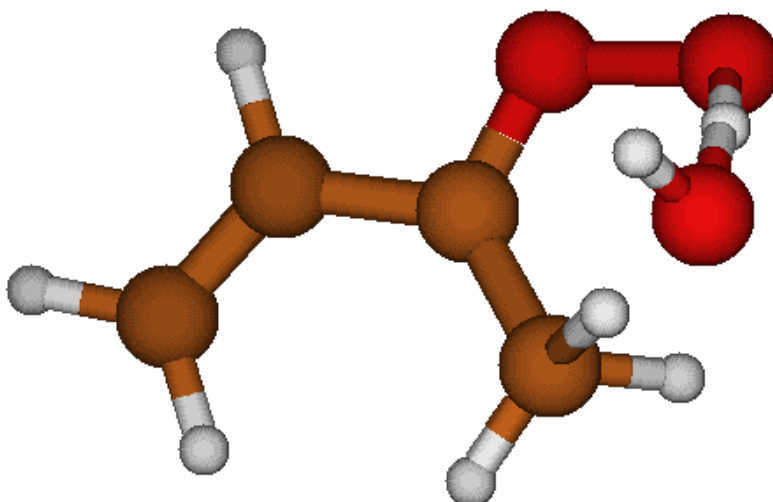

```
  1           6           0        0.017561     0.979653     0.831745
  2           6           0       -0.437134    -0.193406     0.208458
  3           8           0        0.346570    -1.203232    -0.056867
  4           8           0        1.702657    -1.063612     0.372186
  5           6           0       -1.762855    -0.420361    -0.363536
  6           6           0       -2.808885     0.385031    -0.176117
  7           1           0        0.955620     1.304888    -0.040800
  8           1           0       -0.732918     1.726291     1.041317
  9           1           0        0.737971     0.800914     1.624553
 10           1           0        2.038690    -0.022582    -0.234005
 11           8           0        2.110272     1.076252    -0.644381
 12           1           0        2.038345     1.090183    -1.604273
 13           1           0       -1.856471    -1.318329    -0.958422
 14           1           0       -3.763891     0.159187    -0.625186
 15           1           0       -2.745445     1.278690     0.426014
Frequencies --  -1704.6546                73.5736                 135.2417
Frequencies --    253.9871               266.8284                 327.0986
Frequencies --    448.0507               465.5533                 479.3773
Frequencies --    529.5039               573.0349                 642.8930
Frequencies --    663.0429               742.4472                 784.2410
Frequencies --    864.9158               923.6307                 928.7932
Frequencies --    993.5743              1031.5957                1036.8219
Frequencies --   1075.7109              1131.2404                1312.7019
Frequencies --   1355.5910              1363.0013                1430.5355
Frequencies --   1474.4650              1523.4621                1579.7225
Frequencies --   1592.1540              1689.4874                1711.9249
Frequencies --   3125.3620              3178.6245                3202.3754
Frequencies --   3236.7281              3269.4890                3832.7224
```

VHP…H₂O
Geometry a
Relative energy = -17.21 kcal mol^{-1}
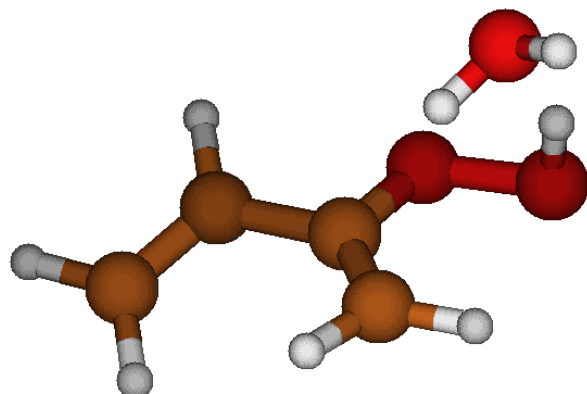
1	6	0	0.181948	-0.635330	1.242252
2	6	0	0.489801	0.140066	0.194460
3	8	0	-0.295599	1.132987	-0.325585
4	8	0	-1.541648	1.264757	0.384997
5	6	0	1.707406	0.046237	-0.623933
6	6	0	2.892433	-0.351740	-0.165837
7	1	0	-1.534739	-1.484385	-0.297638
8	1	0	0.868493	-1.412189	1.533466
9	1	0	-0.698928	-0.455598	1.833045
10	1	0	-2.054653	0.546034	-0.042733
11	8	0	-2.355073	-1.151484	-0.685960
12	1	0	-3.052897	-1.677380	-0.287283
13	1	0	1.595279	0.349109	-1.656808
14	1	0	3.745804	-0.418558	-0.823347
15	1	0	3.040679	-0.612502	0.872026

Frequencies --	58.7952	84.2872	115.4096
Frequencies --	159.5406	204.2848	229.2551
Frequencies --	254.6363	328.1704	359.2160
Frequencies --	424.8692	428.0981	508.6751
Frequencies --	591.0468	687.6844	753.2525
Frequencies --	762.6515	840.0211	867.1096
Frequencies --	926.5550	969.7516	990.3591
Frequencies --	1029.7465	1088.3186	1253.4371
Frequencies --	1333.8494	1421.4485	1469.2171
Frequencies --	1532.4440	1648.7185	1678.3021
Frequencies --	1696.0539	3169.0329	3188.2244
Frequencies --	3202.7754	3260.0955	3301.3985
Frequencies --	3501.1082	3738.0065	3893.0082

Geometry b
Relative energy = -17.66 kcal mol⁻¹
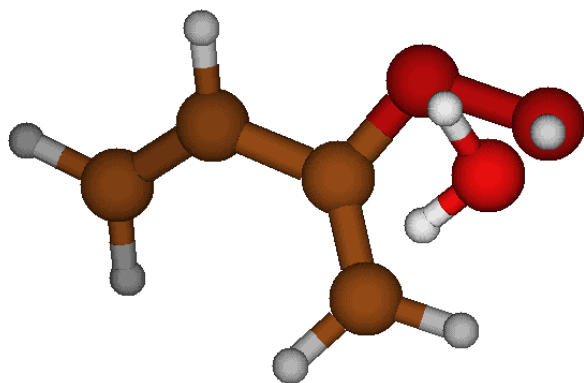
1	6	0	-0.210776	0.510265	1.320295
2	6	0	-0.481730	-0.159872	0.193469
3	8	0	0.340506	-1.073175	-0.412277
4	8	0	1.567478	-1.262266	0.318127
5	6	0	-1.688694	-0.017277	-0.633525
6	6	0	-2.886167	0.333874	-0.169276
7	1	0	1.551801	1.543583	-0.089286
8	1	0	-0.921730	1.235522	1.678301
9	1	0	0.667860	0.297365	1.903575
10	1	0	2.077684	-0.490741	-0.011252
11	8	0	2.378931	1.245669	-0.490758
12	1	0	2.277218	1.419632	-1.430217
13	1	0	-1.559153	-0.244840	-1.683799
14	1	0	-3.729028	0.437647	-0.835426
15	1	0	-3.055777	0.518070	0.881586

Frequencies --	58.8468	77.4634	108.8680
Frequencies --	160.6063	216.8647	229.7746
Frequencies --	257.0245	287.0584	360.3984
Frequencies --	422.0656	461.9540	508.2914
Frequencies --	588.1264	728.0656	751.9346
Frequencies --	786.2670	848.8605	866.6547
Frequencies --	926.0643	969.0438	989.2951
Frequencies --	1029.1321	1087.6721	1250.8469
Frequencies --	1334.7156	1422.3986	1469.9034
Frequencies --	1513.4219	1646.8323	1680.3985
Frequencies --	1696.5475	3169.3860	3184.9715
Frequencies --	3203.0888	3260.5771	3301.2142
Frequencies --	3487.7504	3742.9802	3889.7963

syn-trans…H₂O = VHP…H₂O; spectator
Geometry a
Relative energy = 13.33 kcal mol^{-1}
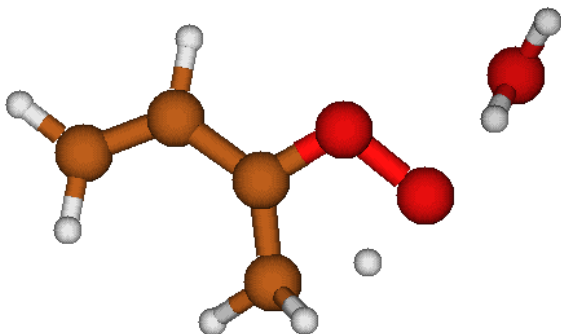
1	6	0	-2.930724	-0.787681	0.220770
2	6	0	-1.654916	-0.904493	-0.154089
3	6	0	-0.732938	0.213944	-0.151998
4	6	0	-0.793171	1.447695	0.516853
5	8	0	0.424719	-0.070353	-0.711769
6	8	0	1.338249	0.976023	-0.443746
7	1	0	-3.344569	0.162601	0.524279
8	1	0	-3.586964	-1.644309	0.230951
9	1	0	-1.248280	-1.852519	-0.478760
10	1	0	0.559711	1.401142	0.539903
11	1	0	-0.655640	2.333809	-0.097706
12	1	0	-1.547993	1.549526	1.281948
13	1	0	2.715570	-0.210671	0.225273
14	8	0	3.248646	-0.937737	0.577960
15	1	0	3.685748	-1.299829	-0.194656

Frequencies --	-1623.8460	11.1229	41.2886
Frequencies --	87.2978	114.7241	168.5606
Frequencies --	246.9054	280.3284	314.7069
Frequencies --	470.7153	488.8173	557.6282
Frequencies --	613.5770	634.1574	742.5515
Frequencies --	760.3229	901.7057	932.4415
Frequencies --	952.4302	999.5443	1027.1984
Frequencies --	1038.1109	1069.4271	1294.8528
Frequencies --	1332.7958	1352.5309	1466.8781
Frequencies --	1472.6696	1554.6363	1678.9579
Frequencies --	1683.3409	1822.6553	3116.6088
Frequencies --	3175.5300	3201.0990	3227.7275
Frequencies --	3269.2147	3700.7887	3901.3284

Geometry b
Relative energy = 12.86 kcal mol^{-1}
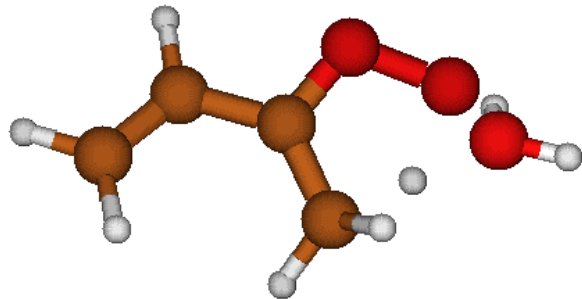
1	6	0	2.842589	-0.738115	-0.255600
2	6	0	1.966605	0.260018	-0.389128
3	6	0	0.600034	0.170898	0.088609
4	6	0	0.014999	-0.690530	1.026894
5	8	0	-0.143951	1.192582	-0.294159
6	8	0	-1.369216	1.166109	0.415969
7	1	0	2.562082	-1.675809	0.200850
8	1	0	3.858683	-0.635924	-0.604630
9	1	0	2.241778	1.187748	-0.872242
10	1	0	-0.837486	0.329887	1.295141
11	1	0	-0.877046	-1.222294	0.695759
12	1	0	0.691416	-1.276894	1.630796
13	1	0	-2.450495	-0.153437	-0.415841
14	8	0	-2.746203	-1.043237	-0.668696
15	1	0	-3.659347	-1.090543	-0.379395

Frequencies --	-1619.7920	40.4798	92.9244
Frequencies --	120.7195	147.0689	182.0655
Frequencies --	249.2568	287.3693	389.6724
Frequencies --	474.4114	502.3374	584.1612
Frequencies --	622.1154	646.6367	747.8941
Frequencies --	773.7153	911.4622	937.2180
Frequencies --	957.8210	999.0272	1027.4762
Frequencies --	1043.2972	1071.3300	1291.0009
Frequencies --	1327.6510	1354.5021	1467.5326
Frequencies --	1473.7311	1561.0778	1679.3621
Frequencies --	1683.7954	1817.5718	3080.9513
Frequencies --	3175.1911	3198.6914	3221.3979
Frequencies --	3268.9692	3639.8589	3897.2997

VHP;trans…H₂O
Geometry a
Relative energy = -14.22 kcal mol^{-1}
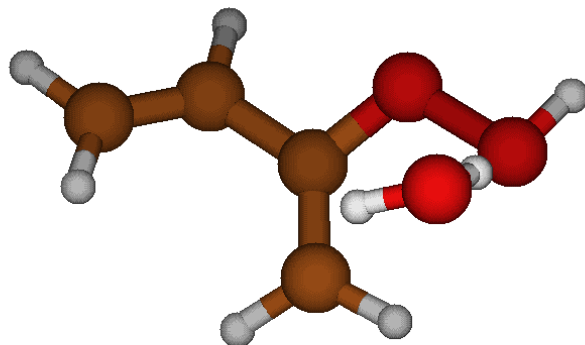
1	6	0	-2.685189	-0.770786	0.346657
2	6	0	-1.868960	0.280972	0.349671
3	6	0	-0.540005	0.296512	-0.274838
4	6	0	-0.165615	-0.361384	-1.372960
5	8	0	0.262290	1.128807	0.470052
6	8	0	1.568971	1.232610	-0.157960
7	1	0	-2.394755	-1.711573	-0.097878
8	1	0	-3.666411	-0.710878	0.791985
9	1	0	-2.165534	1.198849	0.840627
10	1	0	1.872616	2.033779	0.288238
11	1	0	0.833673	-0.305526	-1.765128
12	1	0	-0.902967	-0.944110	-1.898243
13	1	0	2.328571	-0.627562	0.385954
14	8	0	2.430080	-1.571786	0.542455
15	1	0	1.562691	-1.921913	0.326895

Frequencies --	18.8629	62.6694	83.1228
Frequencies --	96.6136	119.9030	168.4570
Frequencies --	178.2037	243.3064	289.5296
Frequencies --	348.5398	408.5999	421.6917
Frequencies --	500.8707	586.6265	730.2464
Frequencies --	741.7971	842.6029	864.2300
Frequencies --	916.8610	968.7429	981.8101
Frequencies --	1024.8529	1090.1636	1250.2508
Frequencies --	1334.0461	1390.7864	1445.1525
Frequencies --	1472.9841	1677.4963	1694.0508
Frequencies --	1701.2668	3169.8590	3185.6676
Frequencies --	3210.6659	3261.8643	3308.9523
Frequencies --	3792.4662	3804.9132	3903.9729

Geometry b
Relative energy = -14.19 kcal mol^{-1}
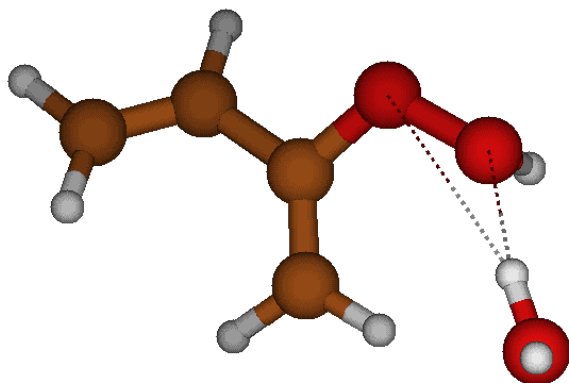
1	6	0	2.938903	-0.772898	-0.363353
2	6	0	2.124956	0.229502	-0.038415
3	6	0	0.680516	0.082433	0.182241
4	6	0	0.054587	-0.981823	0.685862
5	8	0	0.080039	1.271413	-0.194042
6	8	0	-1.335040	1.262729	0.059949
7	1	0	2.568065	-1.775664	-0.518305
8	1	0	3.998854	-0.608408	-0.482922
9	1	0	2.513735	1.234276	0.065338
10	1	0	-1.365997	1.451075	1.010024
11	1	0	-1.015431	-1.042365	0.783287
12	1	0	0.652285	-1.821747	0.997802
13	1	0	-2.679898	-0.188801	-0.445728
14	8	0	-3.293670	-0.912039	-0.274389
15	1	0	-3.076020	-1.568473	-0.939648

Frequencies --	30.0012	81.5532	90.1021
Frequencies --	119.6322	136.3285	176.5566
Frequencies --	184.9440	252.6182	302.6837
Frequencies --	358.6996	412.8368	460.4775
Frequencies --	507.6841	596.5048	742.0151
Frequencies --	757.7345	867.6883	882.2439
Frequencies --	922.5481	968.5072	982.6309
Frequencies --	1026.7891	1090.3249	1233.7579
Frequencies --	1333.1302	1390.2259	1440.9317
Frequencies --	1472.7418	1668.3157	1692.9582
Frequencies --	1698.4573	3169.3909	3185.7531
Frequencies --	3201.8314	3261.1948	3298.0041
Frequencies --	3731.6328	3778.9128	3906.2494

syn-cis…H₂O = VHPOH
Geometry a
Relative energy = 9.17 kcal mol^{-1}
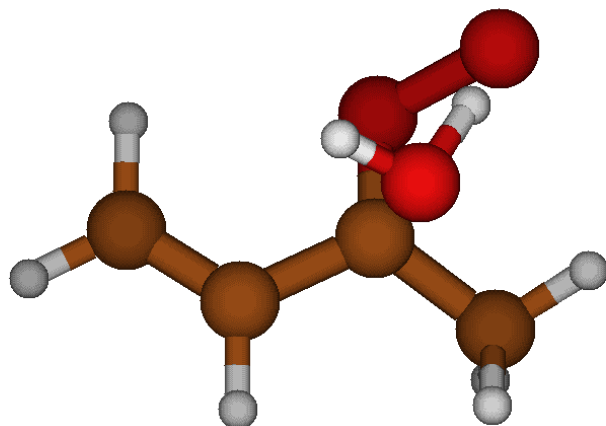
1	6	0	0.076443	0.343639	-0.222305
2	8	0	-0.279064	-0.783420	-0.764280
3	8	0	-1.688818	-1.003933	-0.498672
4	8	0	-0.816056	-0.064608	1.544625
5	1	0	-0.265599	-0.740835	1.954992
6	1	0	-1.434025	-0.593689	0.795269
7	6	0	1.520157	0.469064	0.022322
8	6	0	2.354578	-0.569880	-0.016738
9	1	0	1.877909	1.465077	0.239726
10	1	0	1.993135	-1.565998	-0.224602
11	1	0	3.412755	-0.438554	0.150696
12	6	0	-0.721484	1.590456	-0.408857
13	1	0	-1.772759	1.357662	-0.510082
14	1	0	-0.360663	2.062194	-1.326594
15	1	0	-0.557412	2.270160	0.420681

Frequencies --	-663.2814	84.2144	188.5574
Frequencies --	200.4108	222.8651	309.6968
Frequencies --	331.2155	392.3162	473.1180
Frequencies --	505.8716	573.1798	608.1536
Frequencies --	677.5527	699.0772	796.5091
Frequencies --	896.8130	982.3474	1016.8755
Frequencies --	1028.6415	1032.6439	1079.3518
Frequencies --	1154.8919	1271.7814	1340.1440
Frequencies --	1405.4248	1437.8650	1468.7964
Frequencies --	1499.2398	1515.9329	1612.9980
Frequencies --	1688.2184	1825.4816	3051.7700
Frequencies --	3151.2596	3175.7266	3208.2582
Frequencies --	3214.3332	3271.2382	3820.2684

Geometry b
Relative energy = 10.72 kcal mol^{-1}
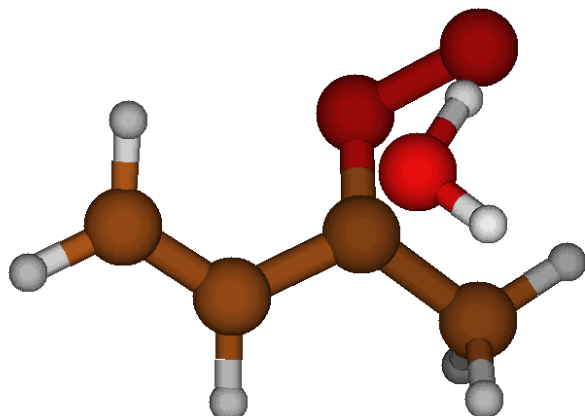
1	6	0	0.076567	0.366363	-0.218684
2	8	0	-0.299432	-0.713357	-0.840192
3	8	0	-1.693006	-0.970608	-0.525976
4	8	0	-0.645585	-0.328771	1.526931
5	1	0	-1.353808	-0.739461	0.756408
6	1	0	-1.126392	0.352549	2.006803
7	6	0	1.528029	0.482429	-0.052944
8	6	0	2.320570	-0.586817	0.010720
9	1	0	1.925418	1.483456	0.037436
10	1	0	1.908308	-1.582951	-0.042442
11	1	0	3.388632	-0.482499	0.127326
12	6	0	-0.738915	1.617774	-0.276881
13	1	0	-1.793759	1.383269	-0.330011
14	1	0	-0.442704	2.148182	-1.185708
15	1	0	-0.519019	2.260845	0.570827

Frequencies --	-778.7290	75.6379	205.7397
Frequencies --	217.5452	228.7024	307.9544
Frequencies --	326.5040	404.1722	460.3552
Frequencies --	507.1050	579.3972	617.1243
Frequencies --	668.3553	700.9135	801.9431
Frequencies --	899.7381	945.7280	1000.6411
Frequencies --	1017.4813	1018.8314	1068.4232
Frequencies --	1112.6826	1267.1694	1341.3092
Frequencies --	1400.5293	1436.2913	1463.3959
Frequencies --	1498.6358	1508.2548	1514.1600
Frequencies --	1689.4044	1873.3174	3049.7893
Frequencies --	3133.2123	3177.6426	3202.8972
Frequencies --	3206.4094	3274.9449	3840.5095

VHPOH
Geometry a
Relative energy = 27.40 kcal mol^{-1}
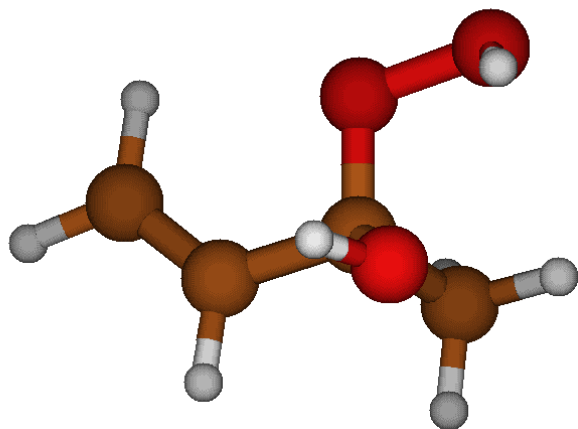
1	6	0	-0.005013	0.341376	0.038973
2	8	0	-0.420685	-1.012154	-0.105800
3	8	0	-1.864638	-1.047694	-0.157160
4	8	0	-0.501348	0.854664	1.269009
5	1	0	0.000751	0.434303	1.976302
6	1	0	-2.081678	-0.755572	0.741079
7	6	0	1.500000	0.308830	0.058301
8	6	0	2.260281	-0.762311	-0.137807
9	1	0	1.945726	1.274459	0.261593
10	1	0	1.831860	-1.729823	-0.348117
11	1	0	3.336779	-0.686503	-0.096153
12	6	0	-0.543207	1.236464	-1.060475
13	1	0	-1.624643	1.295908	-0.994827
14	1	0	-0.263365	0.828401	-2.027879
15	1	0	-0.124425	2.234147	-0.954340

Frequencies --	56.8928	144.5237	208.8953
Frequencies --	236.0355	298.0344	318.0550
Frequencies --	341.6076	395.4223	449.5740
Frequencies --	476.3087	541.6937	586.2015
Frequencies --	705.8692	778.5015	901.7022
Frequencies --	950.1916	960.6471	983.9387
Frequencies --	1035.7976	1048.2743	1110.2349
Frequencies --	1170.8587	1251.0122	1328.5902
Frequencies --	1373.3061	1411.8717	1423.9101
Frequencies --	1464.0146	1498.0495	1503.7572
Frequencies --	1704.1868	3081.4192	3159.2936
Frequencies --	3170.6931	3175.3728	3184.3036
Frequencies --	3267.1688	3724.0059	3798.5698

syn-cis…H₂O = VHP…H₂O
Geometry a
Relative energy = 12.32 kcal mol^{-1}
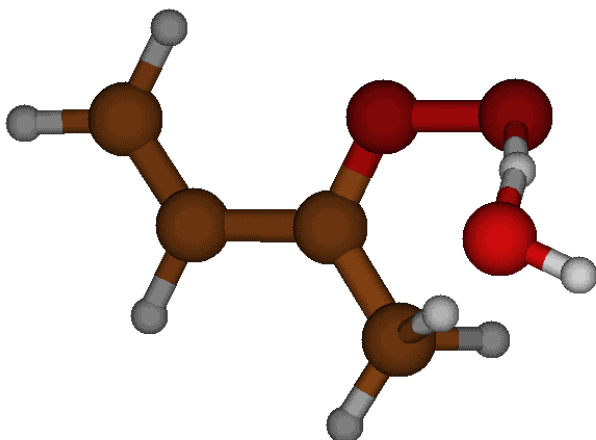
1	6	0	-0.499055	1.296463	-0.683845
2	6	0	0.418244	0.280551	-0.357324
3	8	0	0.089437	-0.974666	-0.285207
4	8	0	-1.291598	-1.259071	-0.543523
5	6	0	1.792620	0.560679	0.059298
6	6	0	2.630785	-0.359543	0.539832
7	1	0	-1.332822	1.109067	0.312575
8	1	0	-0.070087	2.283009	-0.783191
9	1	0	-1.218555	1.011619	-1.445543
10	1	0	-1.839036	-0.540092	0.339258
11	8	0	-2.124681	0.333934	1.063396
12	1	0	-3.050273	0.559693	0.925651
13	1	0	2.104516	1.588599	-0.053833
14	1	0	3.640052	-0.094958	0.815816
15	1	0	2.325374	-1.387406	0.664167

Frequencies --	-1677.2913	51.8937	144.3724
Frequencies --	231.1471	248.9179	330.7382
Frequencies --	436.7246	453.7879	507.8745
Frequencies --	538.0216	582.2478	630.0122
Frequencies --	679.5402	721.6996	774.3263
Frequencies --	871.4765	924.3257	940.2022
Frequencies --	1007.1516	1025.3979	1045.2410
Frequencies --	1086.5071	1101.7038	1321.0917
Frequencies --	1357.4213	1367.0415	1404.6809
Frequencies --	1458.0239	1463.5304	1552.9322
Frequencies --	1604.4416	1692.3058	1839.0213
Frequencies --	3121.8912	3178.4399	3209.9399
Frequencies --	3228.0063	3273.7666	3835.9199

Geometry b
Relative energy = 12.07 kcal mol⁻¹
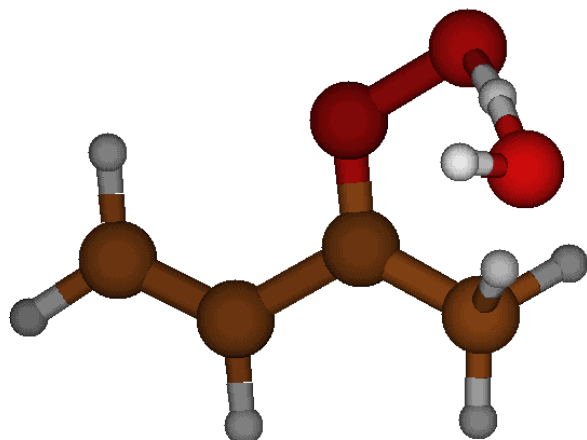
1	6	0	-0.491504	1.299606	-0.681344
2	6	0	0.417691	0.281625	-0.343843
3	8	0	0.080840	-0.970005	-0.254291
4	8	0	-1.291751	-1.259911	-0.550994
5	6	0	1.792297	0.560232	0.075783
6	6	0	2.647392	-0.367793	0.509331
7	1	0	-1.340301	1.118961	0.303040
8	1	0	-0.061269	2.284617	-0.787463
9	1	0	-1.223149	1.015159	-1.431870
10	1	0	-1.880498	-0.524754	0.301016
11	8	0	-2.257045	0.372083	0.932660
12	1	0	-2.053239	0.237915	1.863995
13	1	0	2.092336	1.595025	-0.002573
14	1	0	3.656067	-0.101432	0.785756
15	1	0	2.358435	-1.404837	0.589541

Frequencies --	-1659.8567	54.2417	147.4361
Frequencies --	231.5930	250.0026	328.8234
Frequencies --	431.0516	464.5993	495.2850
Frequencies --	529.5229	582.0860	640.2210
Frequencies --	650.7053	740.1933	794.6366
Frequencies --	859.3922	922.9021	942.8757
Frequencies --	1005.8419	1027.4319	1046.3525
Frequencies --	1096.6992	1153.4891	1323.9984
Frequencies --	1354.6651	1359.2454	1449.9170
Frequencies --	1459.7587	1544.6848	1560.7880
Frequencies --	1599.2501	1692.5124	1704.9322
Frequencies --	3122.4702	3177.9713	3208.8211
Frequencies --	3230.7335	3273.0327	3832.0606

VHP…H₂O
Geometry a
Relative energy = -19.06 kcal mol^{-1}
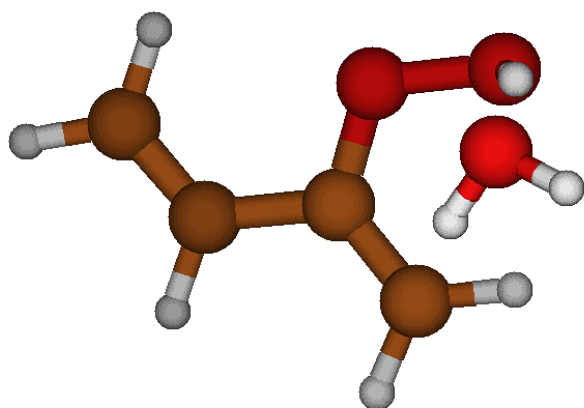
1	6	0	-0.199658	1.441808	-0.817304
2	6	0	0.488350	0.380121	-0.370220
3	8	0	0.054874	-0.914006	-0.386677
4	8	0	-1.254450	-1.034476	-0.974156
5	6	0	1.820564	0.486077	0.224090
6	6	0	2.537175	-0.537614	0.689529
7	1	0	-1.676544	0.830724	1.147424
8	1	0	0.259414	2.414592	-0.756187
9	1	0	-1.155679	1.338582	-1.298763
10	1	0	-1.807053	-0.818365	-0.193138
11	8	0	-2.327582	0.131984	1.291293
12	1	0	-3.178854	0.576376	1.270483
13	1	0	2.214779	1.492341	0.261902
14	1	0	3.518338	-0.375053	1.108811
15	1	0	2.164287	-1.549564	0.659213

Frequencies --		
47.8616	93.7149	128.1673
169.0544	182.4060	225.8452
244.7701	323.4094	366.1745
417.1388	468.4122	490.8694
583.9379	683.9367	749.9291
773.6256	839.4133	857.5646
930.8243	963.7070	994.6559
1022.4231	1072.6067	1326.5761
1333.5519	1417.4114	1466.7914
1535.1374	1642.3979	1649.4228
1708.9027	3176.9886	3194.5157
3202.2470	3270.5188	3302.1174
3506.9285	3755.5070	3895.4757

Geometry b
Relative energy = -19.68 kcal mol^{-1}
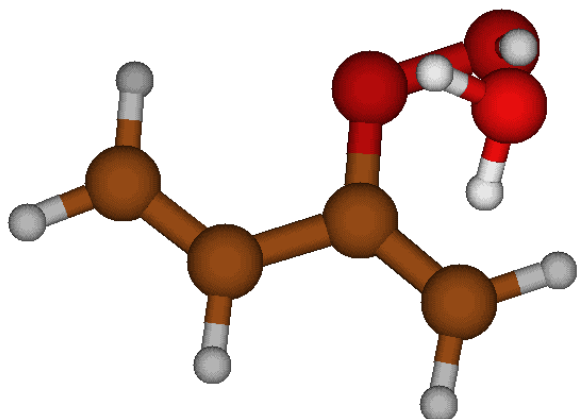
1	6	0	0.170765	1.689933	0.192702
2	6	0	-0.472576	0.513215	0.206915
3	8	0	0.012672	-0.653124	0.726951
4	8	0	1.323327	-0.479436	1.298519
5	6	0	-1.803713	0.324219	-0.368274
6	6	0	-2.480609	-0.825032	-0.378764
7	1	0	1.683513	0.382663	-1.396280
8	1	0	-0.324431	2.541382	-0.243829
9	1	0	1.129955	1.821210	0.661323
10	1	0	1.867041	-0.572603	0.486482
11	8	0	2.291656	-0.358684	-1.281748
12	1	0	1.912302	-1.068801	-1.806883
13	1	0	-2.234190	1.216198	-0.802457
14	1	0	-3.464480	-0.878884	-0.819185
15	1	0	-2.074152	-1.725214	0.055583

Frequencies --	44.9263	89.3525	128.2721
Frequencies --	173.1129	202.8612	228.0720
Frequencies --	246.3972	298.4040	365.6868
Frequencies --	447.6155	468.8739	491.1726
Frequencies --	584.2631	726.2253	770.0856
Frequencies --	787.4620	847.8675	861.2585
Frequencies --	930.4261	961.8039	993.1874
Frequencies --	1024.3212	1072.0825	1326.0816
Frequencies --	1332.2698	1417.6698	1466.9057
Frequencies --	1514.5512	1641.4916	1652.0266
Frequencies --	1708.7184	3176.6255	3194.4279
Frequencies --	3202.1493	3269.6624	3301.6066
Frequencies --	3491.2443	3757.6946	3888.1530

syn-cis…H₂O = VHP…H₂O; spectator
Geometry a
Relative energy = 14.55 kcal mol^{-1}
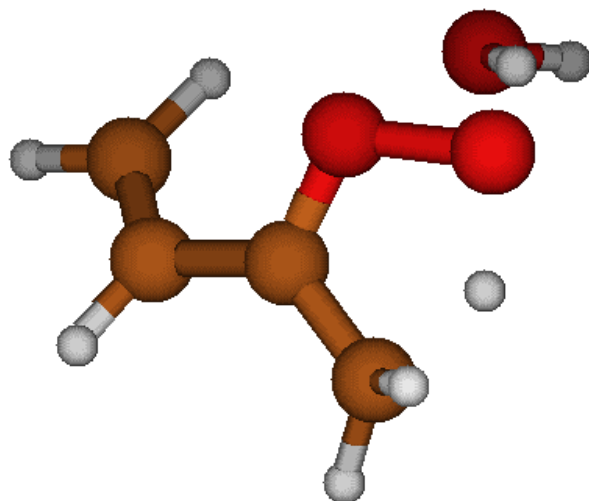
1	6	0	1.481827	1.696796	-0.147649
2	6	0	1.772232	0.402019	0.009845
3	6	0	0.733772	-0.616735	-0.054147
4	6	0	0.531846	-1.726875	0.780324
5	8	0	-0.266886	-0.315440	-0.848219
6	8	0	-1.386619	-1.136105	-0.532343
7	1	0	0.462749	2.019973	-0.307175
8	1	0	2.255553	2.447226	-0.081055
9	1	0	2.772513	0.066408	0.242049
10	1	0	-0.778427	-1.492734	0.614598
11	1	0	0.343642	-2.676351	0.284534
12	1	0	1.163902	-1.795617	1.653138
13	1	0	-2.065358	0.648193	0.105604
14	8	0	-1.926631	1.528585	0.484657
15	1	0	-2.631556	1.635354	1.125310

Frequencies --	-1610.8587	41.6251	64.9473
Frequencies --	80.8787	125.8768	171.5352
Frequencies --	219.9222	290.8253	386.6796
Frequencies --	446.8301	533.1061	562.0907
Frequencies --	589.2097	623.2465	718.0198
Frequencies --	744.7442	901.7159	923.5264
Frequencies --	940.6928	1018.8397	1033.3920
Frequencies --	1042.0176	1090.4185	1313.9961
Frequencies --	1336.1702	1363.2248	1440.9053
Frequencies --	1479.2665	1541.4499	1674.8181
Frequencies --	1679.5495	1830.4941	3112.2610
Frequencies --	3166.9518	3207.1640	3225.1584
Frequencies --	3267.7036	3697.4471	3906.9090

Geometry b
Relative energy = 13.89 kcal mol^{-1}
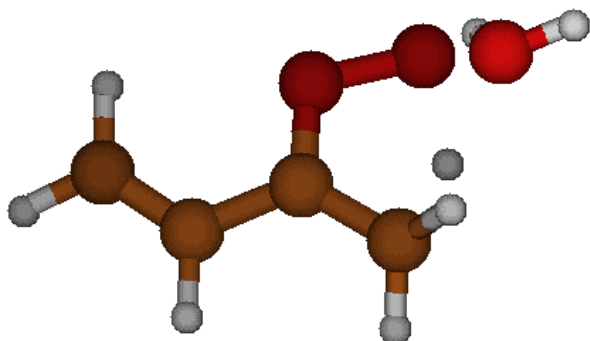
1	6	0	2.772155	-0.460193	0.613818
2	6	0	1.966132	0.529855	0.222269
3	6	0	0.577018	0.345171	-0.163675
4	6	0	-0.329191	1.323088	-0.596079
5	8	0	0.176292	-0.902418	-0.289602
6	8	0	-1.100778	-0.917670	-0.909354
7	1	0	2.431957	-1.484393	0.646766
8	1	0	3.786587	-0.257057	0.920391
9	1	0	2.309364	1.554140	0.213001
10	1	0	-0.912610	0.351812	-1.315616
11	1	0	-1.281541	1.365195	-0.066026
12	1	0	0.091547	2.289866	-0.832257
13	1	0	-2.365642	-0.466964	0.419279
14	8	0	-2.851098	0.096167	1.044819
15	1	0	-3.771672	0.011248	0.789565

Frequencies --	-1615.0701	34.2583	79.7759
Frequencies --	111.3066	150.1824	176.3081
Frequencies --	235.5029	283.6266	394.4130
Frequencies --	483.2131	498.3378	577.4891
Frequencies --	637.2685	651.5047	736.1667
Frequencies --	769.1469	909.4509	940.7370
Frequencies --	957.1199	997.3684	1025.3350
Frequencies --	1041.8259	1084.7334	1314.4620
Frequencies --	1333.1704	1367.8817	1436.6193
Frequencies --	1486.2579	1546.8586	1679.9654
Frequencies --	1687.5295	1821.0748	3072.6479
Frequencies --	3178.0501	3208.6378	3215.1417
Frequencies --	3272.6954	3629.8532	3896.5430

VHP,cis…H₂O
Geometry a
Relative energy = -16.15 kcal mol^{-1}
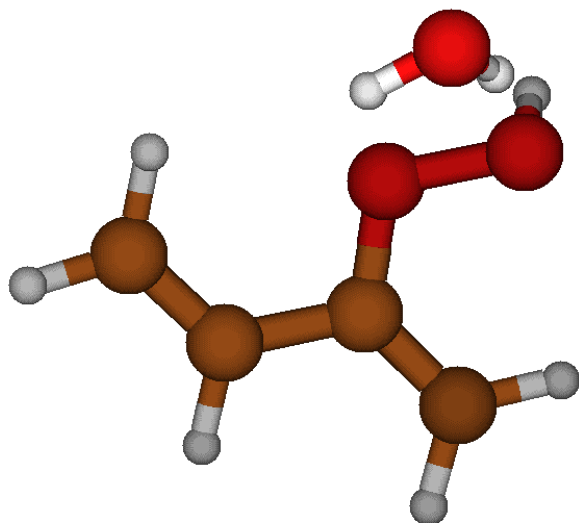
1	6	0	1.775810	1.719398	0.301535
2	6	0	1.849955	0.496614	-0.226932
3	6	0	0.830123	-0.541268	-0.112105
4	6	0	0.916426	-1.742261	-0.687561
5	8	0	-0.223824	-0.099598	0.659119
6	8	0	-1.278757	-1.089266	0.689024
7	1	0	0.921706	2.041230	0.877213
8	1	0	2.579476	2.425974	0.162881
9	1	0	2.717649	0.201281	-0.800444
10	1	0	-1.340187	-1.228984	1.643507
11	1	0	0.140398	-2.480303	-0.599503
12	1	0	1.793486	-1.967153	-1.271073
13	1	0	-2.524862	0.310280	-0.253041
14	8	0	-2.813695	1.127254	-0.670816
15	1	0	-1.991346	1.595661	-0.827778

Frequencies --	9.2016	26.6217	97.4239
Frequencies --	126.0226	136.5129	160.0549
Frequencies --	182.5184	232.5979	255.4877
Frequencies --	360.1208	429.5917	450.1572
Frequencies --	489.3924	578.6185	729.2227
Frequencies --	765.8449	851.5971	863.4689
Frequencies --	923.6757	956.6147	979.0578
Frequencies --	1023.6906	1069.1968	1319.2068
Frequencies --	1327.6300	1379.4509	1426.2499
Frequencies --	1470.6070	1653.8693	1674.2874
Frequencies --	1718.7794	3177.9083	3197.5566
Frequencies --	3208.8633	3269.0984	3310.8547
Frequencies --	3778.6400	3813.3351	3915.1257

Geometry b
Relative energy = 16.07 kcal mol^{-1}
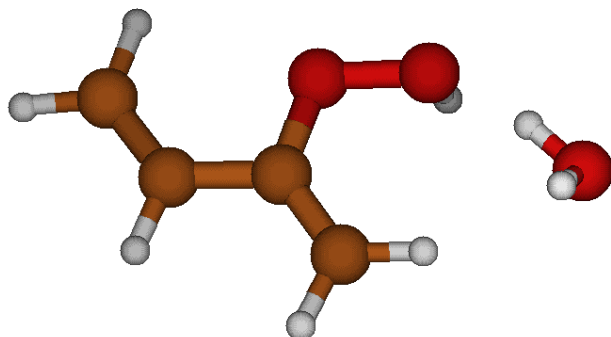
1	6	0	-2.972277	-0.290171	-0.372847
2	6	0	-2.055182	0.635098	-0.086673
3	6	0	-0.636063	0.381440	0.147514
4	6	0	0.254566	1.339591	0.419638
5	8	0	-0.364014	-0.968085	0.057762
6	8	0	1.030535	-1.245275	0.265897
7	1	0	-2.720133	-1.335983	-0.454635
8	1	0	-4.001668	-0.009159	-0.534025
9	1	0	-2.335247	1.676922	-0.013598
10	1	0	1.069701	-1.327877	1.229880
11	1	0	1.303531	1.151305	0.566346
12	1	0	-0.100017	2.355969	0.469892
13	1	0	2.684342	-0.271024	-0.457974
14	8	0	3.471506	0.276853	-0.364030
15	1	0	3.449001	0.856157	-1.128717

Frequencies --	26.3764	80.2553	93.4152
Frequencies --	120.3937	152.5259	181.4691
Frequencies --	192.0226	241.8137	298.0946
Frequencies --	363.9711	439.4282	465.5648
Frequencies --	500.1938	581.9594	735.3764
Frequencies --	774.9849	856.1208	881.4772
Frequencies --	929.2280	958.1029	988.1722
Frequencies --	1022.7305	1069.5849	1317.6924
Frequencies --	1328.8220	1389.0893	1432.1536
Frequencies --	1475.3027	1652.1241	1667.0065
Frequencies --	1715.4983	3178.0457	3195.6407
Frequencies --	3201.0007	3270.1964	3298.2980
Frequencies --	3744.2286	3783.1508	3907.6372

anti,trans…H₂O
Relative energy = -3.96 kcal mol⁻¹
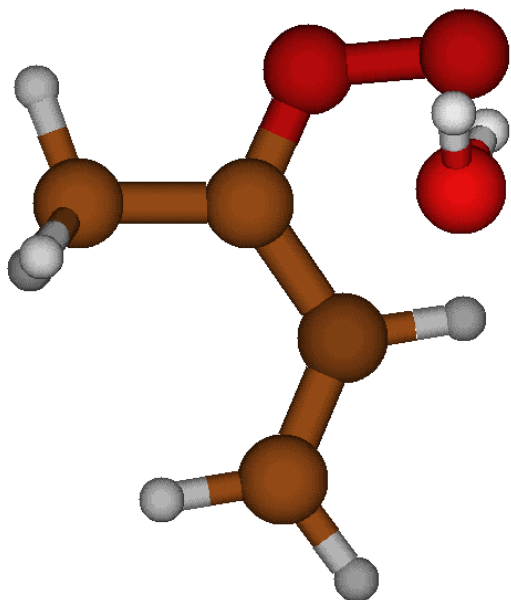
1	6	0	0.502759	-0.530908	-0.040525
2	8	0	-0.557746	-1.204586	-0.283864
3	8	0	-1.565217	-0.632306	-1.026483
4	8	0	-1.865696	1.189809	1.000324
5	1	0	-2.511715	0.878462	1.636905
6	1	0	-1.986430	0.602401	0.228125
7	6	0	0.700039	0.779689	-0.598049
8	6	0	1.794721	1.506221	-0.344643
9	1	0	-0.092263	1.135874	-1.235209
10	1	0	2.582188	1.158439	0.308080
11	1	0	1.919171	2.484508	-0.782971
12	6	0	1.475764	-1.233265	0.838470
13	1	0	1.115678	-2.233429	1.057719
14	1	0	1.589922	-0.684234	1.773165
15	1	0	2.453023	-1.295780	0.362849

Frequencies --	49.4309	69.1601	126.9246
Frequencies --	146.2738	162.4503	214.7714
Frequencies --	256.1720	308.5324	331.6080
Frequencies --	384.0414	405.0895	477.3556
Frequencies --	627.8561	722.8786	774.4368
Frequencies --	801.5273	934.0422	996.6085
Frequencies --	1001.7754	1049.3132	1057.4421
Frequencies --	1067.1525	1292.0431	1371.3492
Frequencies --	1430.2155	1434.0662	1470.9814
Frequencies --	1487.5212	1524.1467	1668.2012
Frequencies --	1678.2292	3063.0967	3126.1236
Frequencies --	3169.8606	3174.5228	3246.6946
Frequencies --	3267.5276	3506.6328	3891.2774

anti,cis…H₂O
Relative energy = -2.88 kcal mol⁻¹
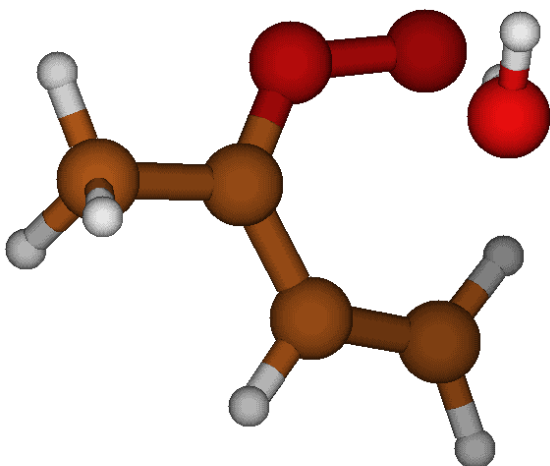
1	6	0	0.492942	2.001152	0.040826
2	6	0	-0.555963	1.257901	-0.353437
3	6	0	-0.897727	-0.073605	0.057168
4	8	0	-0.244460	-0.812669	0.871531
5	8	0	0.953912	-0.371673	1.382346
6	6	0	-2.127248	-0.729000	-0.473605
7	8	0	1.935971	-0.814562	-1.201091
8	1	0	0.599021	3.003775	-0.349259
9	1	0	1.218535	1.617969	0.733413
10	1	0	-1.260002	1.679944	-1.058260
11	1	0	-2.017349	-0.882065	-1.547889
12	1	0	-2.284155	-1.688865	0.007583
13	1	0	-2.997395	-0.093158	-0.316379
14	1	0	1.824254	-0.679011	-0.243089
15	1	0	2.281685	-1.706045	-1.274127

Frequencies --	44.1500	66.0818	125.6064
Frequencies --	142.2799	172.8292	194.7427
Frequencies --	300.0454	312.1421	329.9431
Frequencies --	368.6155	383.4176	413.4903
Frequencies --	634.2084	715.9449	734.7861
Frequencies --	818.1382	954.3371	1025.9549
Frequencies --	1032.6593	1033.4561	1054.7801
Frequencies --	1105.5990	1269.0253	1346.9081
Frequencies --	1416.0047	1459.6556	1469.2495
Frequencies --	1487.1046	1523.6652	1651.8002
Frequencies --	1674.5818	3058.5127	3120.1840
Frequencies --	3171.6983	3173.7647	3189.4565
Frequencies --	3316.6378	3580.4946	3892.2086

anti,trans…H₂O=anti,cis…H₂O

Geometry a

Relative energy = 2.97 kcal mol^{-1}
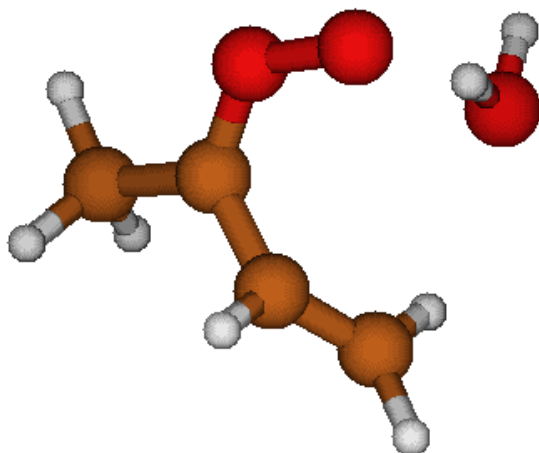
1	6	0	0.163221	2.016779	-0.114447
2	6	0	-0.689443	1.124935	-0.605383
3	6	0	-0.900523	-0.212897	-0.035092
4	6	0	-2.008865	-0.487804	0.913438
5	8	0	-0.193875	-1.214919	-0.349240
6	8	0	0.877192	-1.034809	-1.200961
7	1	0	0.825506	1.772397	0.702310
8	1	0	0.233200	2.998417	-0.558249
9	1	0	-1.329943	1.360660	-1.448599
10	1	0	-2.079190	-1.549448	1.130802
11	1	0	-2.950775	-0.126122	0.500633
12	1	0	-1.829912	0.066755	1.835683
13	1	0	1.937399	-0.377786	0.106745
14	8	0	2.213454	-0.006541	0.969978
15	1	0	2.633215	-0.740795	1.421361

Frequencies --	-156.8769	59.6181	126.7416
Frequencies --	160.2462	173.7484	202.2182
Frequencies --	235.2546	250.6306	313.5951
Frequencies --	337.1840	403.4059	523.8421
Frequencies --	614.4239	691.8397	795.5026
Frequencies --	808.5329	918.1595	992.5158
Frequencies --	1007.9969	1015.3548	1032.6755
Frequencies --	1108.1189	1284.3942	1330.6004
Frequencies --	1413.4804	1454.1093	1475.9875
Frequencies --	1478.2113	1543.2840	1677.6597
Frequencies --	1693.6016	3053.8027	3113.1901
Frequencies --	3153.9258	3165.7002	3173.2901
Frequencies --	3271.0651	3481.9512	3895.7840

Geometry b
Relative energy = 3.19 kcal mol^{-1}
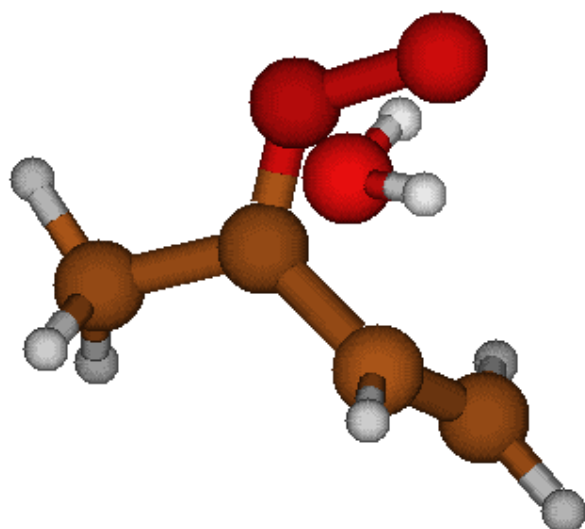
1	6	0	-1.410208	1.824285	0.014094
2	6	0	-0.693551	0.865838	-0.560421
3	6	0	-0.578340	-0.483883	0.008063
4	6	0	-1.368265	-1.621415	-0.524574
5	8	0	0.213131	-0.766137	0.955263
6	8	0	1.055931	0.214863	1.439151
7	1	0	-1.902529	1.675364	0.963950
8	1	0	-1.506085	2.794108	-0.449499
9	1	0	-0.171534	1.012741	-1.496436
10	1	0	-1.148627	-2.533229	0.022531
11	1	0	-1.119236	-1.759756	-1.578106
12	1	0	-2.432566	-1.393692	-0.471263
13	1	0	2.024410	0.185169	-0.096554
14	8	0	2.199222	0.025285	-1.046860
15	1	0	2.812077	0.718254	-1.298023

Frequencies --	-157.0894	48.1979	101.8422
Frequencies --	137.8273	152.8159	203.6406
Frequencies --	227.3128	257.8037	312.0105
Frequencies --	328.9664	470.3643	523.4228
Frequencies --	611.3910	693.7141	709.0625
Frequencies --	799.9243	911.9615	975.0008
Frequencies --	995.6496	1004.6362	1031.9230
Frequencies --	1103.8764	1277.8132	1323.6416
Frequencies --	1412.9140	1453.4750	1472.9391
Frequencies --	1478.6440	1544.1414	1695.4714
Frequencies --	1705.4387	3053.5222	3114.0954
Frequencies --	3167.5622	3170.9889	3194.4822
Frequencies --	3262.6214	3479.4929	3896.9657

anti,trans…H₂O=VHPOH
Geometry a
Relative energy = 9.50 kcal mol^{-1}
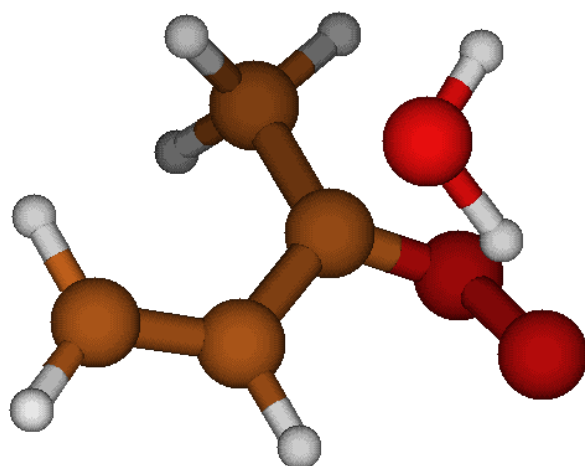
1	6	0	-0.060964	0.348874	-0.257893
2	8	0	1.104144	0.322443	-0.845143
3	8	0	1.775310	-0.892980	-0.423839
4	8	0	0.701112	-0.040932	1.549924
5	1	0	1.208043	0.740233	1.802977
6	1	0	1.368332	-0.593706	0.837969
7	6	0	-0.899577	-0.853879	-0.285482
8	6	0	-2.189293	-0.857695	0.045887
9	1	0	-0.392214	-1.739157	-0.634649
10	1	0	-2.693912	0.016126	0.430868
11	1	0	-2.777556	-1.757576	-0.050120
12	6	0	-0.666046	1.711249	-0.188051
13	1	0	0.116882	2.462255	-0.155407
14	1	0	-1.288423	1.792242	0.698268
15	1	0	-1.290405	1.880042	-1.064208

Frequencies --	-766.0672	76.9871	154.3111
Frequencies --	185.7923	276.3150	292.3097
Frequencies --	330.0388	404.9399	460.2178
Frequencies --	480.1778	598.7133	611.1162
Frequencies --	681.3080	716.3455	774.2926
Frequencies --	885.5082	950.6225	985.5434
Frequencies --	998.1127	1043.4725	1068.2890
Frequencies --	1115.4939	1293.4962	1340.9066
Frequencies --	1421.3128	1422.1262	1464.1920
Frequencies --	1497.9532	1518.3014	1609.4665
Frequencies --	1689.0270	1812.3004	3076.5471
Frequencies --	3151.2677	3174.0378	3177.1669
Frequencies --	3234.2172	3262.9730	3800.2828

Geometry b
Relative energy = 8.81 kcal mol^{-1}
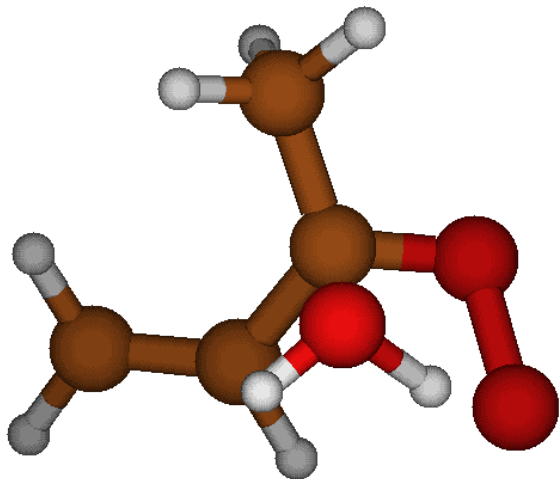
1	6	0	-0.049109	0.377978	-0.240168
2	8	0	1.126947	0.388183	-0.798726
3	8	0	1.792912	-0.850010	-0.447411
4	8	0	0.733872	-0.038785	1.548430
5	1	0	0.176333	-0.704826	1.963800
6	1	0	1.395115	-0.584810	0.834292
7	6	0	-0.883864	-0.824049	-0.364886
8	6	0	-2.178242	-0.861621	-0.047807
9	1	0	-0.366155	-1.676843	-0.776161
10	1	0	-2.695046	-0.018084	0.386214
11	1	0	-2.758985	-1.755870	-0.216151
12	6	0	-0.651197	1.732970	-0.089070
13	1	0	0.135311	2.461576	0.073332
14	1	0	-1.331641	1.744906	0.756808
15	1	0	-1.210309	1.987181	-0.988886

Frequencies --	-745.1645	98.5291	128.3402
Frequencies --	194.7012	274.9690	290.1252
Frequencies --	329.9074	410.0732	459.4679
Frequencies --	470.8369	595.8293	641.6124
Frequencies --	694.0950	719.1753	783.4741
Frequencies --	891.0935	957.4582	983.9842
Frequencies --	1001.3301	1046.8400	1070.7165
Frequencies --	1104.6322	1290.1523	1336.0323
Frequencies --	1419.1908	1426.2368	1460.3318
Frequencies --	1495.2773	1507.5237	1542.5180
Frequencies --	1683.1166	1875.6883	3076.8297
Frequencies --	3154.3186	3172.1687	3186.0913
Frequencies --	3227.7811	3260.6458	3832.2368

VHPOH
Geometry a
Relative energy = -26.38 kcal mol^{-1}
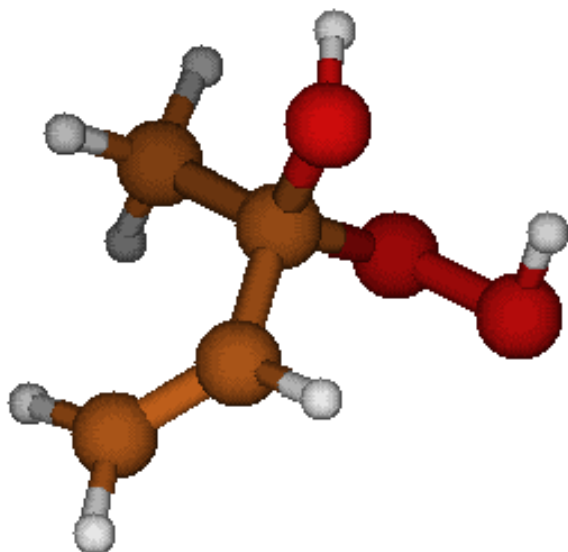
1	6	0	0.001754	0.347355	0.079629
2	8	0	1.051787	0.024753	-0.839713
3	8	0	1.782266	-1.118200	-0.334030
4	8	0	0.574729	0.682899	1.333042
5	1	0	0.996464	1.544131	1.240056
6	1	0	2.202669	-0.729864	0.447526
7	6	0	-0.887106	-0.836140	0.342141
8	6	0	-2.147870	-0.951168	-0.054476
9	1	0	-0.412260	-1.633597	0.893732
10	1	0	-2.656790	-0.177400	-0.609821
11	1	0	-2.715262	-1.842351	0.168318
12	6	0	-0.668586	1.541389	-0.571433
13	1	0	0.066826	2.331241	-0.717579
14	1	0	-1.464649	1.907590	0.070566
15	1	0	-1.076413	1.276020	-1.542358

Frequencies --	58.8681	156.1299	239.5871
Frequencies --	248.4048	288.6436	295.5697
Frequencies --	365.4981	388.6557	404.7531
Frequencies --	454.2048	497.3250	628.5350
Frequencies --	723.2871	762.0343	870.0899
Frequencies --	945.1639	953.4268	970.2892
Frequencies --	1032.0665	1039.5753	1130.1690
Frequencies --	1150.7350	1218.8760	1336.6346
Frequencies --	1394.7020	1406.2260	1426.3282
Frequencies --	1467.5029	1498.6449	1519.3882
Frequencies --	1714.0146	3071.3160	3146.1692
Frequencies --	3169.5006	3171.8245	3215.1879
Frequencies --	3255.8783	3730.8872	3803.7581

Geometry b
Relative energy = -28.54 kcal mol^{-1}
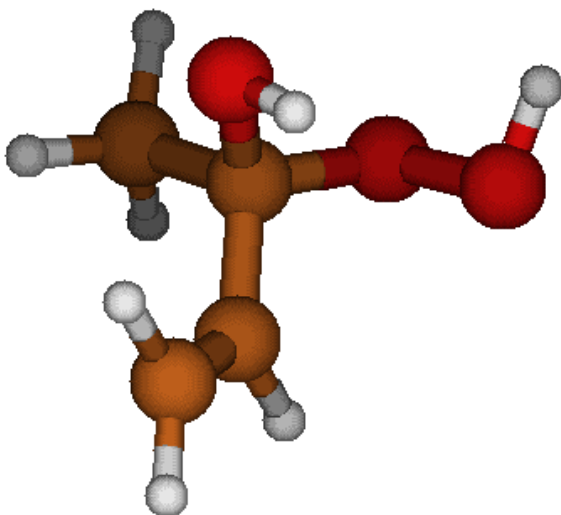
1	6	0	0.032573	0.409777	0.025494
2	8	0	1.329446	0.066005	-0.483071
3	8	0	1.574135	-1.323887	-0.127835
4	8	0	-0.003684	0.310457	1.420449
5	1	0	-0.024930	-0.630092	1.629284
6	1	0	2.277763	-1.198049	0.521191
7	6	0	-1.009151	-0.448695	-0.646571
8	6	0	-2.101219	-0.908592	-0.048255
9	1	0	-0.819681	-0.653808	-1.691858
10	1	0	-2.305128	-0.695446	0.991393
11	1	0	-2.824483	-1.502635	-0.586370
12	6	0	-0.103454	1.876792	-0.341807
13	1	0	0.699993	2.439694	0.126850
14	1	0	-1.060952	2.240390	0.019827
15	1	0	-0.054246	2.003651	-1.419824

Frequencies --	93.2146	136.8482	197.3803
Frequencies --	218.2526	254.2255	293.6399
Frequencies --	311.3784	382.2208	458.2974
Frequencies --	501.9114	533.1771	602.3731
Frequencies --	716.4808	773.6692	876.0991
Frequencies --	937.6960	968.8371	976.2985
Frequencies --	1040.2922	1048.1515	1102.0556
Frequencies --	1171.2961	1263.8172	1319.8772
Frequencies --	1359.9256	1385.0481	1422.5130
Frequencies --	1458.0122	1496.6490	1501.7827
Frequencies --	1703.6625	3077.6217	3161.2562
Frequencies --	3165.8904	3167.6871	3191.8615
Frequencies --	3255.2450	3781.7822	3803.4998

anti,trans…H₂O=AHP…H₂O
Geometry a
Relative energy = 21.68 kcal mol^{-1}
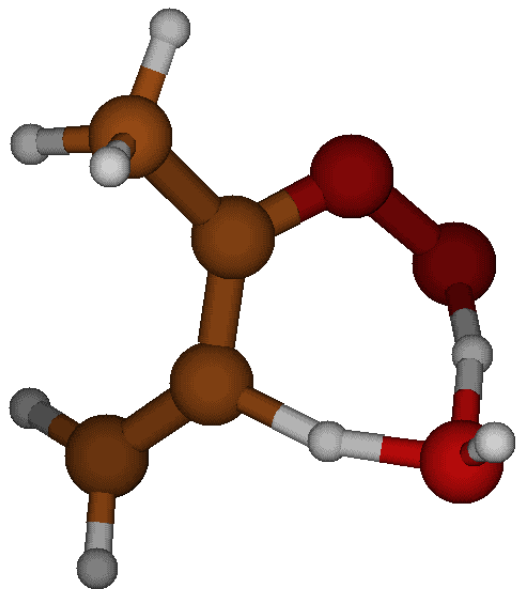
1	6	0	0.303404	0.974816	0.038461
2	6	0	0.721753	-0.363217	0.033286
3	8	0	-0.051964	-1.360414	-0.260270
4	8	0	-1.314260	-1.032972	-0.861754
5	1	0	-0.901826	0.988992	0.565484
6	6	0	0.875077	2.033302	-0.534223
7	6	0	2.036767	-0.805764	0.580613
8	1	0	0.493652	3.029386	-0.356569
9	1	0	1.691124	1.951182	-1.244506
10	1	0	-1.808729	-0.332866	-0.079944
11	8	0	-2.124658	0.607173	0.704286
12	1	0	-2.277368	0.299361	1.603439
13	1	0	2.141304	-0.471189	1.610843
14	1	0	2.827595	-0.324473	0.003950
15	1	0	2.139292	-1.885511	0.530385

Frequencies --	-1617.1316	93.4341	117.5596
Frequencies --	156.1532	209.3185	266.2491
Frequencies --	295.0504	341.4218	469.3560
Frequencies --	513.9825	543.1889	602.5271
Frequencies --	638.5084	661.9232	752.1415
Frequencies --	820.5784	912.6893	991.3215
Frequencies --	1033.8029	1043.2842	1096.6395
Frequencies --	1245.0686	1308.4410	1381.8822
Frequencies --	1392.0930	1406.5819	1436.8604
Frequencies --	1479.1749	1489.8744	1534.4171
Frequencies --	1546.3747	1713.7599	1734.7203
Frequencies --	3060.6175	3122.2553	3128.8256
Frequencies --	3169.5414	3214.8391	3831.7935

Geometry b
Relative energy = 21.29 kcal mol^{-1}
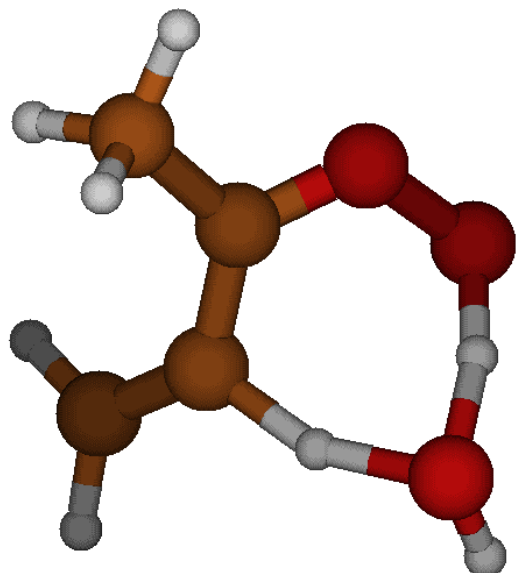
1	6	0	0.283133	0.977742	0.030655
2	6	0	0.726868	-0.353668	0.029436
3	8	0	-0.024171	-1.366579	-0.265828
4	8	0	-1.303151	-1.062739	-0.842170
5	1	0	-0.905621	0.969589	0.580006
6	6	0	0.847140	2.039157	-0.544843
7	6	0	2.048331	-0.767424	0.581303
8	1	0	0.457560	3.033309	-0.372753
9	1	0	1.668587	1.962416	-1.249286
10	1	0	-1.789679	-0.384301	-0.046939
11	8	0	-2.078768	0.492468	0.839930
12	1	0	-2.754779	1.084097	0.494161
13	1	0	2.124963	-0.453197	1.620590
14	1	0	2.832246	-0.249426	0.027996
15	1	0	2.182611	-1.842534	0.511462

Frequencies --	-1579.1606	90.0409	123.4064
Frequencies --	157.6379	209.5987	266.6685
Frequencies --	294.7909	347.5860	455.0434
Frequencies --	526.7034	567.4724	582.2499
Frequencies --	634.0059	685.5202	746.8656
Frequencies --	824.8423	914.8717	985.9504
Frequencies --	1034.7025	1046.2654	1102.7353
Frequencies --	1199.5851	1260.8384	1311.7191
Frequencies --	1351.3159	1402.1852	1432.7856
Frequencies --	1478.6880	1489.9102	1536.7907
Frequencies --	1614.6585	1729.0537	1824.8393
Frequencies --	3061.5159	3122.5845	3129.5143
Frequencies --	3170.0530	3211.7163	3833.7874

AHP…H₂O
Geometry a
Relative energy = -6.91 kcal mol⁻¹
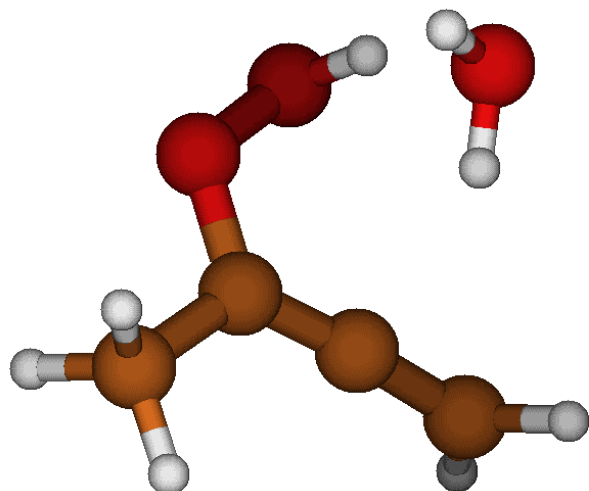
1	6	0	-0.624401	1.015594	0.112446
2	6	0	-0.838068	-0.272220	-0.011432
3	8	0	-0.019619	-1.265056	0.480104
4	8	0	1.016691	-0.712630	1.318904
5	1	0	1.437880	0.546875	-1.183862
6	6	0	-0.516771	2.305151	0.284470
7	6	0	-1.993133	-0.889772	-0.737307
8	1	0	0.025645	2.936970	-0.408967
9	1	0	-0.959780	2.797947	1.141972
10	1	0	1.673610	-0.467461	0.634004
11	8	0	2.279214	0.105767	-1.012504
12	1	0	2.290861	-0.640922	-1.617613
13	1	0	-1.639204	-1.544723	-1.533165
14	1	0	-2.620793	-0.115184	-1.166175
15	1	0	-2.584264	-1.490670	-0.047285

Frequencies --	51.8862	76.4725	146.2370
Frequencies --	149.3252	156.9621	179.0429
Frequencies --	223.6477	233.4389	283.4862
Frequencies --	295.0367	426.1347	444.3698
Frequencies --	477.3723	635.3040	654.5487
Frequencies --	761.0903	778.5411	923.2105
Frequencies --	930.7934	1012.9331	1041.7696
Frequencies --	1072.9719	1207.7811	1335.0640
Frequencies --	1416.8419	1485.5980	1493.4692
Frequencies --	1510.8598	1523.8538	1646.0169
Frequencies --	2049.9484	3058.6593	3119.6405
Frequencies --	3121.2609	3166.0610	3190.6588
Frequencies --	3517.0725	3762.6274	3890.1968
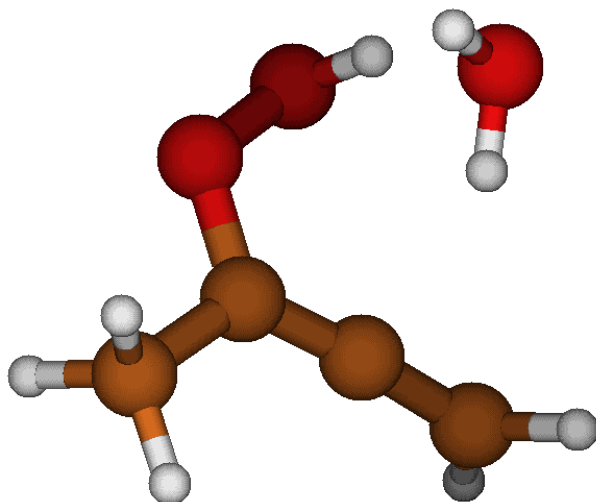
1	6	0	0.415322	1.067370	-0.181275
2	6	0	0.898486	-0.135078	0.022591
3	8	0	0.305726	-1.310940	-0.374304
4	8	0	-0.848575	-1.057362	-1.201633
5	1	0	-1.457498	0.286146	1.218656
6	6	0	0.043327	2.293374	-0.433067
7	6	0	2.167949	-0.438246	0.756979
8	1	0	-0.601963	2.850620	0.236544
9	1	0	0.363287	2.807794	-1.331718
10	1	0	-1.524717	-0.909587	-0.508296
11	8	0	-2.264835	-0.213564	1.043798
12	1	0	-2.922905	0.456118	0.838981
13	1	0	1.968488	-1.088860	1.607745
14	1	0	2.623666	0.481615	1.109145
15	1	0	2.862612	-0.953435	0.094687

```
Frequencies --      50.1646             87.0192            142.9584
Frequencies --     149.3477            158.7080            167.0358
Frequencies --     223.7866            234.6360            288.6377
Frequencies --     318.4374            418.3033            442.6383
Frequencies --     477.3767            632.9827            654.9138
Frequencies --     697.2521            778.8863            920.4341
Frequencies --     929.4444           1014.8930           1042.0460
Frequencies --    1073.3720           1210.0207           1335.2911
Frequencies --    1416.6933           1485.7834           1493.5879
Frequencies --    1523.2201           1533.2856           1650.6912
Frequencies --    2048.0531           3060.5511           3116.9570
Frequencies --    3122.8288           3166.5824           3185.3278
Frequencies --    3525.1606           3761.1085           3891.0181
```

anti,cis…H₂O=VHPOH
Geometry a
Relative energy = 10.86 kcal mol^{-1}
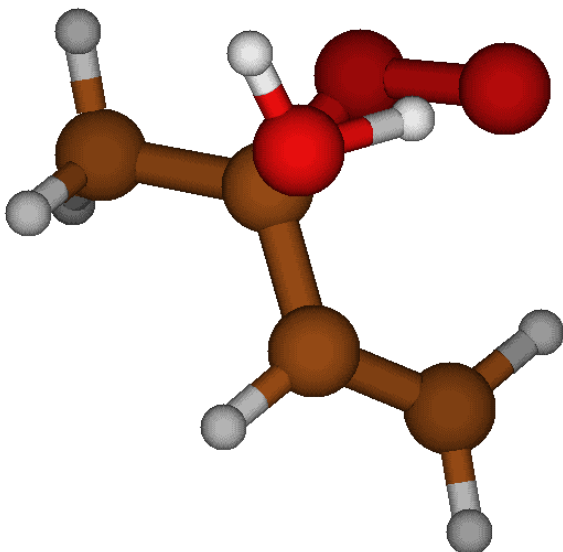
1	6	0	-0.388508	-0.350380	-0.210752
2	8	0	-0.311195	0.656681	-1.023936
3	8	0	0.601097	1.645685	-0.463307
4	8	0	-0.678676	0.806967	1.410648
5	1	0	-1.555363	1.198982	1.318992
6	1	0	-0.027221	1.412091	0.748594
7	6	0	0.772650	-1.023489	0.390931
8	6	0	2.037656	-0.802011	0.040803
9	1	0	0.518239	-1.797717	1.100519
10	1	0	2.291957	-0.006970	-0.641497
11	1	0	2.828880	-1.412160	0.450715
12	6	0	-1.621623	-1.174340	-0.395128
13	1	0	-2.430924	-0.569185	-0.790990
14	1	0	-1.908420	-1.609399	0.558707
15	1	0	-1.408009	-1.988985	-1.087403

Frequencies --	-674.5780	101.8342	148.5727
Frequencies --	195.1035	268.4223	281.8501
Frequencies --	314.7528	394.0978	396.6247
Frequencies --	500.2505	605.5288	617.5990
Frequencies --	664.3580	698.1845	791.3388
Frequencies --	877.3650	990.8995	1009.3404
Frequencies --	1018.1333	1021.4220	1089.3939
Frequencies --	1159.3065	1250.3718	1344.9554
Frequencies --	1409.2663	1451.0265	1465.6964
Frequencies --	1493.0244	1536.3723	1609.0816
Frequencies --	1689.2386	1824.0412	3068.0849
Frequencies --	3141.3853	3174.9886	3176.1005
Frequencies --	3203.7723	3280.3937	3804.9265

Geometry b
Relative energy = 11.00 kcal mol^{-1}
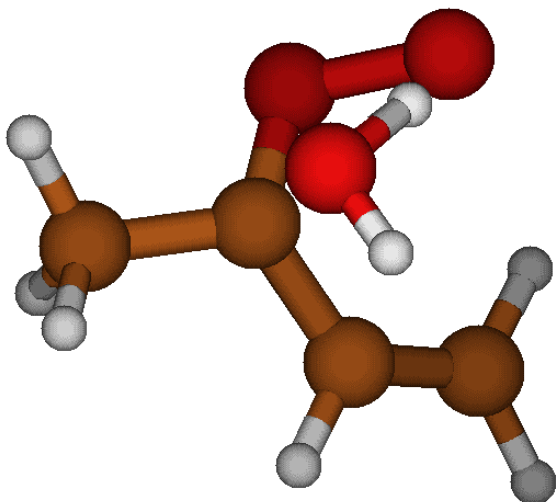
1	6	0	-0.428855	-0.318181	-0.214489
2	8	0	-0.313221	0.702025	-1.004512
3	8	0	0.684613	1.612693	-0.461079
4	8	0	-0.673337	0.866203	1.388133
5	1	0	0.026316	1.433773	0.739005
6	1	0	-0.134718	0.530033	2.112040
7	6	0	0.706631	-1.096416	0.310396
8	6	0	1.985905	-0.906269	-0.011407
9	1	0	0.415112	-1.934469	0.929974
10	1	0	2.282551	-0.062393	-0.613191
11	1	0	2.739967	-1.596739	0.337253
12	6	0	-1.728696	-1.037255	-0.364871
13	1	0	-1.988267	-1.516079	0.575210
14	1	0	-1.625876	-1.811000	-1.126488
15	1	0	-2.509427	-0.341773	-0.651905

Frequencies --	-696.1114	103.3479	118.4113
Frequencies --	203.6312	272.2101	281.8229
Frequencies --	316.3765	393.6546	401.9063
Frequencies --	486.6747	614.5843	635.4449
Frequencies --	674.1498	699.6737	796.5493
Frequencies --	884.5974	983.6792	1013.6366
Frequencies --	1021.5052	1030.7381	1085.6974
Frequencies --	1132.4333	1246.3111	1344.4397
Frequencies --	1411.6678	1445.7731	1457.4424
Frequencies --	1491.9088	1506.4974	1570.4516
Frequencies --	1683.7050	1870.9907	3068.2243
Frequencies --	3144.8718	3170.5353	3184.8291
Frequencies --	3187.6561	3280.2180	3831.2141

VHPOH
Geometry a
Relative energy = -26.98 kcal mol^{-1}
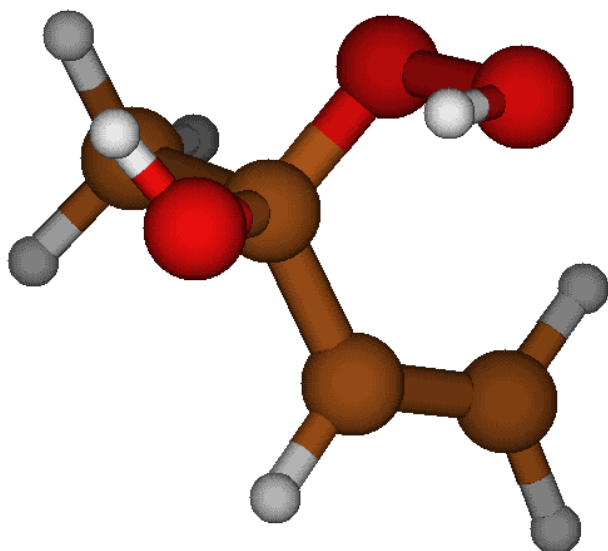
1	6	0	-0.434176	-0.223139	0.049316
2	8	0	-0.160154	0.856789	-0.832798
3	8	0	0.630349	1.851133	-0.134189
4	8	0	-1.108875	0.267069	1.199004
5	1	0	-2.004795	0.501023	0.932304
6	1	0	0.059178	2.025786	0.630414
7	6	0	0.794731	-0.936398	0.544691
8	6	0	1.981395	-0.871087	-0.042331
9	1	0	0.632025	-1.554498	1.417612
10	1	0	2.144981	-0.238779	-0.901861
11	1	0	2.819228	-1.437488	0.335679
12	6	0	-1.326945	-1.138142	-0.775903
13	1	0	-2.234171	-0.610141	-1.070451
14	1	0	-1.593511	-2.010144	-0.183830
15	1	0	-0.803526	-1.463096	-1.670639

Frequencies --		
97.3360	173.2096	221.3963
238.3839	285.0856	306.4104
327.0645	392.1530	449.3677
457.3646	568.7384	601.2449
697.1390	775.6259	882.3414
943.5583	962.9693	977.3258
1028.4957	1052.4216	1112.5386
1180.3117	1204.4873	1320.9402
1382.0702	1411.3412	1423.8875
1460.7418	1493.7442	1508.8581
1712.7621	3059.5616	3139.2879
3163.6236	3171.4476	3191.4398
3264.4236	3705.7594	3801.7305

Geometry b
Relative energy = -27.83 kcal mol^{-1}
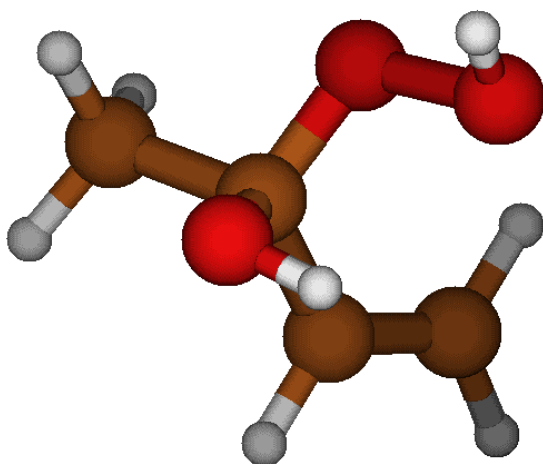
1	6	0	-0.479325	-0.185478	0.054686
2	8	0	-0.043901	0.860097	-0.822213
3	8	0	0.824881	1.746865	-0.064732
4	8	0	-1.093485	0.345171	1.202741
5	1	0	0.230724	2.502545	0.028156
6	1	0	-0.387751	0.688009	1.761486
7	6	0	0.650511	-1.107595	0.437219
8	6	0	1.868978	-1.083358	-0.087795
9	1	0	0.387891	-1.836997	1.193870
10	1	0	2.139508	-0.357824	-0.839729
11	1	0	2.624074	-1.786888	0.230389
12	6	0	-1.551043	-0.894863	-0.751128
13	1	0	-1.889533	-1.771492	-0.204763
14	1	0	-1.149149	-1.205883	-1.711360
15	1	0	-2.390446	-0.220771	-0.902306

Frequencies --	104.1417	154.0731	208.2934
Frequencies --	226.2055	251.2813	299.7956
Frequencies --	325.5446	374.7833	438.7487
Frequencies --	477.1720	561.6252	605.3659
Frequencies --	705.1873	773.2915	882.3863
Frequencies --	935.0130	968.1711	980.5835
Frequencies --	1034.9798	1048.6518	1099.8717
Frequencies --	1194.6209	1238.5412	1324.2960
Frequencies --	1367.9514	1384.6870	1423.8268
Frequencies --	1459.4309	1497.2096	1500.4669
Frequencies --	1706.8475	3075.9029	3158.4723
Frequencies --	3165.3588	3166.8158	3179.7441
Frequencies --	3263.8458	3776.7739	3810.2997

anti,cis…H₂O=VHPOH'

Geometry a

Relative energy = 11.74 kcal mol^{-1}
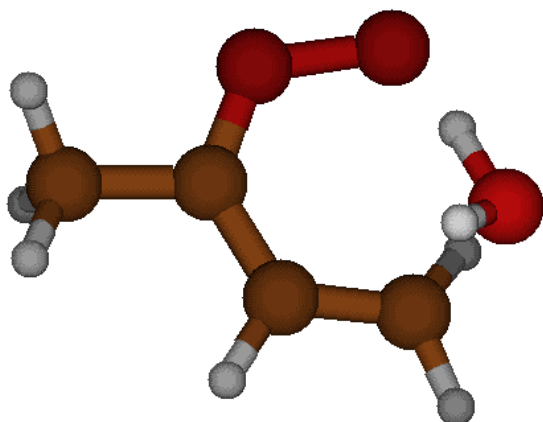
1	6	0	1.181696	-1.105939	-0.621422
2	6	0	-0.123216	-1.180428	-0.152020
3	6	0	-1.011849	-0.110341	-0.021072
4	8	0	-0.739039	1.154097	-0.083319
5	8	0	0.599650	1.560576	-0.359944
6	6	0	-2.459627	-0.341139	0.286392
7	8	0	2.227800	-0.005548	0.668072
8	1	0	1.775451	-2.008299	-0.617786
9	1	0	1.463794	-0.353269	-1.332398
10	1	0	-0.483472	-2.124135	0.229730
11	1	0	-2.578998	-1.209829	0.928832
12	1	0	-2.891005	0.532767	0.765251
13	1	0	-3.001900	-0.532278	-0.639758
14	1	0	1.549947	0.754006	0.378732
15	1	0	1.936864	-0.304869	1.537654

Frequencies --	-451.3264	65.0174	110.6201
Frequencies --	227.7562	278.6256	304.7792
Frequencies --	319.7197	408.6109	448.6185
Frequencies --	562.8341	613.3668	656.3177
Frequencies --	704.6316	739.7717	831.8753
Frequencies --	890.6157	991.4057	1040.1498
Frequencies --	1057.7057	1112.3887	1157.8441
Frequencies --	1229.5522	1258.1369	1290.5621
Frequencies --	1416.7735	1448.8475	1485.2244
Frequencies --	1493.4663	1541.9056	1565.1270
Frequencies --	1697.3704	2060.1566	3066.0558
Frequencies --	3134.0600	3168.0256	3188.4964
Frequencies --	3204.9873	3305.3259	3809.4140

Geometry b
Relative energy = 11.65 kcal mol^{-1}
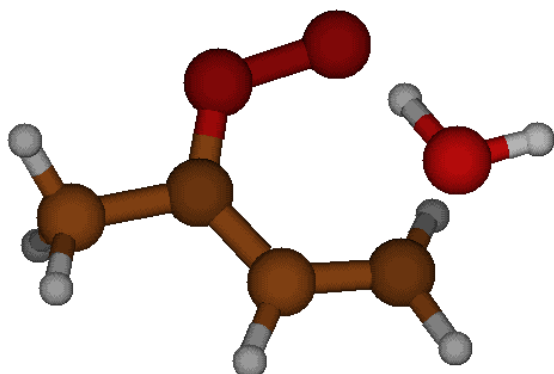
1	6	0	1.176175	-1.119960	-0.598814
2	6	0	-0.134488	-1.181748	-0.143371
3	6	0	-1.015770	-0.108200	-0.022925
4	8	0	-0.739086	1.156601	-0.097632
5	8	0	0.611049	1.541843	-0.359195
6	6	0	-2.464637	-0.327176	0.288110
7	8	0	2.115162	-0.049638	0.772260
8	1	0	1.758732	-2.029269	-0.572430
9	1	0	1.459437	-0.382629	-1.325916
10	1	0	-0.495723	-2.115499	0.259617
11	1	0	-2.589570	-1.205918	0.915094
12	1	0	-2.882251	0.542530	0.786521
13	1	0	-3.014704	-0.493190	-0.638297
14	1	0	1.483994	0.741569	0.412075
15	1	0	3.015408	0.174462	0.501871

Frequencies --	-519.6163	53.1173	109.6619
Frequencies --	227.0268	285.2376	306.7603
Frequencies --	321.4268	417.5422	439.8591
Frequencies --	573.6071	613.3627	657.9144
Frequencies --	732.2839	740.1208	835.3925
Frequencies --	891.0237	983.4814	1040.2060
Frequencies --	1059.3293	1104.9590	1120.0779
Frequencies --	1207.9229	1254.7307	1292.0503
Frequencies --	1416.7748	1445.4571	1485.1901
Frequencies --	1493.8964	1537.9054	1551.6986
Frequencies --	1718.6760	1890.5637	3066.4609
Frequencies --	3135.6372	3168.8694	3184.9716
Frequencies --	3210.8343	3299.5086	3782.1838

VHPOH'
Geometry a
Relative energy = -20.65 kcal mol^{-1}
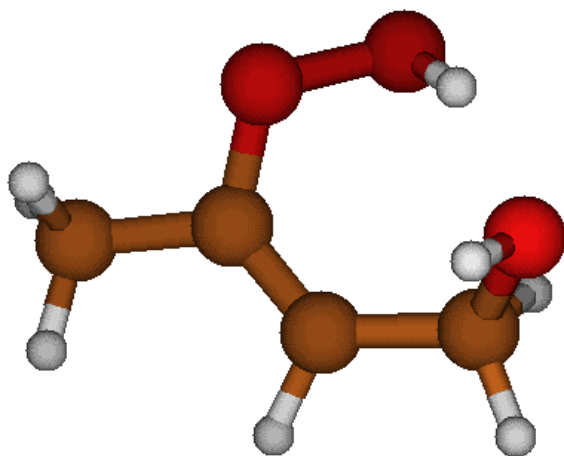
1	6	0	1.502722	-0.866820	-0.424407
2	6	0	0.028286	-1.103276	-0.299031
3	6	0	-0.942073	-0.215242	-0.032206
4	8	0	-0.834620	1.133058	0.142981
5	8	0	0.371928	1.700828	-0.412714
6	6	0	-2.375012	-0.588153	0.191714
7	8	0	2.042984	-0.075121	0.660001
8	1	0	2.017835	-1.826773	-0.458795
9	1	0	1.765791	-0.313658	-1.321493
10	1	0	-0.304730	-2.126605	-0.386805
11	1	0	-2.496462	-1.666392	0.158629
12	1	0	-2.712873	-0.225529	1.162021
13	1	0	-3.005813	-0.129206	-0.568223
14	1	0	1.056242	1.343666	0.193923
15	1	0	1.754139	-0.484672	1.482180

Frequencies --	116.9832	136.7951	170.9232
Frequencies --	237.4197	272.5092	318.6126
Frequencies --	356.1842	420.0098	486.2482
Frequencies --	596.2211	679.0309	733.6570
Frequencies --	769.3643	836.9906	914.3297
Frequencies --	972.5143	1024.5142	1035.6495
Frequencies --	1076.8781	1118.5148	1194.8865
Frequencies --	1224.5794	1364.2247	1379.0228
Frequencies --	1418.7083	1427.0220	1484.0339
Frequencies --	1503.6347	1510.8655	1527.3541
Frequencies --	1712.0466	3062.2105	3066.9710
Frequencies --	3122.0853	3129.4466	3162.2357
Frequencies --	3205.1317	3476.1743	3810.9337
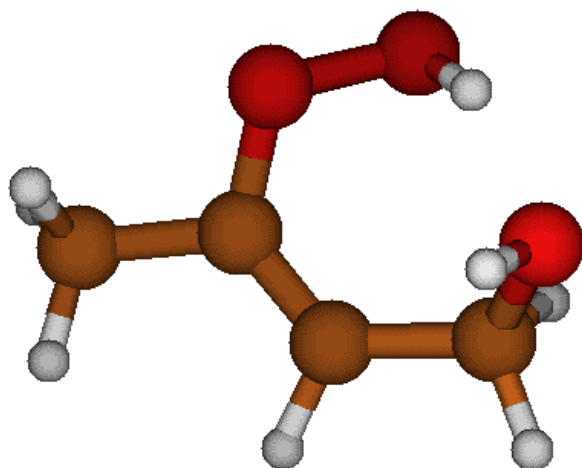
1	6	0	1.490886	-0.866167	-0.425176
2	6	0	0.023667	-1.098123	-0.255849
3	6	0	-0.958991	-0.213597	-0.032898
4	8	0	-0.886408	1.142335	0.080062
5	8	0	0.369535	1.697329	-0.364033
6	6	0	-2.385128	-0.603828	0.207766
7	8	0	1.999327	-0.121700	0.711889
8	1	0	1.992591	-1.832336	-0.470572
9	1	0	1.714718	-0.316972	-1.339932
10	1	0	-0.297312	-2.128072	-0.265130
11	1	0	-2.490620	-1.683769	0.181673
12	1	0	-2.717309	-0.240502	1.179539
13	1	0	-3.030243	-0.160094	-0.549227
14	1	0	0.998547	1.315318	0.284585
15	1	0	2.947393	-0.006993	0.592666

Frequencies --	114.1636	131.0879	164.6963
Frequencies --	231.3946	270.9307	319.2052
Frequencies --	362.3171	390.3695	483.7937
Frequencies --	592.0545	651.4890	697.8492
Frequencies --	765.7936	837.5721	918.0522
Frequencies --	988.3888	1025.9377	1061.2584
Frequencies --	1078.2323	1112.2956	1210.9950
Frequencies --	1241.9220	1283.1551	1387.3697
Frequencies --	1422.5277	1453.1533	1483.9119
Frequencies --	1505.1795	1521.8337	1531.5533
Frequencies --	1720.5676	3052.8464	3063.1287
Frequencies --	3092.5907	3123.0977	3163.6576
Frequencies --	3212.8775	3492.0836	3817.3314

syn,trans…SO₂
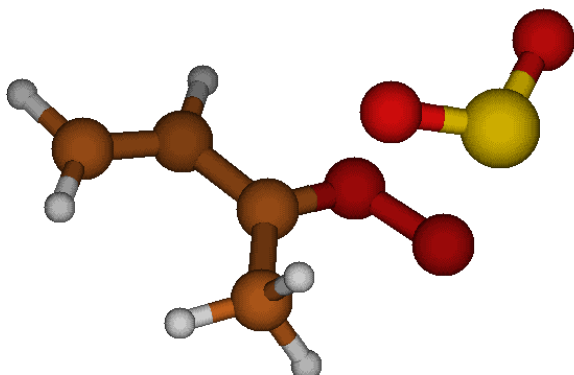
1	6	0	1.311109	0.345350	-0.209375
2	8	0	0.362537	0.503429	-1.056591
3	8	0	-0.632142	1.399004	-0.710766
4	6	0	1.409318	1.217912	0.974013
5	6	0	2.242344	-0.684275	-0.604152
6	1	0	1.155129	2.232114	0.669745
7	1	0	0.660746	0.906862	1.700368
8	1	0	2.397493	1.173493	1.416686
9	1	0	1.999064	-1.194353	-1.525464
10	6	0	3.318454	-1.029680	0.110503
11	1	0	3.572002	-0.548981	1.042587
12	1	0	3.967801	-1.822831	-0.226365
13	16	0	-2.051709	-0.120369	0.400535
14	8	0	-0.930287	-0.777883	1.093355
15	8	0	-2.626639	-0.864081	-0.715005

Frequencies --	43.9908	59.0891	107.1044
Frequencies --	120.3070	151.7698	153.3231
Frequencies --	201.5872	270.5415	291.4578
Frequencies --	340.6993	359.4257	456.4786
Frequencies --	496.1234	526.9041	600.8922
Frequencies --	688.5251	809.4764	942.7130
Frequencies --	995.3231	1014.8939	1028.0444
Frequencies --	1049.5269	1071.1873	1106.3835
Frequencies --	1278.9453	1312.2044	1343.8888
Frequencies --	1398.1147	1454.0322	1471.3221
Frequencies --	1504.1864	1506.2464	1675.7023
Frequencies --	3074.6456	3138.7306	3182.0912
Frequencies --	3189.5210	3209.4786	3275.2279

syn-trans…SO₂ = SOZ
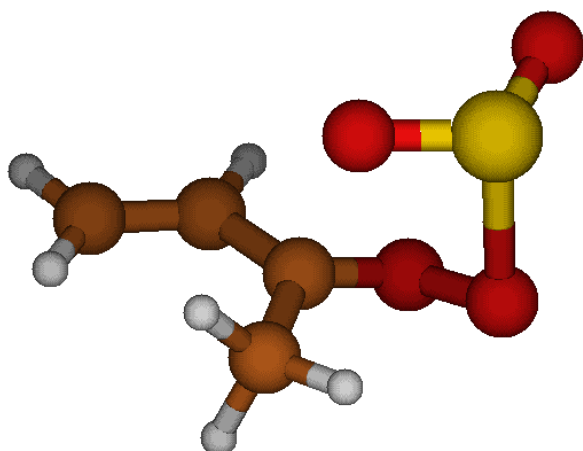
1	6	0	-1.048953	0.326164	0.232035
2	8	0	-0.167040	0.505860	1.168655
3	8	0	0.930174	1.285150	0.769924
4	6	0	-1.349697	1.366447	-0.783806
5	6	0	-1.954410	-0.760475	0.558780
6	1	0	-0.507744	2.036212	-0.890137
7	1	0	-1.580017	0.907446	-1.738432
8	1	0	-2.222431	1.924200	-0.436409
9	1	0	-1.641755	-1.390528	1.378690
10	6	0	-3.082346	-0.997546	-0.113981
11	1	0	-3.393034	-0.385517	-0.947113
12	1	0	-3.718728	-1.826951	0.153285
13	16	0	1.811584	-0.131809	-0.473040
14	8	0	0.483112	-0.516972	-1.065376
15	8	0	2.340104	-1.119471	0.463120

Frequencies --	-172.4600	72.5411	96.7084
Frequencies --	176.3007	188.1187	203.9954
Frequencies --	244.3385	277.0329	354.5020
Frequencies --	375.1692	427.1594	478.1019
Frequencies --	495.1429	552.4431	596.1116
Frequencies --	690.2365	801.6257	940.5472
Frequencies --	978.0869	1001.8076	1008.0748
Frequencies --	1028.9826	1068.6190	1077.9155
Frequencies --	1243.4173	1310.4264	1349.2203
Frequencies --	1401.5745	1443.9629	1464.9777
Frequencies --	1497.4740	1504.4880	1683.5791
Frequencies --	3058.6222	3161.8023	3181.6111
Frequencies --	3215.2830	3218.4911	3272.7976

SOZ
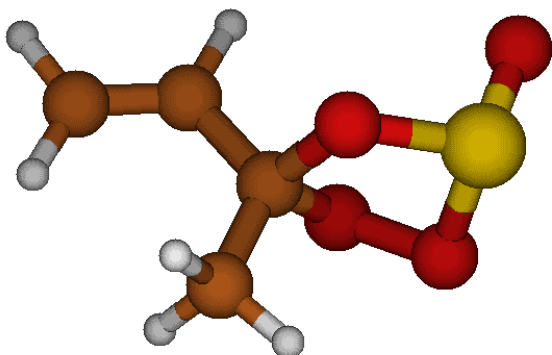
1	6	0	-0.810866	0.210377	-0.022436
2	8	0	-0.115855	0.371045	1.209972
3	8	0	1.142045	1.007981	0.821016
4	6	0	-1.420496	1.503020	-0.509191
5	6	0	-1.728288	-0.951062	0.204200
6	1	0	-0.645604	2.261924	-0.563145
7	1	0	-1.850944	1.365390	-1.497444
8	1	0	-2.191085	1.835134	0.181579
9	1	0	-1.216624	-1.851468	0.514245
10	6	0	-3.044724	-0.918906	0.041466
11	1	0	-3.566516	-0.026945	-0.270702
12	1	0	-3.641479	-1.801243	0.215963
13	16	0	1.739115	-0.003209	-0.404496
14	8	0	0.207454	-0.208514	-0.981424
15	8	0	2.180438	-1.269514	0.151336

Frequencies --	72.1395	83.9393	185.3454
Frequencies --	255.6892	287.8302	290.3490
Frequencies --	323.3446	383.4275	426.5892
Frequencies --	474.0264	485.8914	560.9295
Frequencies --	643.5201	651.0299	664.1314
Frequencies --	744.0322	788.4121	835.6166
Frequencies --	895.6685	934.7505	986.8967
Frequencies --	1034.2859	1036.2261	1117.0259
Frequencies --	1187.2859	1259.7703	1299.4224
Frequencies --	1332.1137	1421.2332	1461.7920
Frequencies --	1501.2734	1508.2993	1709.3089
Frequencies --	3081.2734	3162.8175	3168.5959
Frequencies --	3177.2524	3205.3243	3264.6000

SOZ = SOZ'
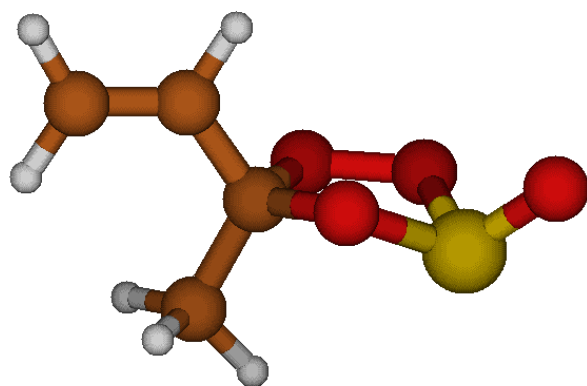
1	6	0	-0.847639	0.162309	-0.060086
2	16	0	1.700713	0.153586	-0.346480
3	8	0	1.138013	0.406572	1.241100
4	8	0	-0.302221	0.585166	1.238309
5	8	0	0.208035	-0.466602	-0.766873
6	6	0	-1.334630	1.398666	-0.782488
7	6	0	-1.865589	-0.890803	0.245541
8	1	0	-2.098553	1.900783	-0.194820
9	1	0	-1.739638	1.131311	-1.755411
10	1	0	-0.502821	2.084971	-0.922412
11	6	0	-3.163093	-0.797152	-0.016721
12	1	0	-1.448557	-1.762579	0.730602
13	1	0	-3.594198	0.067877	-0.497806
14	1	0	-3.837443	-1.597243	0.248066
15	8	0	2.615612	-0.965213	-0.260288

Frequencies --	-180.1149	54.0427	89.1287
Frequencies --	244.6280	271.3617	281.1275
Frequencies --	295.3848	366.1179	392.3921
Frequencies --	435.7800	468.1111	544.9621
Frequencies --	599.8537	656.1245	694.0788
Frequencies --	732.2315	810.4111	866.9843
Frequencies --	931.2864	949.9810	981.3546
Frequencies --	1030.7971	1042.1053	1113.1599
Frequencies --	1192.3260	1271.7153	1288.2060
Frequencies --	1331.2705	1422.6896	1461.8080
Frequencies --	1494.3423	1509.3856	1707.9555
Frequencies --	3074.2157	3153.6338	3161.6426
Frequencies --	3176.4577	3202.1638	3263.2218

SOZ'
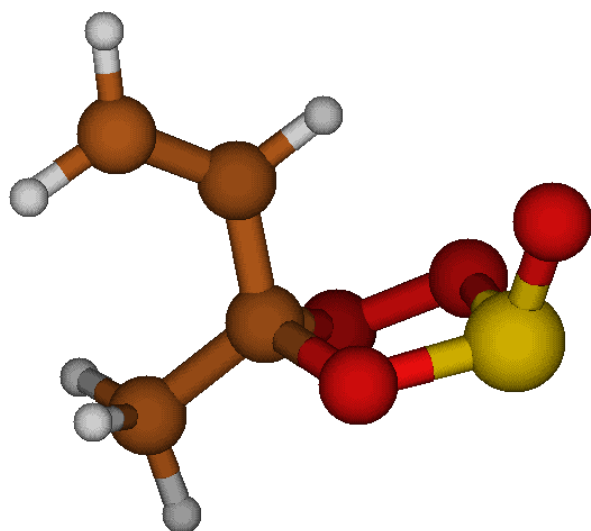
1	6	0	0.848155	-0.372341	-0.050003
2	16	0	-1.700029	-0.127067	-0.332040
3	8	0	-1.015350	-0.443867	1.235632
4	8	0	0.269870	-1.072385	1.042397
5	8	0	-0.232607	-0.358200	-1.035797
6	6	0	1.946571	-1.254082	-0.587142
7	6	0	1.216625	1.033716	0.319336
8	1	0	2.732503	-1.362162	0.155517
9	1	0	2.362417	-0.814681	-1.488923
10	1	0	1.531517	-2.228815	-0.822522
11	6	0	2.407956	1.579909	0.108251
12	1	0	0.425099	1.603019	0.784636
13	1	0	3.219323	1.045240	-0.362458
14	1	0	2.603840	2.598932	0.405799
15	8	0	-2.045672	1.282993	-0.254989

Frequencies --	70.7843	112.9503	188.8152
Frequencies --	216.0415	250.8206	299.2589
Frequencies --	337.5532	360.2643	387.9994
Frequencies --	437.6159	495.8934	547.4546
Frequencies --	606.2036	667.1724	703.4317
Frequencies --	757.4715	784.7002	832.5222
Frequencies --	908.0846	947.0281	979.6173
Frequencies --	1036.3545	1042.5875	1122.9048
Frequencies --	1186.0015	1251.4788	1310.2085
Frequencies --	1352.0258	1421.1886	1466.4078
Frequencies --	1500.7091	1506.7893	1708.8968
Frequencies --	3086.5516	3169.2442	3174.5349
Frequencies --	3177.4720	3213.5355	3260.3609

SOZ' = MVK + SO₃
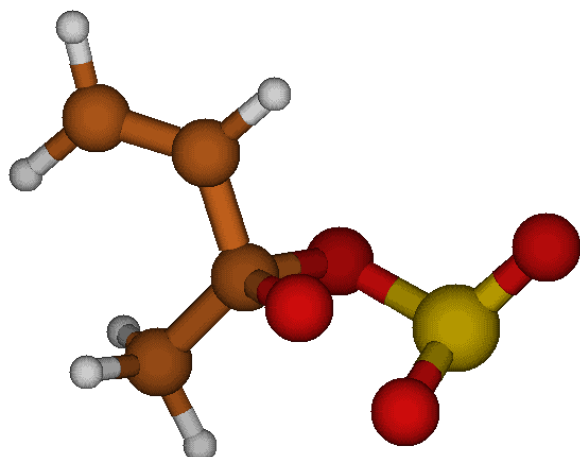
1	8	0	0.268666	0.387733	1.287376
2	6	0	0.854924	0.245856	0.094638
3	8	0	-0.209985	-0.312955	-0.909070
4	16	0	-1.690468	-0.037483	-0.364985
5	8	0	-1.367533	1.082298	0.612173
6	8	0	-2.299841	-1.260266	0.130902
7	6	0	1.393812	1.503594	-0.542399
8	6	0	1.790829	-0.937246	0.239469
9	6	0	3.088824	-0.885572	-0.026553
10	1	0	0.596203	2.238434	-0.594597
11	1	0	1.772095	1.305811	-1.541350
12	1	0	2.191488	1.902718	0.079789
13	1	0	1.308823	-1.828074	0.612782
14	1	0	3.572867	0.007988	-0.389188
15	1	0	3.705215	-1.761415	0.110345

Frequencies --	-450.0671	78.7750	90.7688
Frequencies --	163.8373	254.1774	278.8818
Frequencies --	291.2274	311.7642	359.7220
Frequencies --	407.5348	434.9676	483.7795
Frequencies --	549.3286	556.3118	616.6765
Frequencies --	667.2262	775.1922	832.5499
Frequencies --	907.0316	948.6545	968.4700
Frequencies --	1020.6555	1042.7559	1090.9731
Frequencies --	1187.1692	1252.4011	1290.6189
Frequencies --	1327.4357	1417.1863	1448.0406
Frequencies --	1498.4711	1502.8134	1687.5787
Frequencies --	3079.7277	3159.8213	3172.1172
Frequencies --	3176.9569	3221.7848	3265.9236

MVK
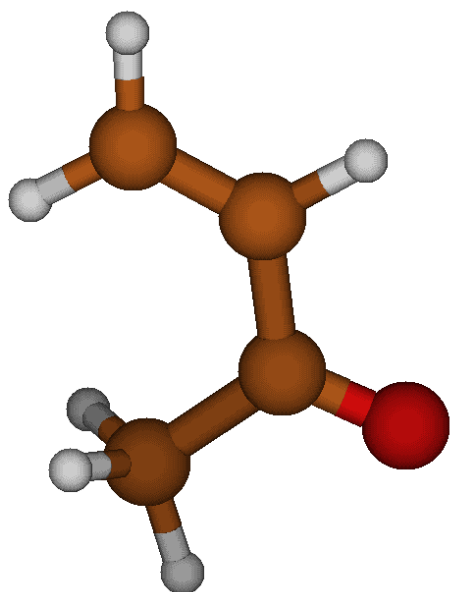
1	6	0	-0.468498	-1.879311	0.000000
2	6	0	-0.887861	-0.614171	0.000000
3	6	0	0.000000	0.574545	0.000000
4	8	0	-0.490257	1.689933	0.000000
5	6	0	1.497998	0.373306	0.000000
6	1	0	0.581237	-2.134287	0.000000
7	1	0	-1.168614	-2.701731	0.000000
8	1	0	-1.942964	-0.375221	0.000000
9	1	0	1.980827	1.344719	0.000000
10	1	0	1.810871	-0.189581	0.878903
11	1	0	1.810871	-0.189581	-0.878903

Frequencies --	121.9725	130.7326	281.7531
Frequencies --	433.2220	489.3543	537.8415
Frequencies --	700.4204	769.8615	951.4588
Frequencies --	994.8900	1047.6423	1055.0048
Frequencies --	1077.8724	1280.3410	1314.1765
Frequencies --	1398.3095	1455.8343	1485.3347
Frequencies --	1492.8355	1679.8415	1738.4354
Frequencies --	3061.5825	3126.2050	3169.3574
Frequencies --	3173.3711	3196.0384	3256.1623

syn-trans; exo
syn-trans…SO₂
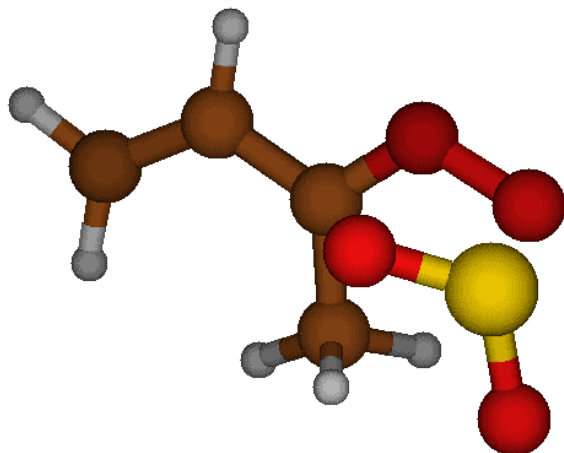
1	6	0	1.236440	0.390605	0.151715
2	8	0	0.531658	1.231267	-0.511902
3	8	0	-0.698475	1.566097	0.030360
4	6	0	0.853829	-0.015215	1.518422
5	6	0	2.440205	0.006535	-0.547209
6	1	0	0.373840	0.833874	2.001684
7	1	0	0.112485	-0.809683	1.476293
8	1	0	1.720614	-0.353260	2.075580
9	1	0	2.567783	0.448503	-1.525056
10	6	0	3.332282	-0.862677	-0.061322
11	1	0	3.213087	-1.333555	0.902154
12	1	0	4.204064	-1.132818	-0.636936
13	16	0	-1.981897	-0.265887	-0.441372
14	8	0	-0.833566	-1.076429	-0.884748
15	8	0	-2.456875	-0.535231	0.916114

Frequencies --	57.0917	72.7004	84.0406
Frequencies --	127.4748	152.7600	183.4696
Frequencies --	224.9502	265.0922	313.7244
Frequencies --	347.3043	366.5307	454.8247
Frequencies --	497.4793	524.0630	602.8360
Frequencies --	690.4562	809.0349	938.2261
Frequencies --	999.9873	1007.4196	1027.3797
Frequencies --	1051.0598	1072.4356	1101.9211
Frequencies --	1265.6009	1312.3075	1346.9207
Frequencies --	1400.8599	1451.5061	1470.9465
Frequencies --	1502.7602	1510.9854	1676.4860
Frequencies --	3079.0081	3147.2198	3180.5378
Frequencies --	3186.1877	3210.9597	3275.6186

syn-trans…SO₂ = SOZ
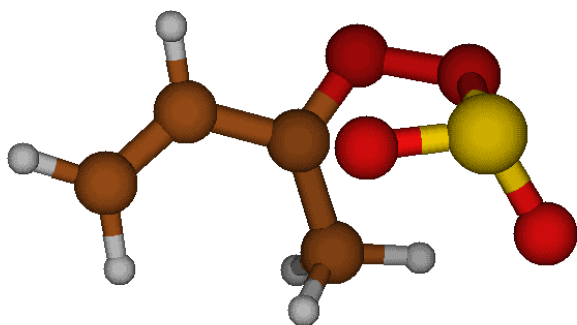
1	6	0	1.015510	0.302431	0.248281
2	8	0	0.388404	1.420436	0.019286
3	8	0	-0.942872	1.412902	0.449094
4	6	0	0.745309	-0.540890	1.442817
5	6	0	2.258943	0.236659	-0.500454
6	1	0	-0.251816	-0.367311	1.822691
7	1	0	0.854319	-1.590591	1.194434
8	1	0	1.485635	-0.277088	2.201787
9	1	0	2.375865	0.984563	-1.271158
10	6	0	3.192724	-0.691806	-0.285424
11	1	0	3.078440	-1.456637	0.467523
12	1	0	4.096171	-0.710615	-0.875189
13	16	0	-1.767337	-0.163050	-0.568130
14	8	0	-0.420516	-0.671740	-1.012252
15	8	0	-2.354532	-0.888083	0.558706

Frequencies --	-167.7993	91.1538	110.1131
Frequencies --	159.7578	187.1136	247.0902
Frequencies --	266.6364	284.8685	345.7335
Frequencies --	394.7844	410.2281	474.9027
Frequencies --	501.1198	537.0575	602.0049
Frequencies --	690.2732	801.1307	948.5216
Frequencies --	983.4073	1000.2142	1006.4490
Frequencies --	1028.6333	1066.6902	1080.4563
Frequencies --	1232.2081	1309.2590	1351.2467
Frequencies --	1407.1312	1438.6424	1464.6375
Frequencies --	1495.2816	1507.5699	1684.6645
Frequencies --	3055.7108	3161.6268	3182.1052
Frequencies --	3213.7608	3218.5836	3273.3685

SOZ
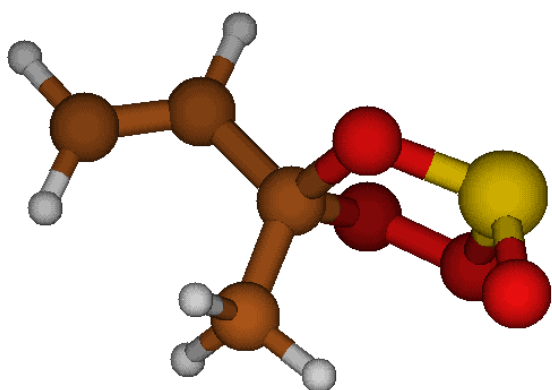
1	6	0	-0.796759	0.007833	0.094681
2	8	0	-0.321012	-1.084616	0.869362
3	8	0	1.097683	-0.838653	1.009361
4	6	0	-0.802549	1.314193	0.854941
5	6	0	-2.095677	-0.456136	-0.484579
6	1	0	0.184364	1.510115	1.260075
7	1	0	-1.072421	2.127871	0.187250
8	1	0	-1.518233	1.259142	1.671205
9	1	0	-2.021490	-1.380097	-1.040618
10	6	0	-3.252938	0.179585	-0.353186
11	1	0	-3.344714	1.104208	0.195975
12	1	0	-4.150914	-0.216053	-0.802877
13	16	0	1.693998	-0.232978	-0.505424
14	8	0	0.157025	0.063183	-1.012056
15	8	0	2.379677	0.991288	-0.123588

Frequencies --	71.8977	101.2198	193.7868
Frequencies --	230.0141	257.3903	306.0574
Frequencies --	344.3281	382.5171	385.3521
Frequencies --	440.0113	498.3458	549.7680
Frequencies --	619.0751	647.3337	662.0985
Frequencies --	746.9057	790.1960	887.5937
Frequencies --	897.4436	942.8491	991.9983
Frequencies --	1031.1810	1034.3584	1118.5892
Frequencies --	1187.8736	1248.3406	1311.2663
Frequencies --	1332.2939	1427.3591	1462.2944
Frequencies --	1504.4116	1511.8488	1710.5720
Frequencies --	3084.0662	3162.3347	3178.0671
Frequencies --	3181.2154	3204.8200	3266.0589

SOZ = SOZ'
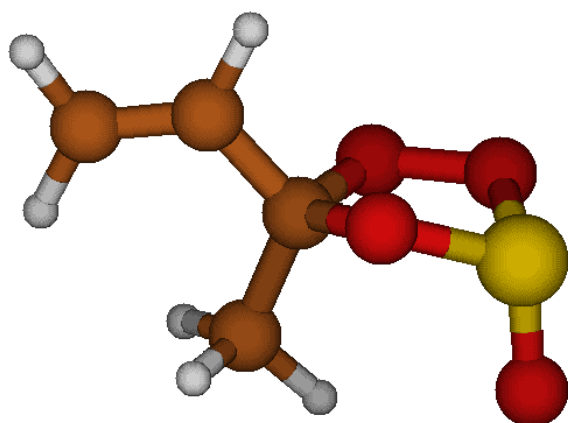
1	6	0	-0.771401	0.079359	0.081826
2	16	0	1.705098	-0.200138	-0.494836
3	8	0	1.146660	-1.153744	0.762592
4	8	0	-0.241030	-0.812745	1.099287
5	8	0	0.159946	0.018694	-1.016757
6	8	0	2.235585	1.049767	0.028730
7	6	0	-0.874703	1.481217	0.641405
8	6	0	-2.039774	-0.553881	-0.401717
9	1	0	-1.569386	1.490702	1.477379
10	1	0	-1.224381	2.165439	-0.127842
11	1	0	0.101665	1.804527	0.986063
12	6	0	-3.244508	-0.003603	-0.322052
13	1	0	-1.897695	-1.539807	-0.822492
14	1	0	-3.403850	0.977072	0.099911
15	1	0	-4.114903	-0.530051	-0.683232

Frequencies --	-128.6963	82.5424	136.2609
Frequencies --	248.9685	255.3495	295.3057
Frequencies --	352.5496	372.8959	388.6703
Frequencies --	411.7868	507.3882	598.7262
Frequencies --	641.4672	652.5990	689.8590
Frequencies --	745.2134	802.6924	849.4882
Frequencies --	886.9147	941.7272	985.4665
Frequencies --	1029.0111	1034.8454	1116.2608
Frequencies --	1182.5865	1244.6799	1290.5690
Frequencies --	1331.4208	1424.6902	1460.5608
Frequencies --	1503.5271	1509.7037	1708.3981
Frequencies --	3080.4549	3158.4946	3176.8937
Frequencies --	3180.8852	3200.6762	3264.4480

SOZ'
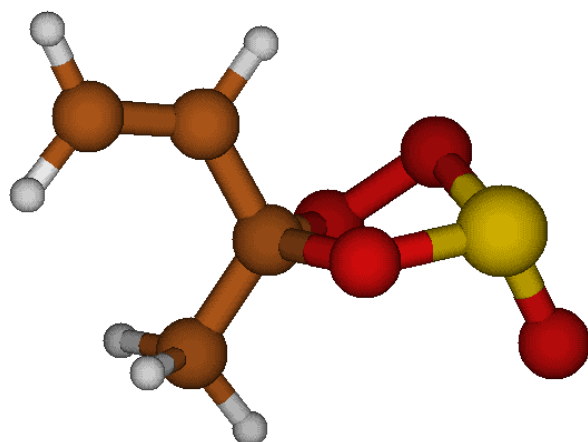
1	6	0	-0.787569	0.291556	0.096676
2	16	0	1.642177	-0.408203	-0.454036
3	8	0	0.871613	-1.005404	0.942438
4	8	0	-0.060773	0.059587	1.299220
5	8	0	0.210895	0.230810	-0.966674
6	8	0	2.525421	0.692026	-0.113254
7	6	0	-1.313489	1.702952	0.193916
8	6	0	-1.782312	-0.801371	-0.150581
9	1	0	-2.019966	1.785733	1.015723
10	1	0	-1.808761	1.973030	-0.734222
11	1	0	-0.476298	2.373112	0.361054
12	6	0	-3.072512	-0.614991	-0.399116
13	1	0	-1.366201	-1.798473	-0.105191
14	1	0	-3.515240	0.368479	-0.451773
15	1	0	-3.730327	-1.455672	-0.560219

Frequencies --	68.6685	88.5478	179.9058
Frequencies --	230.5303	262.9262	297.1211
Frequencies --	333.8729	369.9032	424.6329
Frequencies --	466.1481	483.9051	554.3839
Frequencies --	635.3846	662.1696	692.3499
Frequencies --	763.4537	782.9097	848.0047
Frequencies --	854.4974	945.3141	979.8726
Frequencies --	1032.5001	1037.4845	1124.6301
Frequencies --	1189.4902	1259.8852	1302.3925
Frequencies --	1337.6638	1419.4249	1465.4764
Frequencies --	1500.2241	1507.3283	1710.2486
Frequencies --	3084.2149	3166.5541	3173.4626
Frequencies --	3177.3086	3200.0141	3259.5848

SOZ' = MVK + SO₃
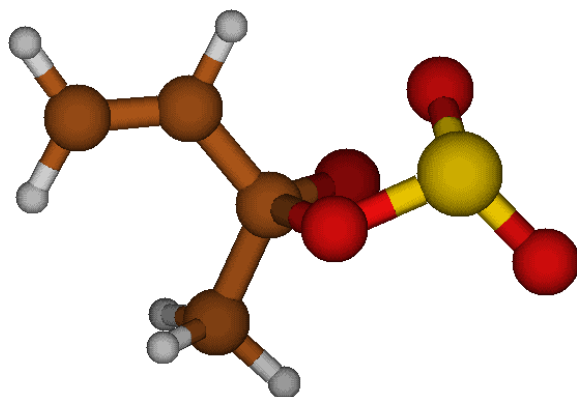
1	8	0	-0.186754	0.192973	1.396827
2	6	0	-0.837553	0.295080	0.233370
3	8	0	0.224710	0.295761	-0.911001
4	16	0	1.598019	-0.362493	-0.406400
5	8	0	1.045713	-1.107803	0.804439
6	8	0	2.614303	0.656553	-0.204869
7	6	0	-1.415870	1.711510	0.133287
8	6	0	-1.756056	-0.847164	-0.075644
9	6	0	-3.007592	-0.729336	-0.501939
10	1	0	-0.625675	2.425789	0.337169
11	1	0	-2.211042	1.818450	0.864416
12	1	0	-1.806436	1.870237	-0.867181
13	1	0	-1.321978	-1.819286	0.113177
14	1	0	-3.468637	0.228894	-0.689570
15	1	0	-3.615890	-1.604613	-0.673224

Frequencies --	-473.4865	74.2209	96.4266
Frequencies --	160.8422	250.7272	261.1170
Frequencies --	285.6100	321.8525	356.5760
Frequencies --	410.8617	439.1278	484.1888
Frequencies --	550.4309	559.5446	620.4054
Frequencies --	714.5322	776.5328	833.6393
Frequencies --	896.7259	977.2618	981.8632
Frequencies --	1002.5179	1033.9802	1076.8321
Frequencies --	1200.8184	1252.2579	1281.5727
Frequencies --	1329.7380	1395.5760	1463.9511
Frequencies --	1494.6021	1505.6603	1704.4290
Frequencies --	3087.7173	3173.3040	3176.9059
Frequencies --	3186.7751	3202.0907	3259.1691

syn-cis; endo
syn-cis…SO₂
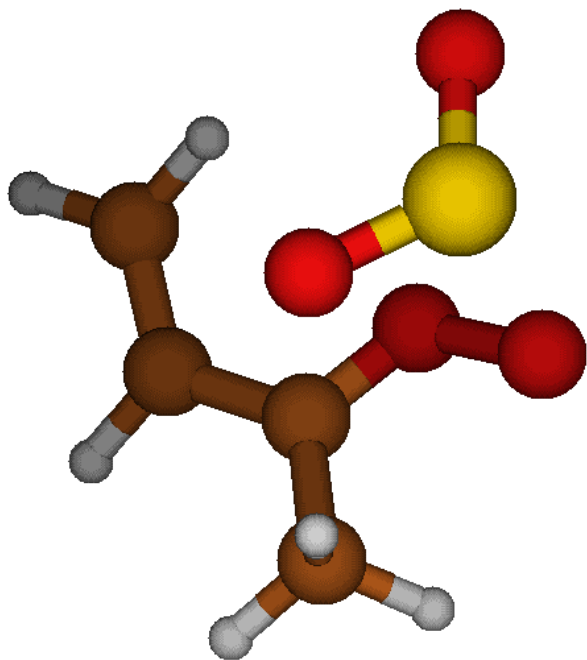
1	6	0	-1.396102	-0.416273	-0.127917
2	8	0	-0.540530	-0.188874	-1.048961
3	8	0	0.480149	-1.133281	-1.173323
4	6	0	-1.486764	-1.735925	0.522970
5	6	0	-2.294559	0.687029	0.150232
6	1	0	-1.295027	-2.510968	-0.217227
7	1	0	-0.699473	-1.807794	1.271641
8	1	0	-2.454860	-1.855646	0.999713
9	16	0	1.892903	-0.070201	0.288799
10	8	0	0.873203	0.007544	1.351876
11	8	0	2.114468	1.181301	-0.434241
12	1	0	-3.266453	0.432495	0.547220
13	6	0	-1.907238	1.958682	0.003600
14	1	0	-0.902133	2.198807	-0.311735
15	1	0	-2.578839	2.771724	0.233492

Frequencies --	43.2671	70.2224	104.1838
Frequencies --	134.6299	158.8260	169.6804
Frequencies --	205.9363	241.2487	308.6136
Frequencies --	341.5754	361.2506	442.9580
Frequencies --	515.1565	532.0978	617.5337
Frequencies --	666.9368	812.7348	929.5168
Frequencies --	1006.0134	1027.1538	1033.5241
Frequencies --	1036.5175	1101.2979	1105.6093
Frequencies --	1263.0818	1284.9026	1343.2089
Frequencies --	1395.4818	1453.2569	1458.6708
Frequencies --	1498.2911	1514.5928	1672.4294
Frequencies --	3069.0380	3138.0126	3171.8518
Frequencies --	3173.9184	3210.2599	3273.9748

syn-cis…SO₂ = SOZ
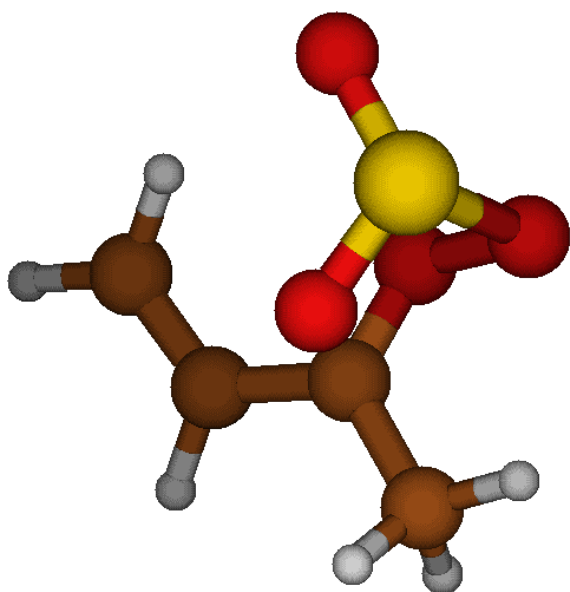
1	6	0	1.203998	-0.416266	0.117429
2	8	0	0.439098	-0.187720	1.137028
3	8	0	-0.701695	-1.011974	1.194873
4	6	0	1.398031	-1.768751	-0.454732
5	6	0	2.139276	0.664026	-0.151845
6	1	0	0.568948	-2.416370	-0.206011
7	1	0	1.517635	-1.701055	-1.531027
8	1	0	2.323953	-2.165313	-0.027205
9	1	0	3.096366	0.383683	-0.567964
10	6	0	1.799172	1.941646	0.037930
11	1	0	0.805490	2.204259	0.371847
12	1	0	2.495474	2.738171	-0.176115
13	16	0	-1.735547	-0.070347	-0.344503
14	8	0	-0.546041	-0.115784	-1.253828
15	8	0	-1.976610	1.260259	0.216405

Frequencies --	-129.5665	64.7575	104.4926
Frequencies --	169.9394	190.3104	194.2593
Frequencies --	237.0143	256.7082	349.0032
Frequencies --	363.4854	432.7902	455.1087
Frequencies --	525.1393	547.2784	612.8386
Frequencies --	681.1048	809.8750	932.1484
Frequencies --	981.2245	1010.1798	1027.1060
Frequencies --	1032.5378	1066.4216	1094.6932
Frequencies --	1229.5193	1292.0716	1346.1600
Frequencies --	1409.7243	1420.0289	1477.7869
Frequencies --	1490.4436	1497.8665	1675.8051
Frequencies --	3043.4646	3150.8782	3171.6071
Frequencies --	3206.2721	3219.4754	3272.1975

SOZ
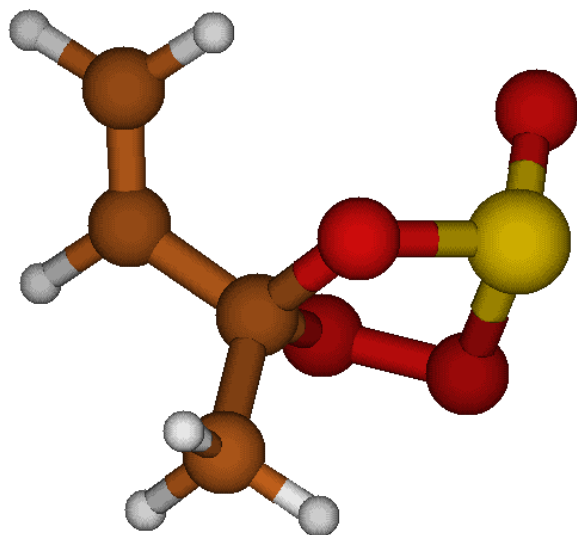
1	6	0	0.907295	-0.405427	-0.025360
2	8	0	0.190774	-0.594452	1.193233
3	8	0	-1.109741	-1.094304	0.746435
4	6	0	1.394320	-1.711856	-0.615207
5	6	0	2.009227	0.558704	0.304050
6	1	0	0.561199	-2.398470	-0.735995
7	1	0	1.850396	-1.525677	-1.584498
8	1	0	2.132902	-2.159123	0.046405
9	1	0	2.861998	0.119246	0.803097
10	6	0	1.966315	1.854067	0.022745
11	1	0	1.115177	2.290310	-0.476584
12	1	0	2.787212	2.502629	0.288658
13	16	0	-1.602317	0.056679	-0.400700
14	8	0	-0.045285	0.190147	-0.937642
15	8	0	-1.952593	1.310022	0.242067

Frequencies --	44.9461	78.5191	189.8789
Frequencies --	241.3992	251.7340	286.2888
Frequencies --	331.3636	364.6086	421.6027
Frequencies --	475.6638	546.6402	569.2323
Frequencies --	607.3737	649.3898	679.1661
Frequencies --	739.8702	801.4266	832.4554
Frequencies --	896.7450	939.2530	997.2198
Frequencies --	1018.4852	1045.0085	1137.7855
Frequencies --	1181.3033	1254.2441	1271.6650
Frequencies --	1332.7052	1418.0835	1457.5890
Frequencies --	1498.1322	1501.3975	1705.1443
Frequencies --	3074.1596	3153.8069	3164.8350
Frequencies --	3177.4631	3197.9810	3273.2407

SOZ = SOZ'
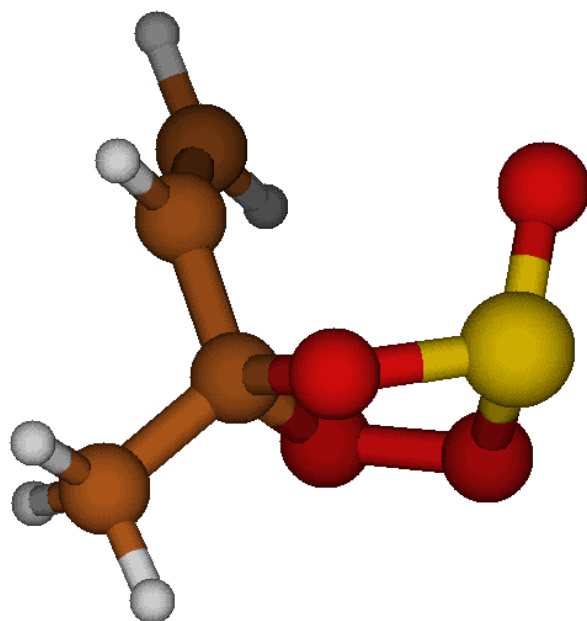
1	6	0	0.911327	-0.378097	-0.142746
2	16	0	-1.635035	-0.222030	-0.250163
3	8	0	-0.987060	-0.576716	1.256376
4	8	0	0.467849	-0.410597	1.230748
5	8	0	-0.231095	-0.716859	-0.954211
6	6	0	1.938869	-1.472741	-0.335160
7	6	0	1.429591	0.987001	-0.501228
8	1	0	2.772196	-1.303076	0.342328
9	1	0	2.309369	-1.456595	-1.357764
10	1	0	1.484812	-2.436986	-0.124481
11	6	0	1.557798	1.990066	0.355837
12	1	0	1.720789	1.092907	-1.538230
13	1	0	1.259404	1.885422	1.387439
14	1	0	1.950759	2.942716	0.035174
15	8	0	-1.794981	1.213011	-0.408173

Frequencies --	-120.1622	82.7292	128.5310
Frequencies --	218.2618	255.5735	285.7301
Frequencies --	300.8523	363.1113	385.3828
Frequencies --	480.4077	531.5594	575.0967
Frequencies --	612.1847	677.0763	712.8606
Frequencies --	736.0692	797.6061	856.6195
Frequencies --	879.9283	953.0834	987.1970
Frequencies --	1024.8840	1041.6467	1139.7834
Frequencies --	1177.9508	1237.2523	1262.4494
Frequencies --	1326.4300	1414.6795	1454.6557
Frequencies --	1493.6399	1496.7896	1707.8902
Frequencies --	3072.5768	3154.7555	3165.7878
Frequencies --	3175.5233	3189.8773	3271.0645

SOZ'
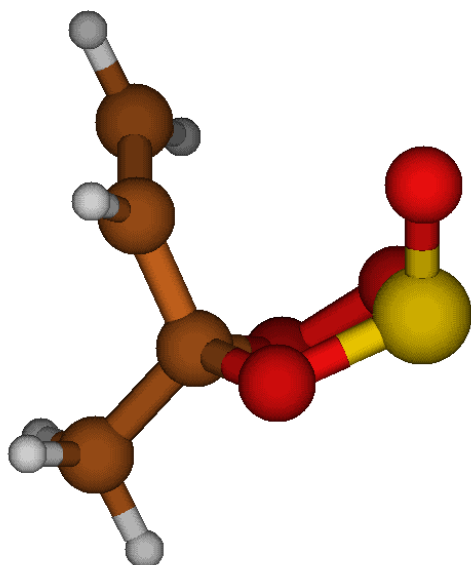
1	6	0	0.931326	-0.385516	-0.124795
2	16	0	-1.628327	-0.383650	-0.049333
3	8	0	-0.716347	0.154814	1.329453
4	8	0	0.616979	-0.406876	1.249533
5	8	0	-0.253763	-0.953088	-0.755124
6	6	0	2.071613	-1.356405	-0.329866
7	6	0	1.202454	0.985707	-0.675468
8	1	0	2.937279	-1.013712	0.231615
9	1	0	2.330764	-1.389564	-1.384874
10	1	0	1.776762	-2.346517	0.005686
11	6	0	1.481012	2.041177	0.076343
12	1	0	1.178911	1.050211	-1.754914
13	1	0	1.484456	1.975092	1.154018
14	1	0	1.692635	3.000023	-0.371416
15	8	0	-2.080119	0.849286	-0.669873

Frequencies --	77.6864	104.4866	171.3643
Frequencies --	207.8023	252.7274	293.5452
Frequencies --	303.9485	352.2568	386.0403
Frequencies --	457.7828	519.8118	562.0009
Frequencies --	605.7655	645.9559	707.9753
Frequencies --	746.8007	796.8104	842.6741
Frequencies --	899.6510	958.0061	982.9617
Frequencies --	1024.1320	1053.8698	1129.8241
Frequencies --	1204.2170	1251.8427	1269.6128
Frequencies --	1325.1640	1415.0838	1456.9714
Frequencies --	1495.4468	1496.9660	1708.3465
Frequencies --	3077.5080	3161.0416	3169.5402
Frequencies --	3174.5091	3195.2092	3266.9753

SOZ' = MVK + SO₃
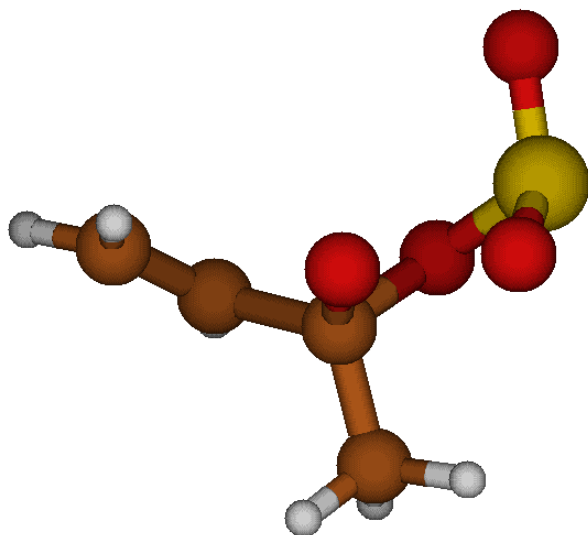
1	8	0	0.482112	0.096044	1.192693
2	6	0	0.888782	0.387026	-0.046778
3	8	0	-0.273751	0.037489	-1.030527
4	16	0	-1.672792	-0.013135	-0.247270
5	8	0	-1.242972	0.775722	0.990566
6	8	0	-2.128139	-1.382450	-0.084597
7	6	0	1.228913	1.838015	-0.316405
8	6	0	1.959296	-0.586127	-0.497241
9	6	0	2.616486	-1.396176	0.321589
10	1	0	0.385361	2.468266	-0.049913
11	1	0	1.478920	1.987490	-1.363823
12	1	0	2.085294	2.108879	0.297519
13	1	0	2.168133	-0.546577	-1.556916
14	1	0	2.402830	-1.428247	1.378545
15	1	0	3.385258	-2.050516	-0.061156

Frequencies --	-503.0963	49.7067	114.2572
Frequencies --	167.4532	238.4033	245.8125
Frequencies --	278.7626	305.0201	349.8186
Frequencies --	426.6553	438.4999	506.6686
Frequencies --	559.1815	564.7677	620.5304
Frequencies --	695.2147	773.8967	833.3841
Frequencies --	884.3514	956.1887	987.0136
Frequencies --	1017.9460	1054.3601	1085.3504
Frequencies --	1208.7140	1238.4825	1259.3925
Frequencies --	1335.8924	1413.3947	1449.7609
Frequencies --	1493.8651	1498.2580	1691.5326
Frequencies --	3073.4758	3153.3649	3166.4758
Frequencies --	3176.1199	3203.1558	3271.4335

MVK
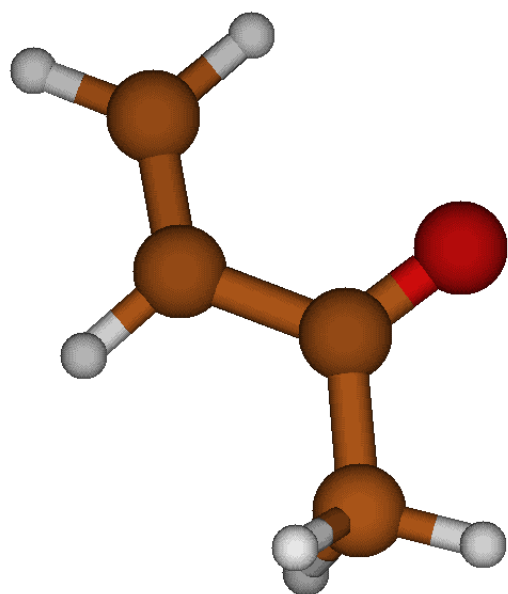
1	6	0	-0.602979	-1.916344	0.000000
2	6	0	0.344205	-0.980834	0.000000
3	6	0	0.000000	0.471355	0.000000
4	8	0	-1.152853	0.859147	0.000000
5	6	0	1.166490	1.427951	0.000000
6	1	0	-1.644059	-1.625329	0.000000
7	1	0	-0.364261	-2.969258	0.000000
8	1	0	1.392679	-1.248799	0.000000
9	1	0	0.809026	2.452241	0.000000
10	1	0	1.791571	1.252604	0.876727
11	1	0	1.791571	1.252604	-0.876727

Frequencies --	95.1011	131.0806	269.1744
Frequencies --	415.7426	462.4459	602.2285
Frequencies --	687.4931	785.7875	967.0014
Frequencies --	1013.9690	1033.2112	1051.5520
Frequencies --	1087.8778	1208.6350	1333.8510
Frequencies --	1393.9406	1447.6324	1477.1397
Frequencies --	1488.2154	1670.7956	1760.3327
Frequencies --	3051.0294	3111.7758	3165.6515
Frequencies --	3172.4552	3186.9241	3262.9738

syn-cis; exo
syn-cis…SO$_2$
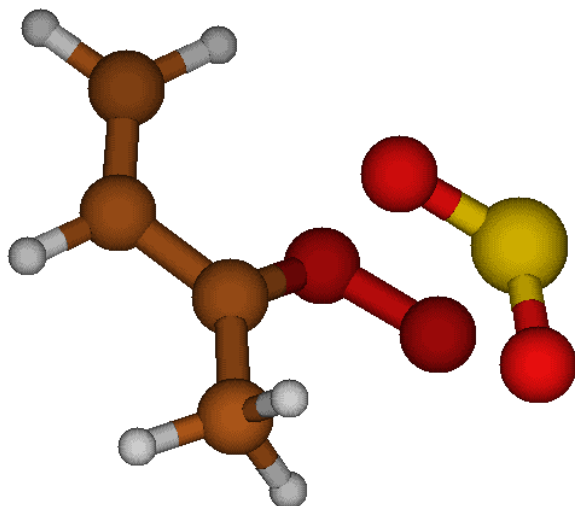
1	6	0	-1.219190	0.620860	0.013608
2	8	0	-0.754735	0.166576	1.114975
3	8	0	0.541528	0.573857	1.432524
4	6	0	-0.568118	1.738745	-0.697170
5	6	0	-2.477938	0.038333	-0.409795
6	1	0	-0.118868	2.408720	0.034103
7	1	0	0.245201	1.360712	-1.313128
8	1	0	-1.291026	2.245408	-1.329957
9	16	0	1.802481	-0.662432	0.043243
10	8	0	0.644867	-1.135470	-0.741838
11	8	0	2.570187	0.423403	-0.568268
12	1	0	-3.085188	0.642949	-1.067294
13	6	0	-2.840666	-1.203969	-0.075669
14	1	0	-2.194285	-1.830054	0.520459
15	1	0	-3.774832	-1.619559	-0.421066

Frequencies --	56.1451	76.6191	93.8906
Frequencies --	117.4857	161.1770	185.9439
Frequencies --	212.7011	257.1847	316.8018
Frequencies --	345.8488	363.2753	438.7743
Frequencies --	507.8252	527.6101	618.6452
Frequencies --	667.4510	811.7390	928.9049
Frequencies --	1005.6513	1018.8100	1029.9406
Frequencies --	1040.2637	1097.3132	1102.8004
Frequencies --	1259.3446	1284.9025	1342.2884
Frequencies --	1400.0391	1450.5955	1457.1662
Frequencies --	1495.6403	1515.8685	1676.5034
Frequencies --	3070.6281	3141.6053	3169.2440
Frequencies --	3180.6319	3212.3966	3278.8832

syn-cis…SO₂ = SOZ
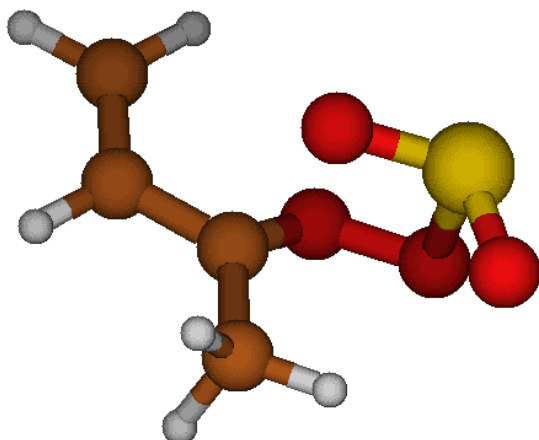
1	6	0	-1.036423	-0.569695	-0.091739
2	8	0	-0.683518	0.031185	-1.183873
3	8	0	0.677129	-0.108934	-1.494635
4	6	0	-0.408801	-1.826235	0.386972
5	6	0	-2.346039	-0.169360	0.401100
6	1	0	0.593102	-1.950930	0.001190
7	1	0	-0.390329	-1.835253	1.472045
8	1	0	-1.049273	-2.646082	0.046857
9	16	0	1.645514	0.703425	0.136307
10	8	0	0.388215	0.749438	0.954793
11	8	0	2.541390	-0.410744	0.448493
12	6	0	-2.854513	1.045537	0.185349
13	1	0	-2.298019	1.791904	-0.360689
14	1	0	-3.824660	1.317313	0.572167
15	1	0	-2.870130	-0.900793	0.999201

Frequencies --	-123.7674	74.4108	107.6976
Frequencies --	160.6666	169.4768	209.1505
Frequencies --	246.9406	288.5004	335.6721
Frequencies --	389.0692	417.0246	450.8684
Frequencies --	504.2118	535.0754	615.6071
Frequencies --	682.2739	807.3926	938.8246
Frequencies --	991.0806	1013.9062	1017.7537
Frequencies --	1020.2132	1064.8532	1092.7112
Frequencies --	1234.3351	1293.9499	1343.9756
Frequencies --	1415.3087	1421.3805	1475.7465
Frequencies --	1489.8036	1501.7213	1682.0705
Frequencies --	3038.9938	3149.7618	3180.8647
Frequencies --	3208.7517	3221.1247	3278.1294

SOZ
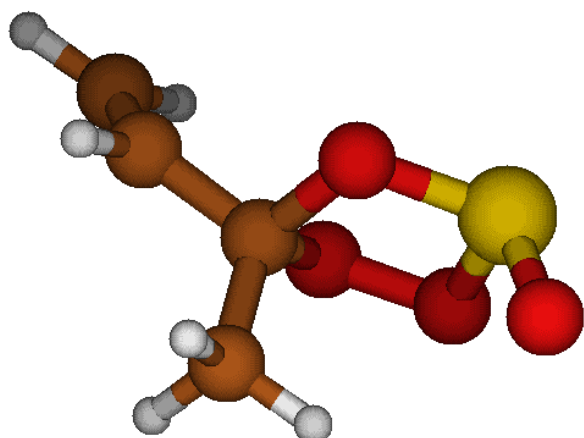
1	6	0	-0.779585	0.384611	0.040320
2	8	0	-0.589124	-0.641560	0.992638
3	8	0	0.843265	-0.732371	1.142240
4	6	0	-0.464132	1.764846	0.580380
5	6	0	-2.165273	0.268516	-0.515729
6	1	0	0.536772	1.794889	0.998165
7	1	0	-0.529988	2.491539	-0.225891
8	1	0	-1.189834	2.019051	1.349825
9	1	0	-2.461803	1.095351	-1.146347
10	6	0	-2.994644	-0.736625	-0.265359
11	1	0	-2.708221	-1.564766	0.364084
12	1	0	-3.987500	-0.746076	-0.688885
13	16	0	1.572727	-0.539794	-0.428120
14	8	0	0.157383	0.030750	-1.030284
15	8	0	2.538319	0.525509	-0.209432

Frequencies --	36.1557	105.3336	175.9085
Frequencies --	231.8567	241.0284	273.8856
Frequencies --	324.7940	362.5611	405.7042
Frequencies --	455.2395	529.9198	539.6025
Frequencies --	605.7772	641.8940	670.6488
Frequencies --	755.3290	786.1635	886.0549
Frequencies --	915.8021	955.1147	994.7821
Frequencies --	1024.3631	1050.3633	1112.5466
Frequencies --	1199.6396	1249.0329	1289.5320
Frequencies --	1338.1200	1424.4544	1463.0970
Frequencies --	1501.1459	1504.3566	1706.9609
Frequencies --	3076.6809	3152.9606	3177.4554
Frequencies --	3178.1646	3198.5264	3271.0558

SOZ = SOZ'
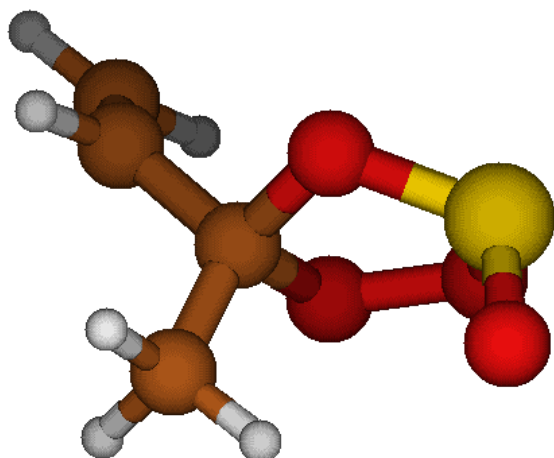
1	6	0	-0.750870	0.425265	0.042461
2	16	0	1.596200	-0.450413	-0.467304
3	8	0	0.780782	-1.214376	0.788980
4	8	0	-0.509122	-0.571852	1.051037
5	8	0	0.175153	0.143042	-1.032326
6	8	0	2.414777	0.625546	0.070978
7	6	0	-0.518499	1.811236	0.613785
8	6	0	-2.134715	0.245429	-0.511245
9	1	0	-1.237852	1.990770	1.409681
10	1	0	-0.659901	2.557137	-0.165752
11	1	0	0.489889	1.892948	1.006593
12	6	0	-2.933819	-0.771690	-0.217300
13	1	0	-2.453715	1.035289	-1.178297
14	1	0	-2.620342	-1.555008	0.454932
15	1	0	-3.922574	-0.834843	-0.645858

Frequencies --	-133.2936	72.1887	142.1014
Frequencies --	216.8127	248.0823	275.0878
Frequencies --	326.4457	358.3408	391.6093
Frequencies --	462.0406	536.0663	585.6902
Frequencies --	610.0290	674.8926	684.2602
Frequencies --	752.9529	804.1265	863.5861
Frequencies --	898.1980	950.8904	996.1242
Frequencies --	1023.8946	1042.0366	1128.0166
Frequencies --	1170.1279	1247.7673	1266.3849
Frequencies --	1331.6613	1422.3919	1455.2068
Frequencies --	1499.6002	1502.1347	1705.9511
Frequencies --	3072.7861	3149.2641	3175.7037
Frequencies --	3176.5065	3193.3570	3272.4330

SOZ'
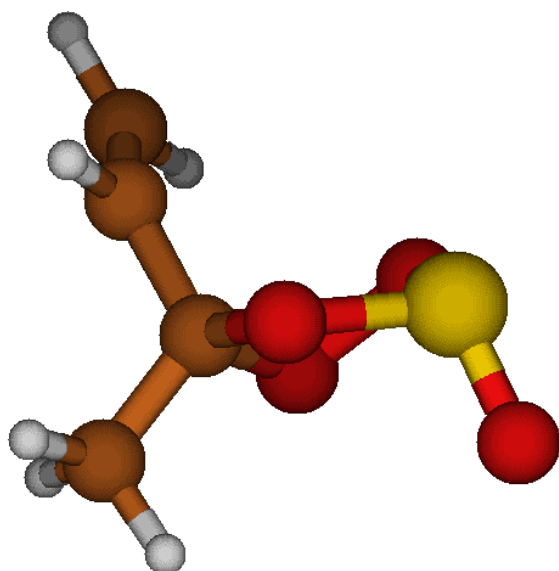
1	6	0	-0.791668	0.527932	-0.012448
2	16	0	1.563227	-0.448364	-0.429741
3	8	0	0.524135	-1.160350	0.710682
4	8	0	-0.308209	-0.052998	1.180502
5	8	0	0.345890	0.554797	-0.921788
6	8	0	2.562073	0.372741	0.229342
7	6	0	-1.172831	1.952046	0.329694
8	6	0	-1.891837	-0.256105	-0.667690
9	1	0	-1.977449	1.947522	1.061019
10	1	0	-1.519975	2.454752	-0.569402
11	1	0	-0.306641	2.472784	0.727433
12	6	0	-2.547812	-1.247738	-0.080676
13	1	0	-2.131355	0.062059	-1.673848
14	1	0	-2.299481	-1.566149	0.920738
15	1	0	-3.342954	-1.767477	-0.593274

Frequencies --	68.2866	103.6043	160.2137
Frequencies --	218.1171	272.8290	299.2199
Frequencies --	313.5158	356.4622	422.0825
Frequencies --	454.8566	532.9197	584.1393
Frequencies --	609.8676	658.9598	705.9982
Frequencies --	745.0954	793.4774	843.6220
Frequencies --	863.4891	954.1695	985.1935
Frequencies --	1028.9074	1051.8352	1130.4946
Frequencies --	1191.6050	1260.8896	1267.7118
Frequencies --	1324.8389	1414.8872	1458.2459
Frequencies --	1496.0492	1497.6730	1708.5752
Frequencies --	3076.6143	3159.2269	3170.8591
Frequencies --	3172.5961	3190.7577	3265.5691

SOZ' = MVK + SO₃
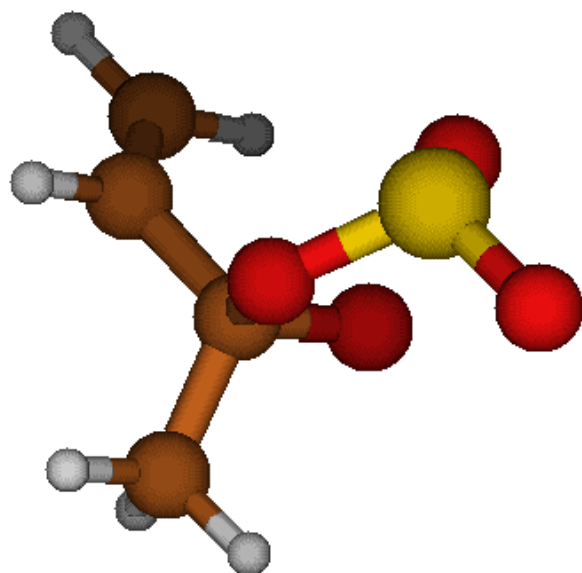
1	8	0	-0.447442	0.071849	1.266523
2	6	0	-0.857914	0.503795	0.074448
3	8	0	0.358966	0.598592	-0.862650
4	16	0	1.532092	-0.393748	-0.366779
5	8	0	0.697451	-1.262461	0.565033
6	8	0	2.637288	0.376643	0.177886
7	6	0	-1.269315	1.981693	0.222449
8	6	0	-1.871802	-0.330398	-0.652632
9	6	0	-2.473618	-1.370723	-0.092318
10	1	0	-0.455653	2.540364	0.673219
11	1	0	-2.154854	2.027636	0.848700
12	1	0	-1.496560	2.379623	-0.762650
13	1	0	-2.097241	-0.016501	-1.662953
14	1	0	-2.231097	-1.669281	0.916754
15	1	0	-3.212284	-1.945054	-0.630622

Frequencies --	-447.2184	81.6922	108.8363
Frequencies --	148.0682	239.3886	274.9905
Frequencies --	288.8271	313.4491	344.0712
Frequencies --	412.0518	448.3199	506.0042
Frequencies --	554.9954	578.1282	651.6463
Frequencies --	703.5862	762.4105	837.8981
Frequencies --	897.4024	991.5857	993.4577
Frequencies --	1027.1804	1050.9033	1058.3022
Frequencies --	1103.8862	1253.0342	1297.1832
Frequencies --	1322.7889	1394.3247	1451.2759
Frequencies --	1489.4554	1498.5584	1702.4875
Frequencies --	3081.3797	3170.8131	3172.1865
Frequencies --	3184.0891	3193.7063	3266.4647

Endo
syn-trans…SO$_2$ = syn-cis…SO$_2$
geometry a
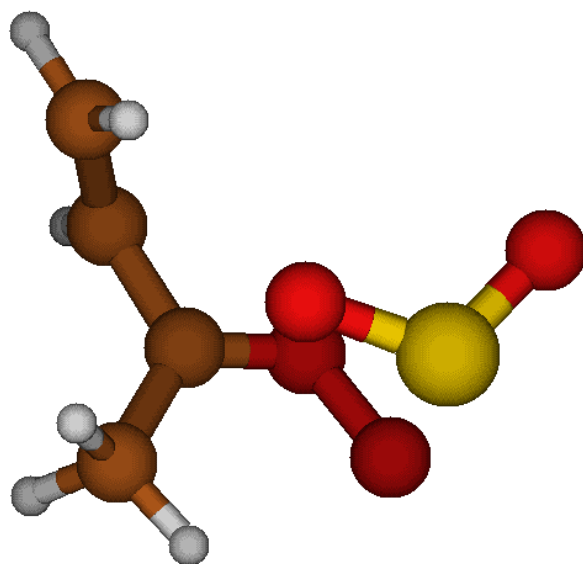
1	6	0	-1.273420	-0.513003	-0.143486
2	8	0	-0.402685	-0.696295	-1.053176
3	8	0	0.708753	-1.471228	-0.714010
4	6	0	-1.360321	-1.322892	1.087101
5	6	0	-2.326425	0.451536	-0.515511
6	1	0	-0.527774	-2.010361	1.157333
7	1	0	-1.386183	-0.659688	1.947609
8	1	0	-2.312399	-1.858843	1.054826
9	16	0	1.845490	0.149620	0.377155
10	8	0	0.621330	0.671981	1.032206
11	8	0	2.349667	0.968348	-0.720124
12	6	0	-2.334332	1.690946	-0.037388
13	1	0	-3.086395	0.093790	-1.199168
14	1	0	-1.550377	2.037002	0.619790
15	1	0	-3.114234	2.382208	-0.318343

Frequencies --	-137.3412	49.2487	83.9355
Frequencies --	113.8335	155.7416	165.5789
Frequencies --	205.5293	252.0622	285.1036
Frequencies --	345.5625	375.5006	405.4768
Frequencies --	526.2842	543.5276	605.0432
Frequencies --	661.5901	806.8491	923.8679
Frequencies --	990.9652	997.9811	1008.8129
Frequencies --	1015.0531	1081.7154	1103.3945
Frequencies --	1262.6065	1301.3353	1328.7103
Frequencies --	1402.7698	1428.1997	1465.8226
Frequencies --	1486.0751	1525.4642	1687.5889
Frequencies --	3052.0485	3138.4154	3170.8435
Frequencies --	3180.9613	3210.2552	3272.6398

syn-trans…SO₂ = syn-cis…SO₂
geometry b
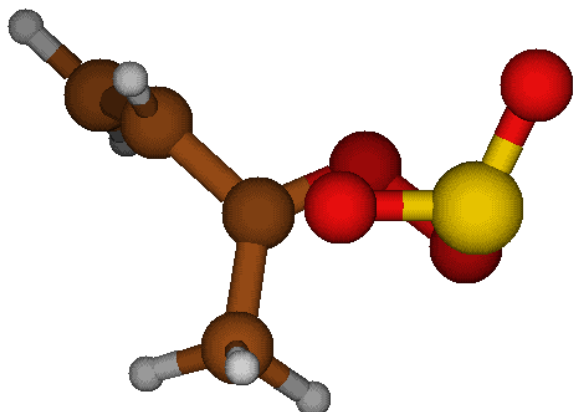
1	6	0	-1.266771	0.268995	0.029727
2	8	0	-0.501188	-0.085406	0.978838
3	8	0	0.512342	0.808108	1.321553
4	6	0	-1.258435	1.637503	-0.517744
5	6	0	-2.197186	-0.783617	-0.419262
6	1	0	-0.930194	2.326887	0.256834
7	1	0	-0.527677	1.682586	-1.325353
8	1	0	-2.240873	1.881066	-0.910803
9	16	0	2.075935	0.063173	-0.234613
10	8	0	1.056567	-0.104028	-1.290300
11	8	0	2.545248	-1.172954	0.380938
12	6	0	-3.405966	-0.954173	0.102755
13	1	0	-1.818610	-1.413450	-1.214539
14	1	0	-3.776151	-0.327131	0.901211
15	1	0	-4.055059	-1.738731	-0.254629

Frequencies --	-143.2147	37.3977	47.3685
Frequencies --	80.0180	139.0395	155.3255
Frequencies --	192.9941	240.4993	277.9177
Frequencies --	323.9631	355.2652	412.9535
Frequencies --	516.4126	529.0533	617.9783
Frequencies --	669.6472	798.8716	918.1594
Frequencies --	988.8932	993.2423	1008.6899
Frequencies --	1029.3298	1087.6807	1105.8856
Frequencies --	1273.5181	1293.3621	1315.8431
Frequencies --	1390.4512	1444.4492	1465.9561
Frequencies --	1487.7166	1526.5271	1696.0014
Frequencies --	3066.8804	3135.4638	3169.9656
Frequencies --	3174.7734	3185.5434	3263.7766

SOZ; cis = trans
geometry a
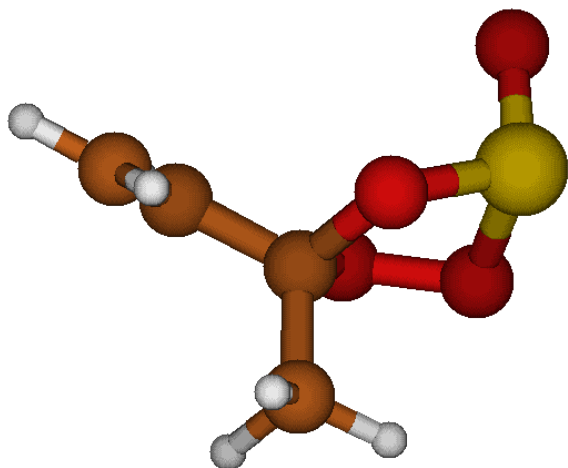
1	6	0	-0.825407	0.343417	0.068557
2	8	0	-0.003366	0.714184	1.164955
3	8	0	1.241652	1.129348	0.534996
4	6	0	-1.370812	1.540569	-0.679878
5	6	0	-1.868915	-0.569714	0.646799
6	1	0	-0.554924	2.185322	-0.994976
7	1	0	-1.920711	1.202062	-1.554498
8	1	0	-2.045891	2.096189	-0.033477
9	1	0	-1.876912	-0.637968	1.725787
10	6	0	-2.719340	-1.262484	-0.098668
11	1	0	-2.699873	-1.216031	-1.178169
12	1	0	-3.448707	-1.915528	0.355223
13	16	0	1.645742	-0.189483	-0.469211
14	8	0	0.051310	-0.396470	-0.834280
15	8	0	2.075652	-1.321193	0.330158

Frequencies --	-96.9181	74.4658	182.5025
Frequencies --	220.9202	260.6107	278.6742
Frequencies --	316.0630	371.3625	443.3348
Frequencies --	467.8152	507.5954	545.2081
Frequencies --	601.5993	652.6251	682.3011
Frequencies --	739.8253	787.5621	863.4692
Frequencies --	898.1504	947.7932	977.4333
Frequencies --	1012.6638	1049.2440	1118.2157
Frequencies --	1191.4095	1260.7514	1273.5871
Frequencies --	1329.6238	1417.3744	1463.2934
Frequencies --	1494.7308	1499.9772	1706.0785
Frequencies --	3075.1257	3156.7556	3164.1626
Frequencies --	3170.2703	3200.0086	3260.6776

SOZ; cis = trans
geometry b
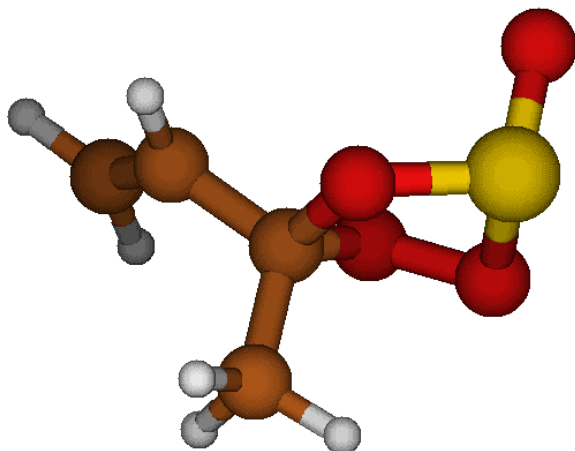
1	6	0	-0.811085	0.267181	-0.201655
2	8	0	-0.333841	0.032089	1.116251
3	8	0	0.958814	0.715487	1.124231
4	6	0	-1.298234	1.687901	-0.398387
5	6	0	-1.843209	-0.786249	-0.485868
6	1	0	-0.512466	2.392837	-0.140672
7	1	0	-1.585197	1.832768	-1.437135
8	1	0	-2.166250	1.860672	0.233273
9	1	0	-1.725135	-1.297950	-1.429676
10	6	0	-2.830102	-1.078940	0.351607
11	1	0	-2.939832	-0.576305	1.301801
12	1	0	-3.549631	-1.846545	0.110903
13	16	0	1.762687	0.073335	-0.232126
14	8	0	0.334793	0.042510	-1.065780
15	8	0	2.161646	-1.299859	0.010468

Frequencies --	-75.8958	75.7866	192.3321
Frequencies --	209.1616	252.5286	286.2159
Frequencies --	325.3928	364.0805	421.0991
Frequencies --	484.6492	488.5934	561.4365
Frequencies --	617.8284	649.1694	685.4120
Frequencies --	736.1086	798.1539	838.8671
Frequencies --	894.8477	946.7115	980.8125
Frequencies --	1019.1964	1052.7240	1144.0676
Frequencies --	1170.7977	1263.8802	1271.3226
Frequencies --	1324.3798	1416.3232	1462.8996
Frequencies --	1496.5251	1498.1685	1700.3838
Frequencies --	3074.1907	3155.8792	3163.4417
Frequencies --	3170.5592	3212.0804	3260.9346

Exo
syn-trans…SO₂ = syn-cis…SO₂
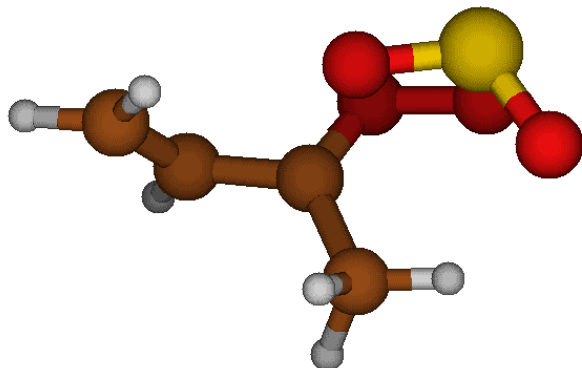
1	6	0	-1.149908	-0.588714	0.112488
2	8	0	-0.582517	-0.934356	-0.975086
3	8	0	0.757829	-1.316590	-0.880511
4	6	0	-0.634704	-0.908268	1.459617
5	6	0	-2.507615	-0.041782	-0.079261
6	1	0	0.348627	-1.357838	1.416132
7	1	0	-0.605422	0.000615	2.054298
8	1	0	-1.359867	-1.581435	1.925265
9	16	0	1.751506	0.558706	-0.330879
10	8	0	0.473985	1.268003	-0.066013
11	8	0	2.456565	0.083986	0.859583
12	6	0	-2.750257	1.263475	-0.042303
13	1	0	-3.295077	-0.768182	-0.239628
14	1	0	-1.950096	1.973357	0.103918
15	1	0	-3.754255	1.637586	-0.172959

Frequencies --	-137.2454	63.5784	82.8236
Frequencies --	111.8508	161.8526	202.8914
Frequencies --	208.9994	277.7327	295.2521
Frequencies --	337.3578	379.4662	411.2342
Frequencies --	520.6840	544.5149	606.8125
Frequencies --	663.9245	807.1788	924.9610
Frequencies --	990.5460	998.8587	1010.3478
Frequencies --	1016.4557	1075.0346	1102.1108
Frequencies --	1249.5330	1300.8653	1329.1910
Frequencies --	1403.7664	1430.4841	1465.7504
Frequencies --	1481.3702	1525.6310	1689.6678
Frequencies --	3047.0326	3139.8321	3170.4656
Frequencies --	3180.5097	3210.4498	3274.3671

SOZ'; cis = trans
geometry a
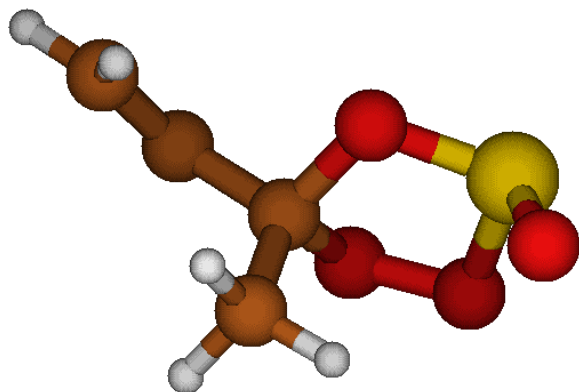
1	6	0	0.802265	0.238964	0.176963
2	8	0	0.227223	1.471521	-0.219784
3	8	0	-1.189799	1.279027	-0.041198
4	6	0	0.716684	-0.011677	1.668587
5	6	0	2.193444	0.245563	-0.382838
6	1	0	-0.310755	0.052771	2.012100
7	1	0	1.101299	-1.004663	1.887015
8	1	0	1.326668	0.723316	2.188280
9	1	0	2.506097	1.180803	-0.826619
10	6	0	2.991468	-0.813592	-0.359609
11	1	0	2.674967	-1.756149	0.063717
12	1	0	3.982951	-0.769724	-0.783391
13	16	0	-1.586169	-0.333454	-0.573674
14	8	0	0.003626	-0.748263	-0.550434
15	8	0	-2.306759	-0.883116	0.563799

Frequencies --	-85.2953	108.2796	164.6015
Frequencies --	226.5849	247.3041	285.7631
Frequencies --	323.0215	367.6012	394.3238
Frequencies --	470.6404	506.7293	532.9293
Frequencies --	590.6467	640.9903	679.1629
Frequencies --	748.2718	783.7174	886.9478
Frequencies --	918.1605	958.4712	980.5447
Frequencies --	1013.7737	1050.6370	1116.2086
Frequencies --	1190.7427	1248.7770	1286.3933
Frequencies --	1329.5052	1424.2112	1464.4160
Frequencies --	1498.3918	1503.0747	1707.3309
Frequencies --	3079.1284	3156.7240	3170.4471
Frequencies --	3177.3317	3198.1728	3260.8380

SOZ'; cis = trans
 geometry b
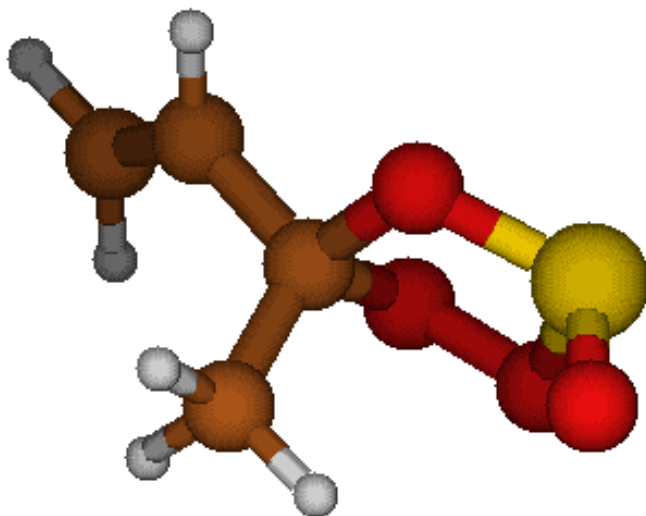
1	6	0	-0.776471	0.225102	-0.016391
2	8	0	-0.542500	-1.019942	0.625930
3	8	0	0.874359	-0.997109	0.918638
4	6	0	-0.663208	1.411817	0.919891
5	6	0	-2.097256	0.114034	-0.719034
6	1	0	0.302463	1.424109	1.415045
7	1	0	-0.781565	2.329649	0.349149
8	1	0	-1.457819	1.354279	1.659970
9	1	0	-2.083319	0.371506	-1.768108
10	6	0	-3.208192	-0.277765	-0.108239
11	1	0	-3.218239	-0.547389	0.938131
12	1	0	-4.139809	-0.351690	-0.648058
13	16	0	1.687166	-0.326453	-0.464242
14	8	0	0.262058	0.273024	-1.033948
15	8	0	2.512883	0.719484	0.117428

Frequencies --	-71.8617	102.0041	170.8726
Frequencies --	218.3242	245.3680	294.2465
Frequencies --	308.4214	361.3665	407.1019
Frequencies --	452.6191	503.4032	541.2898
Frequencies --	613.9883	643.8508	682.6372
Frequencies --	742.6893	804.5322	878.0768
Frequencies --	898.6595	952.1154	982.0569
Frequencies --	1019.2087	1053.6853	1147.0870
Frequencies --	1164.9783	1250.1096	1283.0711
Frequencies --	1325.1509	1423.2133	1463.6601
Frequencies --	1499.3624	1501.4061	1702.2779
Frequencies --	3078.1819	3155.5483	3170.4671
Frequencies --	3176.7499	3209.7600	3260.9465
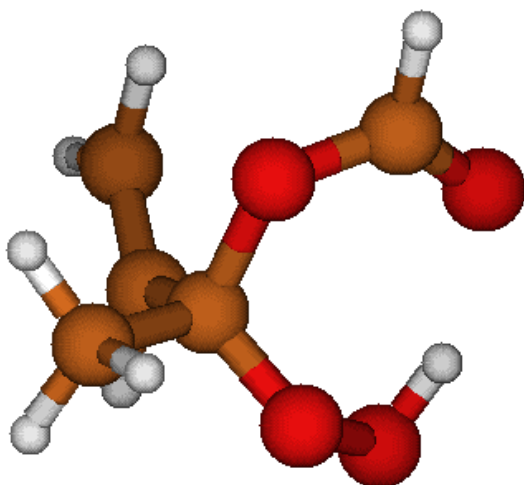
1	6	0	0.887132	1.833521	1.149484
2	6	0	1.033689	0.527588	0.972696
3	6	0	0.655613	-0.227145	-0.267388
4	6	0	1.835608	-0.472676	-1.191309
5	8	0	-0.260085	0.585337	-1.104488
6	6	0	-1.552793	0.721494	-0.833135
7	8	0	-2.195196	0.212668	0.056200
8	8	0	0.132622	-1.493107	-0.001688
9	8	0	-0.587135	-1.525235	1.253677
10	1	0	0.420651	2.462359	0.406039
11	1	0	1.231685	2.308060	2.055470
12	1	0	1.500777	-0.089177	1.726790
13	1	0	2.187882	0.473424	-1.590896
14	1	0	2.634065	-0.953481	-0.633335
15	1	0	1.526081	-1.122352	-2.006823
16	1	0	-1.997569	1.392848	-1.573025
17	1	0	-1.380709	-1.005674	1.004085

Frequencies --	76.1711	98.5487	202.2302
Frequencies --	212.1820	245.8493	273.2042
Frequencies --	294.7566	305.7585	332.8620
Frequencies --	358.8855	474.2877	526.6551
Frequencies --	574.6422	651.1098	692.8068
Frequencies --	702.5734	816.1616	842.2435
Frequencies --	933.2481	971.5763	989.7281
Frequencies --	1026.8053	1051.0905	1054.6095
Frequencies --	1135.3447	1177.4427	1242.9183
Frequencies --	1267.6844	1327.9383	1415.4150
Frequencies --	1422.0319	1461.0597	1496.5182
Frequencies --	1499.6406	1508.0581	1708.5395
Frequencies --	1757.0750	3077.5436	3079.7063
Frequencies --	3160.6890	3172.7467	3174.6443
Frequencies --	3210.0141	3262.9315	3497.3191

Conformer 2

1	6	0	2.800298	-0.078238	-0.575578
2	6	0	1.782497	-0.747966	-0.051368
3	6	0	0.432501	-0.145439	0.222837
4	6	0	0.223710	0.169153	1.691010
5	8	0	-0.492656	-1.270099	-0.139905
6	6	0	-1.787283	-1.075385	-0.335491
7	8	0	-2.405703	-0.033684	-0.298248
8	8	0	0.282190	0.928971	-0.645465
9	8	0	-0.617024	1.935990	-0.127875
10	1	0	2.700249	0.953942	-0.873023
11	1	0	3.755913	-0.558716	-0.721603
12	1	0	1.877501	-1.784268	0.241133
13	1	0	-0.805109	0.443408	1.896868
14	1	0	0.490531	-0.707676	2.275645
15	1	0	0.871135	0.996327	1.967941
16	1	0	-2.264274	-2.035198	-0.552882
17	1	0	-1.470738	1.470002	-0.250589

Frequencies --	72.6077	109.6505	174.0443
Frequencies --	228.3544	254.0508	270.5366
Frequencies --	291.2392	294.2404	351.8090
Frequencies --	383.7694	472.9525	504.0488
Frequencies --	563.2571	652.0546	686.6383
Frequencies --	723.4533	807.2726	833.4947
Frequencies --	930.3300	980.5030	990.2689
Frequencies --	1030.8915	1052.6003	1062.0250
Frequencies --	1102.4706	1204.3290	1252.8101
Frequencies --	1280.8337	1329.9264	1419.0313
Frequencies --	1421.4803	1456.2740	1496.2891
Frequencies --	1500.3208	1502.3878	1707.3000
Frequencies --	1744.7778	3079.4897	3084.3109
Frequencies --	3163.5218	3176.6857	3180.1701
Frequencies --	3202.7073	3271.2215	3511.0775

Conformer 3

1	6	0	-2.700863	0.677522	-0.396425
2	6	0	-1.907555	-0.354897	-0.145113
3	6	0	-0.436016	-0.293236	0.160140
4	6	0	-0.115599	-0.828123	1.542376
5	8	0	-0.083298	1.144070	0.126040
6	6	0	1.168304	1.567049	0.019593
7	8	0	2.177512	0.909985	-0.102894
8	8	0	0.158020	-0.992693	-0.896774
9	8	0	1.411122	-1.612816	-0.519061
10	1	0	-2.330660	1.690002	-0.403682
11	1	0	-3.749164	0.522127	-0.602266
12	1	0	-2.291444	-1.365908	-0.148592
13	1	0	-0.705340	-0.277363	2.270200
14	1	0	-0.377204	-1.882051	1.586777
15	1	0	0.939547	-0.726421	1.769854
16	1	0	1.176309	2.659874	0.056525
17	1	0	1.981476	-0.818516	-0.470734

Frequencies --	70.9725	83.0563	183.1175
Frequencies --	225.3040	248.2182	255.7482
Frequencies --	281.4223	308.5218	352.2594
Frequencies --	411.3527	443.2096	499.0019
Frequencies --	581.2000	645.2795	689.4894
Frequencies --	702.6669	820.9861	848.7920
Frequencies --	924.5984	965.8192	982.8748
Frequencies --	1029.9415	1050.2296	1052.6445
Frequencies --	1135.8451	1187.7340	1245.4425
Frequencies --	1273.9436	1330.7779	1419.6062
Frequencies --	1422.4236	1459.7448	1490.5004
Frequencies --	1498.5693	1501.6175	1709.8954
Frequencies --	1752.1261	3081.3073	3085.3122
Frequencies --	3163.9066	3179.2747	3182.0759
Frequencies --	3199.4308	3274.0408	3533.6429

Conformer 4

1	6	0	2.256691	0.310569	-1.343272
2	6	0	0.990230	0.369548	-0.951865
3	6	0	0.478134	-0.196689	0.339340
4	6	0	1.474675	-0.945423	1.195306
5	8	0	-0.507320	-1.274408	-0.025416
6	6	0	-1.723094	-1.009747	-0.476735
7	8	0	-2.252354	0.069999	-0.628895
8	8	0	-0.101405	0.735899	1.200238
9	8	0	-0.655706	1.876741	0.504841
10	1	0	3.031646	-0.140918	-0.742866
11	1	0	2.555588	0.729250	-2.292392
12	1	0	0.248588	0.838287	-1.578912
13	1	0	1.855298	-1.810345	0.661139
14	1	0	2.291198	-0.284501	1.468692
15	1	0	0.972995	-1.278056	2.099917
16	1	0	-2.229915	-1.950814	-0.708395
17	1	0	-1.450921	1.461696	0.110020

Frequencies --	66.3568	77.8885	190.0123
Frequencies --	230.3490	260.2765	270.6017
Frequencies --	295.5257	316.5064	332.6341
Frequencies --	385.9255	431.7643	497.2633
Frequencies --	555.9009	640.1973	673.5732
Frequencies --	747.1058	796.5578	827.1998
Frequencies --	929.0861	981.1652	987.1140
Frequencies --	1029.8110	1039.1963	1053.2775
Frequencies --	1098.1228	1196.3029	1249.1956
Frequencies --	1319.5007	1347.1306	1417.1866
Frequencies --	1423.5562	1465.3969	1500.1482
Frequencies --	1502.9957	1509.3740	1708.8388
Frequencies --	1743.1153	3079.0016	3086.9559
Frequencies --	3167.8822	3176.3493	3178.8435
Frequencies --	3227.3268	3263.0480	3515.1882

Conformer 5

1	6	0	1.862518	-1.184768	1.034523
2	6	0	1.028076	-0.154746	1.079421
3	6	0	0.442672	0.538891	-0.116905
4	6	0	1.240147	1.769321	-0.515581
5	8	0	-0.864598	1.141518	0.312323
6	6	0	-1.957120	0.419068	0.502308
7	8	0	-2.122102	-0.762068	0.290876
8	8	0	0.316997	-0.188064	-1.293753
9	8	0	-0.021816	-1.583978	-1.105457
10	1	0	2.116602	-1.670192	0.106395
11	1	0	2.296389	-1.572963	1.943961
12	1	0	0.779032	0.314646	2.021722
13	1	0	0.761089	2.250422	-1.365013
14	1	0	1.280144	2.466068	0.316859
15	1	0	2.246722	1.464274	-0.784319
16	1	0	-2.749873	1.063724	0.892065
17	1	0	-0.895706	-1.501825	-0.666180

Frequencies --	54.8229	92.8148	192.7587
Frequencies --	219.1158	241.3391	261.0966
Frequencies --	293.4826	303.5717	333.2831
Frequencies --	345.7920	456.9745	495.2362
Frequencies --	557.3205	649.4915	680.8286
Frequencies --	720.5705	794.9812	828.8467
Frequencies --	927.9457	982.7147	992.9715
Frequencies --	1026.7125	1054.9495	1063.3596
Frequencies --	1099.9610	1183.3088	1244.2319
Frequencies --	1292.9000	1334.9112	1413.6882
Frequencies --	1418.7588	1461.7528	1496.2354
Frequencies --	1498.4557	1528.3866	1706.7823
Frequencies --	1749.0698	3078.5776	3080.3184
Frequencies --	3162.1624	3174.5581	3176.6790
Frequencies --	3192.2964	3276.2387	3477.4975

Conformer 6

1	6	0	-1.674338	1.722750	-0.541696
2	6	0	-0.454659	1.238912	-0.347264
3	6	0	-0.171135	-0.034434	0.397970
4	6	0	0.358532	0.204850	1.800976
5	8	0	0.757458	-0.881697	-0.368160
6	6	0	2.001743	-0.471506	-0.646335
7	8	0	2.512511	0.572308	-0.337010
8	8	0	-1.287380	-0.858438	0.595436
9	8	0	-1.864228	-1.227222	-0.681641
10	1	0	-2.555267	1.189274	-0.220298
11	1	0	-1.814029	2.671058	-1.038620
12	1	0	0.421650	1.782799	-0.666625
13	1	0	0.638567	-0.743559	2.253615
14	1	0	1.220340	0.861903	1.760179
15	1	0	-0.424830	0.671901	2.391634
16	1	0	2.504292	-1.260193	-1.216057
17	1	0	-1.298470	-1.976214	-0.914732

Frequencies --	94.0340	103.6592	157.2415
Frequencies --	190.1500	220.9352	240.4219
Frequencies --	244.4562	249.4702	300.9962
Frequencies --	333.4790	383.8830	444.1606
Frequencies --	503.3586	582.5964	697.1762
Frequencies --	732.8237	807.6844	863.5570
Frequencies --	918.6703	975.7838	982.8918
Frequencies --	1041.8929	1045.2582	1064.5126
Frequencies --	1119.1812	1183.6051	1212.0479
Frequencies --	1289.0441	1332.9549	1399.6695
Frequencies --	1409.8760	1416.0447	1462.5033
Frequencies --	1498.3652	1505.3240	1707.8531
Frequencies --	1778.2308	3061.1112	3079.9520
Frequencies --	3160.4578	3175.8834	3184.6688
Frequencies --	3218.8248	3268.4147	3759.2248

Conformer 7

1	6	0	-1.154950	2.330792	-0.297869
2	6	0	-0.166662	1.519720	0.059372
3	6	0	-0.284853	0.025600	0.181687
4	6	0	-0.069336	-0.470952	1.597731
5	8	0	0.660637	-0.634168	-0.742234
6	6	0	1.983137	-0.476287	-0.610022
7	8	0	2.562074	0.195441	0.202901
8	8	0	-1.538893	-0.317469	-0.339124
9	8	0	-1.755794	-1.737260	-0.177692
10	1	0	-2.137316	1.962781	-0.548197
11	1	0	-0.992013	3.397291	-0.341954
12	1	0	0.809941	1.902402	0.314622
13	1	0	-0.066720	-1.555864	1.619678
14	1	0	0.871984	-0.093347	1.982129
15	1	0	-0.886613	-0.103740	2.213683
16	1	0	2.479600	-1.069218	-1.385580
17	1	0	-1.347074	-2.065893	-0.990579

Frequencies --	43.5490	98.7842	129.3191
Frequencies --	204.3070	220.6656	228.5749
Frequencies --	257.1323	286.9489	310.2734
Frequencies --	329.8679	409.7847	462.0348
Frequencies --	494.7611	565.4119	673.7914
Frequencies --	728.2247	811.0002	882.7275
Frequencies --	926.8690	968.2530	986.9309
Frequencies --	1044.4577	1049.5988	1062.7698
Frequencies --	1112.4270	1195.7764	1234.0116
Frequencies --	1276.9768	1336.0482	1399.0534
Frequencies --	1413.0014	1416.2748	1463.8452
Frequencies --	1500.1601	1508.0085	1704.9298
Frequencies --	1776.6319	3058.8456	3087.0457
Frequencies --	3167.7082	3177.0361	3185.7857
Frequencies --	3221.5582	3270.1645	3756.4166

Conformer 8

1	6	0	1.374023	2.111856	-0.111803
2	6	0	0.491501	1.311409	-0.693233
3	6	0	-0.326886	0.267698	0.010845
4	6	0	-0.264716	0.243469	1.519962
5	8	0	-0.004544	-1.053816	-0.554967
6	6	0	1.197586	-1.613519	-0.342556
7	8	0	2.104060	-1.171405	0.309191
8	8	0	-1.626102	0.517698	-0.476233
9	8	0	-2.552744	-0.439415	0.093444
10	1	0	1.583744	2.066793	0.945605
11	1	0	1.926988	2.833964	-0.693269
12	1	0	0.306226	1.365362	-1.757726
13	1	0	-0.653922	1.185063	1.898671
14	1	0	-0.884449	-0.565279	1.891787
15	1	0	0.755498	0.101316	1.856682
16	1	0	1.226826	-2.569634	-0.876707
17	1	0	-2.455328	-1.167558	-0.535813

Frequencies --	52.1622	89.8422	135.6378
Frequencies --	206.3076	224.1317	228.7328
Frequencies --	249.9107	294.4314	321.0038
Frequencies --	345.9323	416.8605	428.2077
Frequencies --	500.8694	576.9841	649.4785
Frequencies --	723.2063	814.0751	893.0125
Frequencies --	915.3274	948.4706	985.5456
Frequencies --	1028.1844	1034.5877	1043.4320
Frequencies --	1123.9488	1192.9246	1202.0943
Frequencies --	1309.1027	1335.3283	1390.6948
Frequencies --	1415.4315	1418.8487	1462.9530
Frequencies --	1504.6030	1516.2279	1713.2945
Frequencies --	1784.8432	3053.8729	3092.9023
Frequencies --	3172.8335	3177.1970	3193.3726
Frequencies --	3194.1770	3266.4829	3757.5812

Conformer 9

1	6	0	0.627628	2.218261	-0.568681
2	6	0	-0.196589	1.185170	-0.683224
3	6	0	-0.352857	0.093177	0.333459
4	6	0	0.191471	0.361097	1.719807
5	8	0	0.183918	-1.161909	-0.220115
6	6	0	1.501334	-1.305401	-0.436957
7	8	0	2.373677	-0.524157	-0.170905
8	8	0	-1.709244	-0.212846	0.568126
9	8	0	-2.374427	-0.506072	-0.683757
10	1	0	1.284994	2.345963	0.277405
11	1	0	0.673746	2.970015	-1.342422
12	1	0	-0.830933	1.074822	-1.549560
13	1	0	-0.336420	1.206486	2.151773
14	1	0	0.027127	-0.517213	2.338472
15	1	0	1.252867	0.572415	1.673367
16	1	0	1.665968	-2.283242	-0.902688
17	1	0	-2.154657	-1.443186	-0.779567

Frequencies --	50.6800	98.0937	141.9017
Frequencies --	203.3189	216.9084	237.9371
Frequencies --	259.0828	292.6021	311.8059
Frequencies --	369.4189	374.2639	428.9182
Frequencies --	498.3528	594.6826	660.0609
Frequencies --	731.4627	821.3215	853.9187
Frequencies --	920.3430	965.4445	980.6762
Frequencies --	1030.1599	1038.8639	1042.9657
Frequencies --	1123.0195	1192.0355	1207.5967
Frequencies --	1306.8671	1335.7605	1395.9644
Frequencies --	1414.2006	1417.6825	1465.4207
Frequencies --	1500.4944	1515.6410	1710.1232
Frequencies --	1783.9694	3054.5957	3088.6734
Frequencies --	3164.8523	3175.8920	3195.6310
Frequencies --	3220.5255	3263.3052	3757.8764

5.4 MVK-oxide + formic acid
Planar minimum
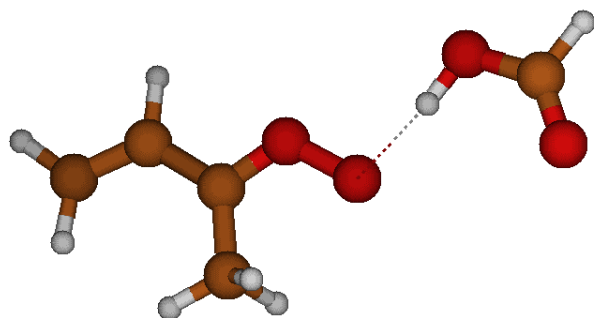
1	6	0	1.741217	0.130226	0.000189
2	8	0	0.555319	-0.358983	0.000568
3	8	0	-0.473966	0.542452	0.000064
4	8	0	-3.904313	0.798072	0.000785
5	6	0	-3.759207	-0.399502	-0.000162
6	8	0	-2.604470	-1.054101	-0.000957
7	1	0	-4.594850	-1.110732	-0.000285
8	1	0	-1.846557	-0.401643	-0.000741
9	6	0	1.899630	1.592252	-0.000496
10	6	0	2.776238	-0.871954	0.000469
11	6	0	4.087061	-0.601848	-0.000134
12	1	0	2.939955	1.892743	0.000320
13	1	0	1.372547	1.997505	0.864787
14	1	0	1.374324	1.996632	-0.867284
15	1	0	2.423735	-1.894328	0.001128
16	1	0	4.469782	0.407095	-0.000845
17	1	0	4.810873	-1.401840	0.000045

Frequencies --	-11.2128	28.0164	28.5450
Frequencies --	93.0419	114.4863	187.3679
Frequencies --	187.6019	202.7433	283.9468
Frequencies --	288.2781	374.3504	466.6073
Frequencies --	499.7103	613.3722	688.0206
Frequencies --	700.7362	816.1089	960.2787
Frequencies --	971.2524	981.8794	1023.7979
Frequencies --	1028.5016	1046.9966	1070.0874
Frequencies --	1078.7956	1223.0542	1307.2149
Frequencies --	1340.6752	1402.9329	1407.4447
Frequencies --	1452.4933	1462.4560	1478.6718
Frequencies --	1489.8396	1505.6518	1670.7873
Frequencies --	1790.6366	3027.2501	3058.1226
Frequencies --	3105.0973	3130.1696	3182.2002
Frequencies --	3195.2472	3202.5521	3274.2473

van der Waals minimum
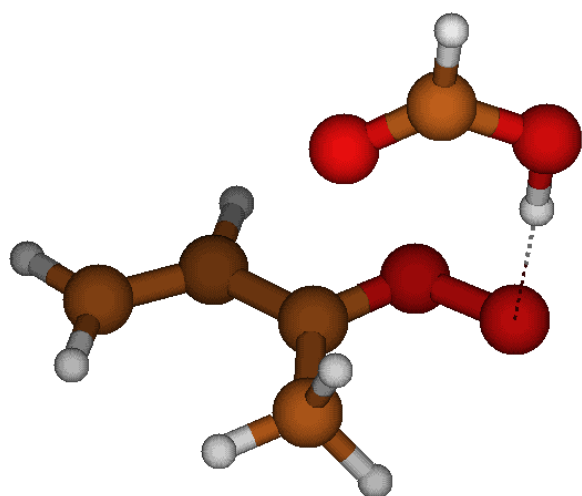

```
  1           6           0       0.000000     0.000000     0.000000
  2           8           0       0.000000     0.000000     1.275955
  3           8           0       1.245775     0.000000     1.892005
  4           8           0       0.606398    -2.800437     0.381749
  5           6           0       1.017466    -3.231013     1.441733
  6           8           0       1.418780    -2.525602     2.475900
  7           1           0       1.096188    -4.304566     1.647652
  8           1           0       1.354816    -1.531258     2.273211
  9           6           0       1.271230     0.075133    -0.735745
 10           6           0      -1.329184    -0.043379    -0.564140
 11           6           0      -1.585380    -0.054876    -1.875686
 12           1           0       1.115967     0.238392    -1.795234
 13           1           0       1.804535    -0.859772    -0.570167
 14           1           0       1.877193     0.865388    -0.294599
 15           1           0      -2.132100    -0.086121     0.158207
 16           1           0      -0.802662    -0.028630    -2.617617
 17           1           0      -2.601700    -0.103459    -2.234886
```

```
Frequencies --     46.8365                56.9407                93.3520
Frequencies --    126.3653               148.3550               156.9454
Frequencies --    221.9254               247.4525               269.3290
Frequencies --    338.2014               358.9841               455.7681
Frequencies --    493.3374               597.9164               688.1404
Frequencies --    708.0896               808.8531               926.4019
Frequencies --    991.7365              1019.5153              1028.1072
Frequencies --   1041.7520              1047.0099              1071.0999
Frequencies --   1116.5869              1260.2678              1313.3572
Frequencies --   1342.3675              1392.1696              1408.1414
Frequencies --   1457.3675              1471.1291              1492.7186
Frequencies --   1502.5265              1519.0126              1678.8845
Frequencies --   1747.2199              2799.5379              3051.0151
Frequencies --   3073.7270              3135.1225              3183.0650
Frequencies --   3193.5201              3207.7761              3275.1933
```

van der Waals minimum = HPBF
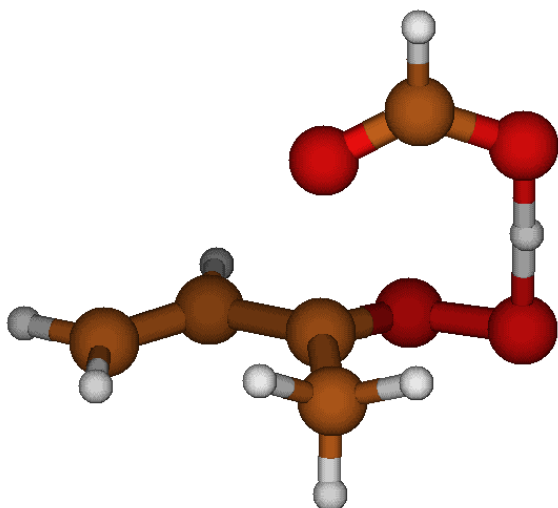
1	6	0	0.735502	0.454862	0.005429
2	8	0	-0.012061	1.158611	-0.764566
3	8	0	-1.165269	1.718647	-0.142895
4	8	0	-0.488945	-1.447803	0.047960
5	6	0	-1.725710	-1.379711	-0.017457
6	8	0	-2.456497	-0.330435	-0.094877
7	1	0	-2.299636	-2.314001	-0.008477
8	1	0	-1.862852	0.675446	-0.120004
9	6	0	0.665065	0.556642	1.481842
10	6	0	1.860444	-0.120030	-0.717072
11	6	0	2.908772	-0.687222	-0.120910
12	1	0	1.082850	-0.330317	1.941562
13	1	0	1.249719	1.432001	1.776493
14	1	0	-0.355806	0.708391	1.801768
15	1	0	1.796939	-0.048340	-1.793121
16	1	0	2.983701	-0.776058	0.951796
17	1	0	3.722827	-1.086513	-0.705978

Frequencies --	-598.0338	58.5295	83.8810
Frequencies --	142.1704	169.6873	192.1403
Frequencies --	250.3268	271.1921	305.4575
Frequencies --	345.1720	376.8882	461.5846
Frequencies --	484.5414	575.6331	662.7502
Frequencies --	706.2328	774.5847	819.0039
Frequencies --	939.2021	995.0411	1000.5989
Frequencies --	1028.5869	1060.3462	1066.7508
Frequencies --	1078.1853	1271.7963	1318.4128
Frequencies --	1346.0554	1354.1718	1403.3264
Frequencies --	1417.4923	1456.9270	1475.3778
Frequencies --	1496.8015	1526.9577	1669.0611
Frequencies --	1691.6501	1744.9004	3039.1798
Frequencies --	3057.8435	3169.0449	3183.6576
Frequencies --	3213.6016	3225.2961	3273.7312

HPBF
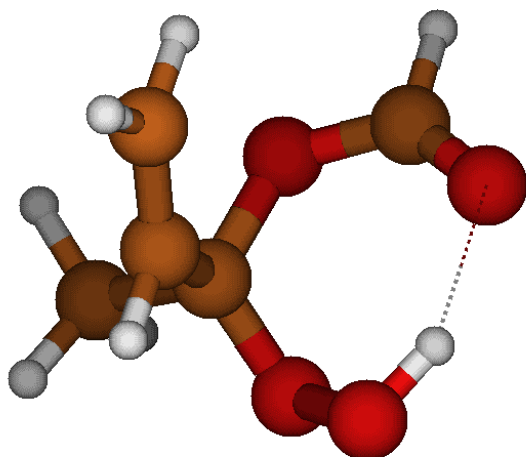
1	6	0	-0.883500	1.834737	1.149530
2	6	0	-1.034160	0.529419	0.971859
3	1	0	-1.227925	2.310005	2.055163
4	1	0	-0.413804	2.462367	0.407125
5	6	0	-0.655954	-0.226175	-0.267616
6	1	0	-1.504382	-0.086180	1.724944
7	6	0	-1.836046	-0.471726	-1.191482
8	8	0	0.260416	0.584631	-1.104752
9	8	0	-0.134272	-1.492675	-0.000581
10	1	0	-2.188107	0.474285	-1.591477
11	1	0	-1.526585	-1.121755	-2.006710
12	1	0	-2.634634	-0.952142	-0.633379
13	6	0	1.553524	0.719314	-0.833830
14	8	0	0.585099	-1.524915	1.255073
15	8	0	2.195498	0.210024	0.055430
16	1	0	1.998607	1.390186	-1.573964
17	1	0	1.379722	-1.006701	1.006175

Frequencies --	76.0580	98.5864	202.2503
Frequencies --	212.1732	245.6072	272.8544
Frequencies --	294.5828	305.7747	332.8314
Frequencies --	358.7746	474.4106	526.5001
Frequencies --	574.6054	651.3611	692.4755
Frequencies --	702.5520	816.2610	842.2525
Frequencies --	933.1789	971.4580	989.3940
Frequencies --	1026.7452	1051.0041	1054.5359
Frequencies --	1135.5926	1177.0500	1242.5607
Frequencies --	1267.6093	1327.8929	1415.3733
Frequencies --	1422.0245	1461.0687	1496.5053
Frequencies --	1499.6251	1507.1182	1708.6714
Frequencies --	1757.4064	3077.6396	3079.7797
Frequencies --	3160.8343	3172.7541	3174.8347
Frequencies --	3210.0886	3263.1153	3498.3543

Alkoxy
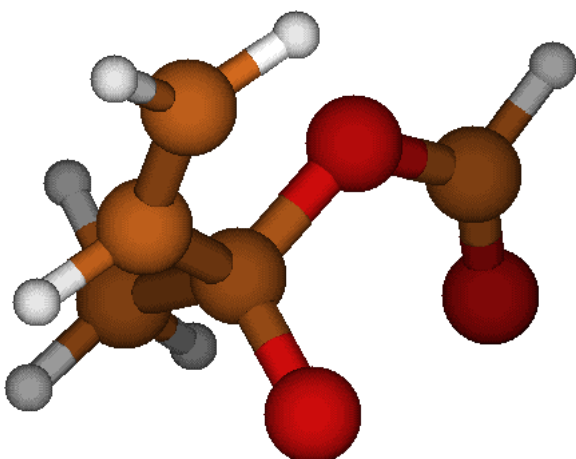
1	6	0	2.372674	-1.020834	-0.081462
2	6	0	1.802909	0.171921	0.034423
3	1	0	3.448819	-1.110346	-0.098440
4	1	0	1.785744	-1.919485	-0.181417
5	6	0	0.297368	0.406274	0.068797
6	1	0	2.382535	1.074785	0.156943
7	6	0	-0.114558	1.570558	-0.832022
8	8	0	0.074864	0.636804	1.370559
9	8	0	-0.331173	-0.831697	-0.394272
10	1	0	0.095177	1.310963	-1.866845
11	1	0	0.457472	2.451934	-0.554932
12	1	0	-1.172513	1.773592	-0.706715
13	6	0	-1.655823	-0.957260	-0.204460
14	8	0	-2.399740	-0.137245	0.260446
15	1	0	-1.964267	-1.948301	-0.554118

Frequencies --	62.0861	107.9899	173.0780
Frequencies --	223.5841	239.7966	262.0089
Frequencies --	307.7685	348.7095	425.4105
Frequencies --	511.1594	545.8325	649.3337
Frequencies --	691.0476	828.4077	891.6562
Frequencies --	951.9134	987.3386	1018.9171
Frequencies --	1034.7477	1043.9681	1102.8519
Frequencies --	1162.2461	1169.2324	1230.4460
Frequencies --	1324.1390	1399.1923	1412.1628
Frequencies --	1443.1028	1491.2506	1513.5205
Frequencies --	1685.8150	1784.4604	3057.9617
Frequencies --	3078.6667	3160.3187	3178.1332
Frequencies --	3184.1275	3215.5311	3276.1918

6. References

1. L. Sheps, D. W. Chandler (2013) Time-resolved broadband cavity-enhanced absorption spectroscopy for chemical kinetics. (Sandia National Laboratories (SNL-CA), Livermore, CA (United States)).
2. L. Sheps, Absolute ultraviolet absorption spectrum of a Criegee intermediate CH_2OO. *J Phys Chem Lett* **4**, 4201-4205 (2013).
3. V. P. Barber *et al.*, Four-carbon Criegee intermediate from isoprene ozonolysis: methyl vinyl ketone oxide synthesis, infrared spectrum, and OH production. *J Am Chem Soc* **140**, 10866-10880 (2018).
4. D. L. Osborn *et al.*, The multiplexed chemical kinetic photoionization mass spectrometer: A new approach to isomer-resolved chemical kinetics. *Rev Sci Instrum* **79**, 104103 (2008).
5. S. Lias, Ionization energy evaluation. *NIST Chemistry WebBook, NIST Standard Reference Database* **69** (2005).
6. M.-N. Su, J. J.-M. Lin, Note: A transient absorption spectrometer using an ultra bright laser-driven light source. *Rev Sci Instrum* **84**, 086106 (2013).
7. W. Chao, J.-T. Hsieh, C.-H. Chang, J. J.-M. Lin, Direct kinetic measurement of the reaction of the simplest Criegee intermediate with water vapor. *Science* **347**, 751-754 (2015).
8. S. L. Manatt, A. L. Lane, A compilation of the absorption cross-sections of SO_2 from 106 to 403 nm. *J Quant Spectrosc Radiat Transf* **50**, 267-276 (1993).
9. T. C. Johns *et al.*, The second Hadley Centre coupled ocean-atmosphere GCM: model description, spinup and validation. *Clim Dynam* **13**, 103-134 (1997).
10. W. Collins, D. S. Stevenson, C. Johnson, R. Derwent, Tropospheric ozone in a global-scale three-dimensional Lagrangian model and its response to NO x emission controls. *J Atmos Chem* **26**, 223-274 (1997).
11. R. Derwent, W. Collins, M. Jenkin, C. Johnson, D. Stevenson, The global distribution of secondary particulate matter in a 3-D Lagrangian chemistry transport model. *J Atmos Chem* **44**, 57-95 (2003).
12. M. Jenkin, L. Watson, S. Utembe, D. Shallcross, A Common Representative Intermediates (CRI) mechanism for VOC degradation. Part 1: gas phase mechanism development. *Atmos Environ* **42**, 7185-7195 (2008).
13. L. Watson, D. Shallcross, S. Utembe, M. Jenkin, A Common Representative Intermediates (CRI) mechanism for VOC degradation. Part 2: gas phase mechanism reduction. *Atmos Environ* **42**, 7196-7204 (2008).
14. S. R. Utembe *et al.*, Simulating secondary organic aerosol in a 3-D Lagrangian chemistry transport model using the reduced Common Representative Intermediates mechanism (CRI v2-R5). *Atmos Environ* **45**, 1604-1614 (2011).
15. M. A. H. Khan *et al.*, A modeling study of secondary organic aerosol formation from sesquiterpenes using the STOCHEM global chemistry and transport model. *J Geophys Res Atmos* **122**, 4426-4439 (2017).
16. J. G. Olivier *et al.*, Description of EDGAR Version 2.0: A set of global emission inventories of greenhouse gases and ozone-depleting substances for all anthropogenic and most natural sources on a per country basis and on 1 degree x 1 degree grid. (1996).
17. J. Cofala, M. Amann, R. Mechler, Scenarios of world anthropogenic emissions of air pollutants and methane up to 2030. *International Institute for Applied Systems Analysis (IIASA)), Laxenburg, Austria* (2005).
18. M. A. H. Khan *et al.*, Reassessing the photochemical production of methanol from peroxy radical self and cross reactions using the STOCHEM-CRI global chemistry and transport model. *Atmos Environ* **99**, 77-84 (2014).
19. M. R. McGillen *et al.*, Criegee Intermediate–Alcohol Reactions, A Potential Source of Functionalized Hydroperoxides in the Atmosphere. *ACS Earth Space Chem* **1**, 664-672 (2017).
20. R. Chhantyal-Pun *et al.*, Direct Kinetic and Atmospheric Modeling Studies of Criegee Intermediate Reactions with Acetone. *ACS Earth Space Chem* **3**, 2368-2371 (2019).
21. L. Sheps *et al.*, The reaction of Criegee intermediate CH_2OO with water dimer: primary products and atmospheric impact. *Phys Chem Chem Phys* **19**, 21970-21979 (2017).

22. M. C. Smith *et al.*, Strong Negative Temperature Dependence of the Simplest Criegee Intermediate CH_2OO Reaction with Water Dimer. *J Phys Chem Lett* **6**, 2708-2713 (2015).

23. Y. Fang *et al.*, Communication: Real time observation of unimolecular decay of Criegee intermediates to OH radical products. *J Chem Phys* **144**, 061102 (2016).

24. C. A. Taatjes *et al.*, Direct Measurements of Conformer-Dependent Reactivity of the Criegee Intermediate CH_3CHOO. *Science* **12**, 177-180 (2013).

25. O. Welz *et al.*, Rate coefficients of C1 and C2 Criegee intermediate reactions with formic and acetic acid near the collision limit: direct kinetics measurements and atmospheric implications. *Angew Chem Int Ed* **53**, 4547-4550 (2014).

26. L.-C. Lin, W. Chao, C.-H. Chang, K. Takahashi, J. J.-M. Lin, Temperature dependence of the reaction of *anti*-CH_3CHOO with water vapor. *Phys Chem Chem Phys* **18**, 28189-28197 (2016).

27. J. M. Anglada, A. Solé, Impact of the water dimer on the atmospheric reactivity of carbonyl oxides. *Phys Chem Chem Phys* **18**, 17698-17712 (2016).

28. L. Vereecken, A. Novelli, D. Taraborrelli, Unimolecular decay strongly limits the atmospheric impact of Criegee intermediates. *Phys Chem Chem Phys* **19**, 31599-31612 (2017).

29. Anonymous, MOLPRO, version 2012.1, A Package of Ab Initio Programs. Werner, H.-J.; Knowles, P. J.; Knizia, G.; Manby, F. R.; Schutz, M.; Celani, P.; Korona, T.; Lindh, R.; Mitrushenkov, A.; Rauhut, G.; et al. see http://www.molpro.net.

30. Anonymous, MRCC, A String-Based Quantum Chemical Program Suite; written by M. Kállay, see also Kállay, M.; Surján, P. R. Higher Excitations in Coupled-Cluster Theory. J. Chem. Phys. 2001, 115, 2945-2954

31. Anonymous, Gaussian 09, Revision D.01, Frisch, M. J.; Trucks, G. W.; Schlegel, H. B.; Scuseria, G. E.; Robb, M. A.; Cheeseman, J. R.; Scalmani, G.; Barone, V.; Mennucci, B.; Petersson, G. A.; et al. Gaussian, Inc., Wallingford CT, 2009.

32. Y. Georgieskii, J. A. Miller, M. P. Burke, S. J. Klippenstein, Reformulation and Solution of the Master Equation for Multiple-Well Chemical Reactions. *J Phys Chem A* **46**, 12146-12154 (2013).

33. Y. Georgieskii, S. J. Klippenstein, MESS.2016.3.23; Argonne National Laboratory, see https://tcg.cse.anl.gov/papr/codes/mess.html. (2016).

34. Y. Georgieskii, L. B. Harding, S. J. Klippenstein, VaReCoF, Argonne National Laboratory, see https://tcg.cse.anl.gov/papr/codes/varecof.html. (2011).

35. O. Welz *et al.*, Direct kinetic measurements of Criegee intermediate (CH_2OO) formed by reaction of CH_2I with O_2. *Science* **335**, 204-207 (2012).

36. P. Aplincourt, M. F. Ruiz-López, Theoretical investigation of reaction mechanisms for carboxylic acid formation in the atmosphere. *J Am Chem Soc* **122**, 8990-8997 (2000).

37. L. Jiang, Y.-s. Xu, A.-z. Ding, Reaction of Stabilized Criegee Intermediates from Ozonolysis of Limonene with Sulfur Dioxide: Ab Initio and DFT Study. *J Phys Chem A* **114**, 12452-12461 (2010).

38. T. Kurtén, J. R. Lane, S. Jørgensen, H. G. Kjaergaard, A computational study of the oxidation of SO_2 to SO_3 by gas-phase organic oxidants. *J Phys Chem A* **115**, 8669-8681 (2011).

39. L. Vereecken, H. Harder, A. Novelli, The reaction of Criegee intermediates with NO, RO_2, and SO_2, and their fate in the atmosphere. *Phys Chem Chem Phys* **14**, 14682-14695 (2012).

40. K. T. Kuwata *et al.*, A Computational Re-examination of the Criegee Intermediate–Sulfur Dioxide Reaction. *J Phys Chem A* **119**, 10316-10335 (2015).

41. M. Pfeifle *et al.*, Nascent energy distribution of the Criegee intermediate CH_2OO from direct dynamics calculations of primary ozonide dissociation. *J Chem Phys* **148**, 174306 (2018).

42. T. H. Dunning Jr., K. A. Peterson, A. K. Wilson, Gaussian basis sets for use in correlated molecular calculations. X. The atoms aluminum through argon revisited. *J Chem Phys* **114**, 9244-9253 (2001).

43. Y. Georgievskii, S. J. Klippenstein, Long-range transition state theory. *J Chem Phys* **122**, 194103 (2005).

44. L. Vereecken, The reaction of Criegee intermediates with acids and enols. *Phys Chem Chem Phys* **19**, 28630-28640 (2017).

45. J.-D. Chai, M. Head-Gordon, Long-range corrected hybrid density functionals with damped atom–atom dispersion corrections. *Phys Chem Chem Phys* **10**, 6615-6620 (2008).

46.   S. Grimme, J. Antony, S. Ehrlich, H. Krieg, A consistent and accurate ab initio parametrization of density functional dispersion correction (DFT-D) for the 94 elements H-Pu. *J Chem Phys* **132**, 154104 (2010).

47.   G. Knizia, T. B. Adler, H.-J. Werner, Simplified CCSD(T)-F12 methods: Theory and benchmarks. *J Chem Phys* **130**, 054104 (2009).

48.   J. Anglada, J. Gonzalez, M. Torrent-Sucarrat, Effects of the substituents on the reactivity of carbonyl oxides. A theoretical study on the reaction of substituted carbonyl oxides with water. *Phys Chem Chem Phys* **13**, 13034-13045 (2011).

49.   P. Aplincourt, J. M. Anglada, Theoretical studies on isoprene ozonolysis under tropospheric conditions. 1. Reaction of substituted carbonyl oxides with water. *J Phys Chem A* **107**, 5798-5811 (2003).

50.   K. T. Kuwata, M. R. Hermes, M. J. Carlson, C. K. Zogg, Computational studies of the isomerization and hydration reactions of acetaldehyde oxide and methyl vinyl carbonyl oxide. *J Phys Chem A* **114**, 9192-9204 (2010).

51.   S. J. Klippenstein, L. B. Harding, B. Ruscic, Ab Initio Computations and Active Thermochemical Tables Hand in Hand: Heats of Formation of Core Combustion Species. *J Phys Chem A* **121**, 6580-6602 (2017).

52.   B. Long, J. L. Bao, D. G. Truhlar, Atmospheric chemistry of Criegee intermediates: unimolecular reactions and reactions with water. *J Am Chem Soc* **138**, 14409-14422 (2016).

53.   T. Berndt *et al.*, Kinetics of the unimolecular reaction of CH_2OO and the bimolecular reactions with the water monomer, acetaldehyde and acetone under atmospheric conditions. *Phys Chem Chem Phys* **17**, 19862-19873 (2015).

54.   B. Long, J. L. Bao, D. G. Truhlar, Unimolecular reaction of acetone oxide and its reaction with water in the atmosphere. *Proc Natl Acad U S A* **115**, 6135-6140 (2018).

55.   C. Kuang, P. H. McMurry, A. V. McCormick, F. L. Eisele, Dependence of nucleation rates on sulfuric acid vapor concentration in diverse atmospheric locations. *J Geophys Res Atmos* **113** (2008).

56.   J. Kirkby *et al.*, Role of sulphuric acid, ammonia and galactic cosmic rays in atmospheric aerosol nucleation. *Nature* **476**, 429 (2011).